Novel Monitoring System to Diagnose Rail Track Foundation Problems

by

AW, ENG SEW

MEng, Civil and Environmental Engineering (2001)
Imperial College of Science, Technology and Medicine, London, UK

Submitted to the
Department of Civil and Environmental Engineering
in Partial Fulfilment of the Requirements for the Degree of

Masters of Science in Civil and Environmental Engineering

at the

MASSACHUSETTS INSTITUTE OF TECHNOLOGY
February 2004

Signature of Author _____
Department of Civil and Environmental Engineering
September 2003

Certified by _____
Dr John T Germaine
Thesis Supervisor

Certified by_____
Professor Andrew J. Whittle
Thesis Supervisor

Accepted by _____
Heidi Nepf, Chairman,
Departmental Committee on Graduate Studies

Novel Monitoring System to Diagnose Rail Track Foundation Problems

by

Aw, Eng Sew

Submitted to the Department of Civil and Environmental Engineering
on February 2004
in Partial Fulfilment of the Requirements for the Degree of
Masters of Science in Civil and Environmental Engineering

ABSTRACT

A low cost, remote monitoring system has been developed to diagnose rail track subgrade failures. The portable monitoring system consists of five liquid vertical settlement probes, one piezometer, a small data acquisition system and laptop, and an Internet communication with remote control capabilities. The probes are designed to be small, easily installed (within railbeds using a one-man auger), easily manufactured, and low cost.

The sensors and data acquisition have been rigorously tested and calibrated in the laboratory. The settlement probes and piezometer are sensitive to changes in the atmospheric pressure and temperature, and calibration curves have been obtained to correct for these effects. The settlement probes are further subjected to silicone oil density changes due to differential temperature between the atmosphere and the ground, and these effects are minimised by a proposed correction method.

The prototype monitoring system was installed through a two phase installation exercise at the bridge approach site in FAST (Facility for Accelerated Service Testing) at Transportation Technology Centre Inc (TTCI), Pueblo, Colorado, USA. Since there are virtually no settlements at the stiff, sandy bridge approach site, the sensors are evaluated for ideal stability and robustness while being subjected to well-defined Heavy Axle Train (HAL) loadings.

A detailed evaluation of the prototype system found that probes installed at depths 1.0 to 1.5m within the subgrade did not achieve satisfactory measurement stability (i.e. measurements have a spurious drift), due principally to manufacturing defects. The prototype probes were sufficiently robust to survive installation within the subgrade but not within the ballast itself. The probe designs have subsequently been refined to eliminate sources of drift, and have undergone more extensive calibration to account for differential temperature effects. These second generation probes are scheduled for field deployment as part of the on-going research

Thesis Supervisor: Dr. John T. Germaine
Title: Doctor of Civil and Environmental Engineering

Thesis Supervisor: Professor Andrew J. Whittle
Title: Professor of Civil and Environmental Engineering

ACKNOWLEDGEMENTS

I would extend my greatest gratitude and appreciation to several people who were involved in the completion of this thesis. They are:

Dr John T. Germaine and Professor Andrew J. Whittle for their invaluable advice, guidance, inspiration and friendship throughout my two years at MIT.

The TTCI (Transportation Technology Centre Inc) for their interest and support in this research project: Dave Davis, Brian Doe, Steve Renshaw and colleagues; Dio Yoshino for spending hours with us in the subzero site and maintaining the monitoring system throughout the testing period

Stephen Rudolph for machining the probes and equipments

Alice Kalemkarian for meeting my constant quest for equipment purchasing, often at a moment's notice

Nabi Kartal Toker, Maria A. Nikolinakou , Pei Jianyong , Anamika Prasad, Jean-Louis S. Loscin and the geotechnical group for the friendship, great company and many spontaneous outings

My parents and my brother for their love, understanding, and unwavering support that provides me with the determination to see this thesis through to a successful completion.

CONTENTS

Abstract ……..3
Acknowledgement……5
Contents……7
List of Figures……10
List of Tables……14

Chapter 1: Introduction 17
1.1 Introduction 17
1.2 Research Objectives 18
1.3 Thesis organisation 18

Chapter 2: Background 21
2.1 Introduction 21
2.2 Subgrade Problems Overview 21
2.3 Factors affecting the subgrade problems 23
2.3.1 Pore ware pressure 23
2.3.2 Water content 23
2.3.3 Imposed Stresses 24
2.3.4 Conclusion 24
2.3.5 Maintenance as a Solution for Subgrade Problems 27
2.3.5.1 Tamping 27
2.3.6 Geosynthetics and other forms of subgrade improvements 29
2.4 Instrumentations overview 32
2.4.1 Piezometer 34
2.4.1.1 Casagrande Porous Tube Piezometer 35
2.4.1.2 Push-in Vibrating Wire Piezometer 37
2.4.1.3 Pneumatic Piezometers 39
2.4.1.4 Hydraulic Piezometer 40
2.4.2 Vertical deformation 41
2.4.2.1 Extensometers 43
2.4.2.2 Inclinometers 43
2.4.2.3 Liquid level gage 45
2.4.2.3.1 Single liquid level gage – both ends on same level 46
2.4.2.3.2 Single liquid level gage – Pressure transducer on one end 47
2.4.2.3.3 Single liquid level gage – Pressure transducer on one end 48
2.4.3 Data Acquisition System 49
2.4.4 Remote Data Communication 50
2.4.4.1 Modem Internet 51
2.4.4.2 Cellular Wireless Internet 52
2.4.4.3 Satellite Internet 52

Chapter 3: Equipment Development 57
3.1 Introduction 57
3.2 The monitoring system 58
3.3 Piezometer Probe 60
3.3.1 Introduction 60
3.3.2 Conceptual design 61
3.3.3 Components of Piezometer 64
3.3.3.1 Body 64
3.3.3.2 Sealing 67
3.3.3.3 Porous Filter 67
3.3.3.4 Data cable and BX cable 67
3.3.3.5 Pressure Transducer 68

3.3.3.6 Thermistor 73
3.3.3.7 Silicone Fluid 74
3.3.3.8 Assembling the electronic components 77
3.3.3.9 Saturation 79
3.4 Liquid vertical settlement probe 80
3.4.1 Introduction 80
3.4.2 Conceptual design and components 82
3.4.2.1 Body 82
3.4.2.2 Sealing 84
3.4.2.3 Tubing 84
3.4.2.4 Cable and BX cable 84
3.4.2.5 Transducer and Thermistor 84
3.4.2.6 Reservoir 87
3.4.2.7 Assembling the electronic components 88
3.4.2.8 Silicone oil 88
3.4.2.9 Saturation of the settlement probe 88
3.4.2.10 Temperature effects 89
3.5 Junction Box 90
3.5.1 Electrical Grounding 91
3.6 Data acquisition system 93
3.7 Remote Control System 96

Chapter 4: Laboratory Testing 99
4.1 Introduction 99
4.1.1 Noise and signal management 99
4.2 Data acquisition 100
4.2.1 Iotech Personal DAQ 55 100
4.2.2 Central Data Acquisition 103
4.3 Motorola MPX pressure transducer 103
4.3.1 Stability 103
4.3.2 Temperature Calibration 106
4.4 Settlement Probe 108
4.4.1 Pressure calibration 108
4.4.2 Temperature Calibration 111
4.4.2.1 Pressure Transducer, Temperature Calibration 111
4.4.2.2 Silicone Oil, Temperature Calibration 113
4.4.3 Noise evaluation 116
4.5 Piezometer 118
4.6 Conclusions 119

Chapter 5: Field Installation 123
5.1 FAST site at TTCI 123
5.1.1 HAL Trains at HTL 123
5.1.2 Weather at TTCI 124
5.2 Monitoring system at TTCI 127
5.2.1 Introduction 127
5.2.2 Aim of the installation 127
5.3 Monitoring System Layout 129
5.4 Installation of the monitoring system 129
5.4.1 Setting up the Data acquisition 129
5.4.2 Field installation of the sensors 131
Saturation of probes 132
5.4.2.1 Installation methods 133
5.4.2.1.1 Excavation from top of ballast 133
5.4.2.1.2 Hand-augering 134
5.4.2.2 Compaction 135

5.4.3 Junction Box 136
5.5 System testing 138

Chapter 6: First Field Test Results 141
6.1 Data collection 141
6.2 Methods of data interpretation 142
6.3 Data interpretation 144
6.3.1 HAL train operation 144
6.3.2 Performance of the prototype probes 144
6.3.2.1 Reservoir Transducer 145
6.3.2.2 Piezometer (PZT-P) 147
6.3.2.3 Settlement Probe 1 and 3 147
6.3.2.4 Settlement Probe 2 157
6.3.2.5 Settlement Probe 4 158
6.3.2.6 Settlement Probe 5 160
6.3.2.7 Remarks about P2, P4 and P5 162

Chapter 7: Conclusions 167
7.1 Instrumentation 167
7.1.1 The monitoring system 167
7.1.2 Design and fabrication of sensors 168
7.1.3 Laboratory Testing 168
7.1.4 Installation process 169
7.1.5 Field Data Interpretation and Discussions 169
7.2 Recommendations for future research 170

Chapter 8: References 175

LIST OF FIGURES

Figure 2.1: Progressive shear failure (LI 2000a) 22
Figure 2.2: (LI 2000) Typical settlement profile of soft subgrade section at TTCI 22
Figure 2.3: Distorted columns indicating progressive shear failure. (SELIG & WATERS 1994) 25
Figure 2.4: SELIG & WATERS (1994): Rehabilitation of the ballast using tamping machine 27
Figure 2.5: SELIG & WATERS (1994): Effect of progressive fouling on length of tamping cycle 28
Figure 2.6: LI (2000) Settlement and tamping operation under the standard 0.46m (18") granular ballast. (Arrow indicating surfacing and tamping maintenance) ... 29
Figure 2.7: Schematic of open standpipe piezometer installed in a borehole (DUNNICLIFF 1998). 36
Figure 2.8: (Slope Indicator) Small push in vibrating wire piezometers 37
Figure 2.9: DUNNICLIFF (1988). Principle of the vibrating wire..... 38
Figure 2.10: (DUNNICLIFF 1988): Pneumatic Piezometers, read under a condition of no gas flow 39
Figure 2.11: (DUNNICLIFF 1988) Schematic of twin-tube hydraulic piezometer installed in fill 40
Figure 2.12: (HANNA 1985) Types of hydraulic piezometers in boreholes..... 40
Figure 2.13: Principle of horizontal in-placed inclinometer operation..... 44
Figure 2.14: Casing..... 44
Figure 2.15: Inclinometer (Courtesy of Slope Indicator, Inc, USA)..... 44
Figure 2.16: Installation of a horizontal inclinometer 45
Figure 2.17: (DUNNICLIFF 1988). Schematic of single liquid level overflow gage with both ends at the same elevation..... 46
Figure 2.18: (DUNNICLIFF 1988) Schematic of liquid level gage with pressure transducer 47
Figure 2.19: Multipoint gage for vertical settlement (Geokon, Inc., Lebanon, NH)..... 48
Figure 2.20: Standalone data logger (Iotech Logbook 360)..... 49
Figure 2.21: Laptop based data acquisition (Iotech DAQ 55) 50
Figure 2.22: Satellite Internet communication infrastructure (courtesy of Tachyon). 52
Figure 2.23: Schematic diagram showing possible communication methods between the remote system and host system at MIT..... 54
Figure 3.1: The prototype monitoring system consisting of one piezometer and five settlement probes. 59
Figure 3.2: Piezometer..... 60
Figure 3.3: Pore pressure measurement 61
Figure 3.4: Pore pressure response of partially saturated piezocone to step pressure using water as the medium of pressure transfer (Rad & Tumay 1985). 62
Figure 3.5: Design of the piezometer probe..... 63
Figure 3.6: Component i..... 64
Figure 3.7: 64
Figure 3.8: From the bottom: Component ii, iii and v. 65
Figure 3.9: Component vi)..... 66
Figure 3.10: Component vii) BX gripper..... 66
Figure 3.11: Fluid path and sealing of the piezometer 67
Figure 3.12: Temperature Stability Omega PX-26 gage pressure transducer. 70

Figure 3.13: a) and b) shows the main schematic diagram of the Omega PX-26 transducer, without the outer shell.....70
Figure 3.14: Motorola MPX2200A and MPX2100A pressure transducers. (Courtesy of Motorola) 71
Figure 3.15: Omega 44005 thermistor 73
Figure 3.16: Schematic diagram of Thermistor configuration. 73
Figure 3.17: Variation of voltage (mV/V) output across the Wheatstone bridge versus the change in temperature.....74
Figure 3.18: Molecular structure of polydimethylsiloxane silicone oil.....75
Figure 3.19: Density vs. Temperature graph for 20cSt silicone oil.....76
Figure 3.20: Transducer, Thermistor and Wheatstone bridge configuration.....77
Figure 3.21: Epoxying the transducer element 78
Figure 3.22: Saturating the piezometer.....79
Figure 3.23: Liquid settlement probe.....80
Figure 3.24: Design of Settlement Probe (to scale) 81
Figure 3.25: Component i: Conical head.....82
Figure 3.26: Component ii.....82
Figure 3.27: Left (component iv) and right (component iii).....83
Figure 3.28: Component v.....83
Figure 3.29: Component vi: BX gripper.....83
Figure 3.30: Quick connect mechanism for the reservoir.....87
Figure 3.31: Assembling the electronic components for settlement probe 88
Figure 3.32: Variation of ground and atmospheric temperature with time (from TTCI field data) 90
Figure 3.33: Schematic of the electrical grounding. 91
Figure 3.34: Schematic of the wire connection in the junction box 92
Figure 3.35: Iotech Personal DAQ 55 connected to the expansion module (Courtesy of Iotech, DAQ 55).....93
Figure 3.36: More PDQs can be connected to a USB hub, thus increasing the data acquisition capacity of the system. (Courtesy of Iotech, DAQ 55).....94
Figure 4.1: Automatic calibration for the DAQ 55.....101
Figure 4.2: Laboratory Stability of DAQ 55 at 24^0C.....102
Figure 4.3: Influence of temperature on the stability of the IOTECH DAQ 55.....102
Figure 4.4: Configuration of stability and temperature testing for MPX series transducers 103
Figure 4.5: Stability of the pressure transducers in mV/V 104
Figure 4.6: Stability of three different pressure transducers (two MPX2200A and one MPX2100A) 105
Figure 4.7: Absolute stability of the transducers (normalised by MPX2200A (2)).....106
Figure 4.8: Effect of temperature on the MPX2100A 107
Figure 4.9: Temperature Calibration for MPX2100A (exposed to air) 108
Figure 4.10: Calibration process 109
Figure 4.11: Calibration of the settlement probes (including silicone oil) 110
Figure 4.12: Calibration of the settlement probes (matching at the origin).....111
Figure 4.13: Temperature calibration equipment set up for the settlement probes.....112
Figure 4.14: Temperature Calibration for P3, P4, P5 and RES 113
Figure 4.15: Profile of density changes between the ground and atmospheric temperature 114
Figure 4.16: Principle of variable model temperature-density correction 115
Figure 4.17: Influence of the differential temperature on the density changes of the silicone oil (with ground temperature set at 10°C).....116

Figure 4.18: Stability of settlement cell transducers at constant temperature 24°C. 117
Figure 4.19: Absolute Stability of probe (no atmospheric pressure influence) 118
Figure 5.1: Map of TTCI in Pueblo, Colorado 123
Figure 5.2: FAST section and the bridge approach 123
Figure 5.3: HAL main engine. 124
Figure 5.4: 320 tonnes cargo carriage. 124
Figure 5.5: Typical daily atmospheric temperature in Pueblo, Colorado at various times of the year (Weather Underground)..... 125
Figure 5.6: Typical daily atmospheric pressure in Pueblo, Colorado at various times of the year (Weather Underground)..... 125
Figure 5.7: Typical hot and dry climate at TTCI and Colorado where temperatures could soar up to 50°C and rain is few and far between..... 126
Figure 5.8: Colorado is not all hot and dry. With temperatures dipping subzero during winter, it is vital that the monitoring system is able to perform in all weather conditions. 126
Figure 5.9: Location and layout of the monitoring system at TTCI..... 128
Figure 5.10: Layout of the data acquisition trailer on the site..... 129
Figure 5.11: Layout of the system in the trailer 130
Figure 5.12: Digital surveillance camera 130
Figure 5.13: Location of the sensors installed in the subgrade..... 132
Figure 5.14: Saturating the piezometer..... 132
Figure 5.15: Field Saturation of the settlement probes. 133
Figure 5.16: Excavating the top of the ballast by shovel. 134
Figure 5.17: Installing settlement probe 2 from the top of ballast 134
Figure 5.18: Excavation of the rail ballast using a front-end-loader 134
Figure 5.19: The augered hole is back-filled with sand. 135
Figure 5.20: Hand installation of the probe in the augered hole using a rod. 135
Figure 5.21: Compaction process of the ballast after installation of the probe. 135
Figure 5.22: Picture of the sensors after the installation is completed. The BX cables runs out from the side of the ballast. 136
Figure 5.23: Junction box and lightning protection rod. 137
Figure 5.24 Junction box installed at the bridge. 137
Figure 5.25: Reservoir for the settlement probe..... 137
Figure 6.1 : a) Comparison between the reservoir pressure transducer (RES-P) and the atmospheric pressure (from weather station), and b) comparison between the reservoir thermistor and the atmospheric temperature for the period 18 April – 12 May 2003..... 146
Figure 6.2: Comparison between density-corrected P3-P (for silicone oil in the tubing) and no density correction. 148
Figure 6.3: Absolute stability of settlement probe 1, 3, and piezometer (18 April – 12 May 2003)..... 150
Figure 6.4: Stability of settlement probe 1, 3, and piezometer (18 April – 12 May 2003) 151
Figure 6.5: Temperature readings for settlement probe 1, 3, piezometer and reservoir thermistor (18 April – 12 May 2003) 152
Figure 6.6: a) Stability and b) Absolute stability of sensors between 18 – 24 April 2003 153
Figure 6.7: a) Stability and b) Absolute stability of sensors between 25 - 30 April 2003 154
Figure 6.8: a) Stability and b) Absolute stability of sensors between 30 April – 6 May 2003..... 155

Figure 6.9: a) Stability and b) Absolute stability of sensors between 6 – 12 May 2003 ..... ……..156
Figure 6.10: Stability of P2 during the laboratory temperature calibration testing (compare with P3) 157
Figure 6.11: Stability of P2 after field installation. 157
Figure 6.12: Performance of P4: First phase (16 to 20 Jan 2003) 158
Figure 6.13: Performance of P4: Second phase (26 – 30 May 2003) 159
Figure 6.14: P5 clipped on the rail tie. 160
Figure 6.15: Performance of P5 (at rail tie) after first installation phase (16 – 20 Jan 03) 161
Figure 6.16: Performance of P5 three months after installation (18-23 April 03.) 161
Figure 6.17: Performance of thermistor in P5 (18-23 April 03). 162
Figure 7.1: Remote monitoring system package of the future. 171

LIST OF TABLES

Table 2.1: (adapted from LI & SELIG 1995). Major subgrade problems and features. 26
Table 2.2: Types of geosynthetic and functions (SELIG & WATERS 1994) 31
Table 2.3: Categories of Instruments for Measuring Deformation (DUNNICLIFF 1988) 42
Table 3.1: Manufacturer Specification for MPX2200A (Motorola). 72
Table 3.2: Solubility of gasses in silicone oil. 76
Table 3.3: Manufacturer Specification for MPX2100A (Motorola). 86
Table 3.4: Sampling integration rate and resolution. (modified from Iotech) 95
Table 3.5: Iotech recommendation of the inherent system noise in DAQ 55. 95
Table 4.1: Noise characterisation in the measuring system. 100
Table 4.2: Resolution and stability of settlement probe and piezometers 119
Table 5.1: Location of the sensors installed at TTCI 131
Table 6.1: Data collection at TTCI 141
Table 6.2: Prototype I System Performance 142
Table 6.3: Calibration and corrections for the sensors 143
Table 6.4: Performance of settlement probe P2, P4, and P5, before and after installation. 162
Table 7.1: Performance of the sensors. 170


Introduction

Chapter 1: Introduction

1.1 Introduction

The demand for more cost efficient railroad cargo deliveries has led to use of increasingly heavier trains, termed Heavy Axle Load (HAL) vehicles. The HAL cargo trains (36 to 38T/axle) are typically five times the weight and three times the length of a normal passenger train. Unfortunately, there are many locations where rail track beds are not suitable for handling this change in loading conditions, leading to excessive track settlements, particularly in areas of weak subgrade (manifested by low track modulus). Settlements as high as 5 to 8 cm have occurred (Li 2000) and cause difficulties in maintaining track alignment. Track failure will occur if the problematic site is left untreated.

Differential settlements have been observed to occur at some bridge approaches, resulting in introduction of speed restrictions at the bridge approach and more frequent track maintenance (10 MGT (Mega Gross Ton) at 3 to 5 months intervals). Track maintenance, consists mainly of rail tamping, is costly, usually ineffective and does not address the fundamental cause of the problem. Similarly, various subgrade improvement methods such as Hot Mix Asphalt (HMA) and geo-synthetic membrane (Geoweb) are expensive and not always effective in reducing the differential settlements (Li 2002).

The current efforts made to understand subgrade failure mechanisms have been mostly limited to theoretical predictions and laboratory experiments. There is a lack of reliable field measurements necessary to diagnose the underlying causes of track settlements and failure mechanisms. There are too main challenges in monitoring rail bed subgrade problems: a) the remoteness of the problematic sites, and b) the lack of robust instrumentation. Electronic and remote instrumentation are gaining popularity in other fields of geotechnical engineering, notably in large deep excavation projects and embankments. And it is timely that remote instrumentation should be encouraged in the railway geotechnical monitoring realm.

1.2 Research Objectives

This research is funded by the American Association of Railroads (AAR) in an effort to understand mechanisms controlling subgrade failures and to promote the usage of subgrade monitoring system in railroad engineering. The aim of this thesis is to:

1. Develop a modular, low-cost, expendable, and robust remote monitoring system aimed at characterising railway subgrade failures. In this first phase of development, a prototype monitoring system has been developed with capabilities for measuring vertical deformation and pore water pressures. The analogue signals from these sensors are processed by an on-site data acquisition system and the digital data are transmitted remotely, with real time options, via the Internet for further analyses.

2. Evaluate monitoring system at an artificial bridge approach site on the FAST loop (Facility for Accelerated Service Testing) at TTCI (Transportation Technology Centre Inc) in Pueblo, Colorado, USA. This special track loop was designed for testing HAL trains. The HAL trains are in operation throughout the monitoring period, replicating real site loading conditions.

3. Evaluate the performance and long-term stability of the prototype monitoring system, identify deficiencies in the hardware and software, and recommend further system development and refinement. This work is being carried out as part of the on-going research project.

1.3 Thesis organisation

This thesis is organised into 7 chapters, with the first being the Introduction. Chapter 2 provides detailed background information on the subgrade problems and an overview of the pore pressure and vertical deformation instrumentation used in subgrade monitoring. The design, fabrication and set up of the monitoring system are presented in Chapter 3. The electronic sensors are laboratory calibrated (Chapter 4) before the site installation at TTCI (Chapter 5). The field performance of the monitoring system is analysed in Chapter 6, with conclusions and recommendations in Chapter 7.


II
Background

Chapter 2: Background

2.1 Introduction

There is a current trend towards using heavier cargo trains on existing trackbeds in order to reduce operating cost and increase competitiveness in the rail freight market. These heavy-haul trains, better known as the Heavy Axle Load (HAL) trains, normally weigh about 25 T/axle to 30 T/axle (there are efforts of pushing above the limit of 38 T/axle) with length of up to 70 cars. By packing more cargos on a single journey, the economics of reducing shipping costs is clearly attractive. However, it comes with another cost – HAL vehicles may cause more severe rail defects and subgrade failure problems. Even on stable subgrade, increasing the axle load by 20% (25 T/axle to 30 T/axle) and train length by 50% accelerates the deterioration of the track and increases the total track maintenance cost by 3% (NIELSON & STENSSON 1999). The track maintenance cost would be substantially higher in areas where there are pervasive track failures[1] due to soft subgrade conditions.

2.2 Subgrade Problems Overview

The usage of HAL vehicles increases the stresses in the subgrade, and has caused large settlement of tracks in areas of soft subgrade (manifested by low track modulus) and bridge approaches. The soft subgrades generally consist of fine-grained materials such as silts, clays and organic soils. In some severe site cases, the track deteriorates to unsafe conditions within 20 to 30 MGT[2] before the maintenance program is required (READ and LI 1995). However, the importance of the subgrade failure is very often being overlooked during the design and maintenance phase, where greater emphases are being placed in designing and maintaining the ballast, sleepers and rail components.

[1] Defined as track settlement of

[2] It is often convenient to express loading in terms of million gross ton (MGT), which refers to cumulative axle loading. A typical HAL train of 38 T/axle, 4 axles per carriage, and 76 carriages per train may clock up to 0.011 MGT per crossing (as opposed to 0.0008 MGT for a typical passenger train)

Table 2.1 presents 11 common types of subgrade failures, their causes and features. Two subgrade failures which are of particular interest in this research are progressive shear failures and the bridge approach settlements.

The progressive shear failure is a type of surface failure where cyclical loading produces large plastic deformations on the soft subgrade, leading to excessive settlement of the ballast and rail (*Figure 2.1* and *Figure 2.3*). Previous measurements at the soft subgrade section at TTCI suggested that settlements and heave up to 8cm and 10cm in the rail and the shoulder can occur (LI, 1994). SELIG & WATERS (1994) and LI *et al.* (1998a, 1998b) provide further discussions on the progressive shear failure.

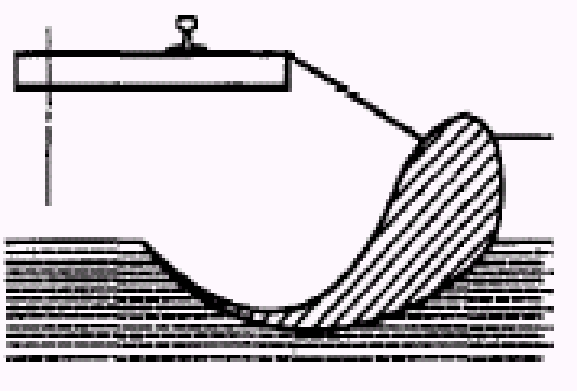

Figure 2.1: Progressive shear failure (Li 2000a)

Another pervasive subgrade failure is the bridge approach problem where significant settlement occurs typically at a half carriage length from a stiff bridge abutment. Little is known about the cause of the settlement.

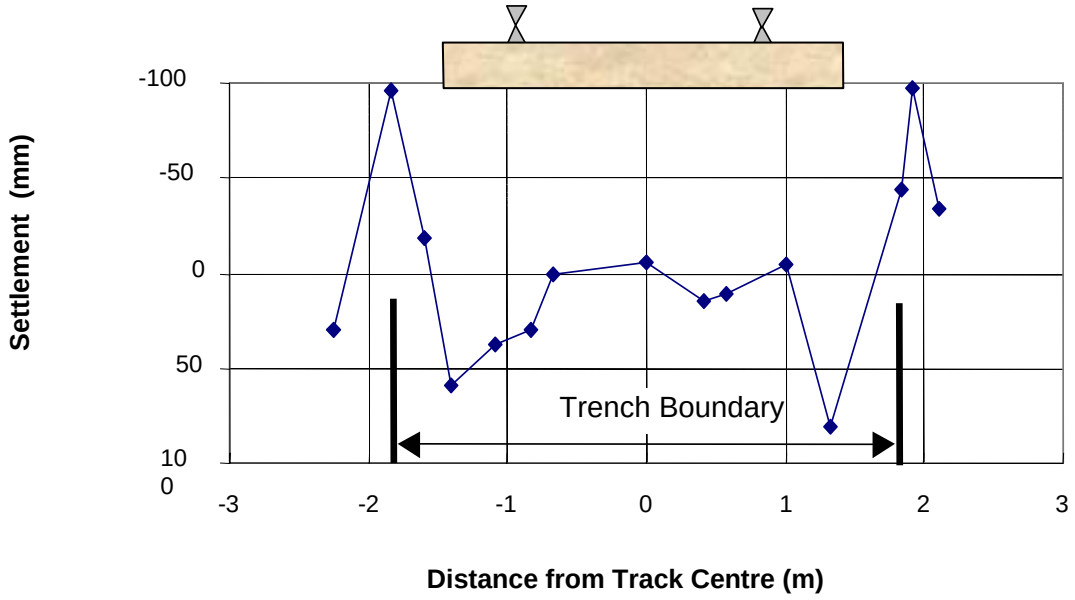

Figure 2.2: (LI 2000) Typical settlement profile of soft subgrade section at TTCI

Rail tracks are generally intolerant to vertical and differential settlements before being rendered unsafe of usage. *Figure 2.2* shows a settlement profile under a rail tie subjected to cyclical loading (LI 2000). Settlements up to 5cm occur under the rail tie and heaves of up to 10cm have been recorded at distance of 2m from the centre of the rail. This is a typical soft subgrade progressive failure, with the soil being pushed outwards and upwards from the side of the rail

2.3 Factors affecting the subgrade problems

The underlying mechanics behind these failures are still poorly understood. In recent years, extensive laboratory research has been performed to characterise and address the issue of the progressive failure. The following are some of the critical parameters involved in causing subgrade failures:

2.3.1 Pore water pressure

Pore water pressure affects the effective stresses in the subgrade; increase in pore water pressure results in decrease of effective stress and reduce the factor of safety in the subgrade (especially in low permeability fine-grained subgrades where excess pore pressure dissipation is slow). Experimental results have shown that pore water pressure increases with cyclical loading for both normally consolidated and over[3] consolidated soils (ANDERSEN *et al*. 1976, MITCHELL and KING 1977, MATSUI *et al*. 1980). At some areas with poor drainage system, development of excess pore pressure as a result of cyclical loading has led to pumping of fines[4] (ALOBAIDI & DAVID 1996)

2.3.2 Water content

Subgrade water content influences the subgrade resilient modulus[5]; a small increase in the water content may result in substantial decrease in the subgrade resilient modulus (e.g. 27.1% to 30.1% increase in water content reduces subgrade resilient

[3] Excess pore water pressure decreases at initial load cycles due to the dilative behaviour of over consolidated soils, but increases again after a certain number of loading cycles
[4] Migration of fines from the subgrade to the ballast (or subgrade layer)
[5] Effective “stiffness” of the subgrade. Smaller the resilient modulus, bigger the deformation of the subgrade

modulus from 130 to 70 MPa (DRUMM *et al*. 1997)), and has been confirmed by field measurements (LI 1996).

2.3.3 Imposed Stresses

The rail loading stress is normally included under the deviator stress ($\sigma_d = \sigma_1 - \sigma_3$). Increase in deviator stress (heavier HAL trains) will lead to an increase in plastic strain and hence vertical deformation. There exist critical deviator stress states which, once surpassed, will result in exponential increase of plastic straining with cyclic loading (LAREW & LEONARDS 1962; LI 1996). It is, therefore, important to ensure that the cyclical stresses in the subgrade do not exceed the critical values (either by limiting the imposed train loads, using thicker ballast layer to redistribute the stresses, and etc)

2.3.4 Conclusion

In recent years, extensive laboratory research has been performed to characterise and address the issue of subgrade failures. However there is still a general lack of reliable field data (such as pore pressure, stresses and ground movement) available in order to properly understand and characterize the subgrade failures. One of the possible reasons is the lack of suitable monitoring system tailored to the subgrade environment monitoring (and meeting the demands of heavy train loadings), the relatively high cost of remote site monitoring, high cost of power supply, personnel and means of data transmission. Therefore, there is a strong demand for instrumentation to obtain field measurements of the pore water pressure, deformation and soil stresses for the reasons mentioned above.

Figure 2.3: Distorted columns indicating progressive shear failure. (SELIG & WATERS 1994)

Table 2.1: (adapted from LI & SELIG 1995). Major subgrade problems and features.

Type	Causes	Features
Progressive Shear Failure	– repeated over-stressing – fine-grained soils – high water content	– squeezing near subgrade surface – heaves in crib and shoulder – depression under ties
Bridge Approach	– repeated loading – differential stiffness between the bridge and the soft subgrade	– depression of the ballast and subgrade at distance about one half carriage from the abutment of the bridge
Excessive plastic deformation (ballast pocket)	– repeated loading – soft or loose soils	– differential subgrade settlement – ballast pockets
Subgrade attrition and mud pumping	– repeated loading of subgrade by ballast – contact between ballast and subgrade – clay rich rocks or soils	– muddy ballast – inadequate subballast
Liquefaction	– repeated loading – saturated silt and fine sand	– large displacement – more severe with vibration
Massive shear failure (slope stability)	– soil and train weight – inadequate soil strength	– high embankment and cut slope – often triggered by increase in water content
Consolidation settlement	– soil weight – saturated fine-grained soils	– increased static soil stress as from newly constructed embankment
Frost action (heave and softening)	– periodic freezing temperature – free water – frost susceptible soils	– occur in winter/spring period – rough track surface
Swelling/Shrinkage	– highly plastic soils – changing moisture content	– rough track surface
Slope erosion	– running surface and subsurface water – wind	– soil washed or blown away
Soil collapse	– water inundation of loose soil deposits	– ground settlement

2.3.5 Maintenance as a Solution for Subgrade Problems

Maintenance programs, such as tamping, are commonly used to revitalise sections of track which have undergone substantial deterioration. Tamping programs are costly and are not always effective in solving foundation problems especially those related to underlying subgrade. In cases where maintenance tamping has proven to be ineffective, various sophisticated and more expensive solutions such as Geoweb confinements (Geogrid), Hot-Mix Asphalts underlay (HMA), and soil improvement methods (e.g.. lime stabilization) have been used with varying degrees of success. These methods are briefly described in the following paragraphs.

2.3.5.1 Tamping

Rail tamping machines are used to repack ballast below the ties and elevate the track to a specified vertical alignment. The rails and the ties are lifted to the desired level, and tamping tools are used to sweep the ballast back under the voids in the ties as shown in *Figure 2.4.* The ballast is then compacted by vibrating the tamping tools in the ballast. Additional gravel may be added to restore the ballast to its original existing level. This is known as the start of the serviceability cycle, which will end when the track settles above a predetermined level.

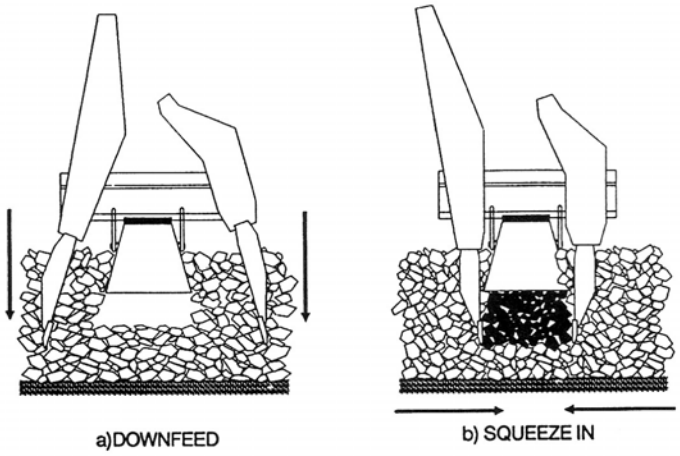

Figure 2.4: SELIG & WATERS (1994): Rehabilitation of the ballast using tamping machine

Tamping track maintenance is never a sustainable exercise, with the serviceability life cycle decaying exponentially with subsequent tamping. *Figure 2.5* presents the effect of subsequent tamping on the tamping cycle of the track (SELIG & WATERS 1994). The physical mechanics of the operation are as follows: a) the track settles with increasing cumulative traffic and is restored to the original height by tamping; b) with subsequent loading and tamping operation, the stiffness of the track decreases, causing bigger settlement with a shorter serviceability life; and c) the tamping cycle will continue to shorten until it is no longer feasible to keep up with the tamping process and complete reconstruction of the rail track has to be performed. *Figure 2.6* further shows typical field measurements of a tamping service cycle. The first two tamping cycles progressively reduces from 12 MGT to 9 MGT, and towards the end of the test, tamping needs to be performed at every 1 MGT.

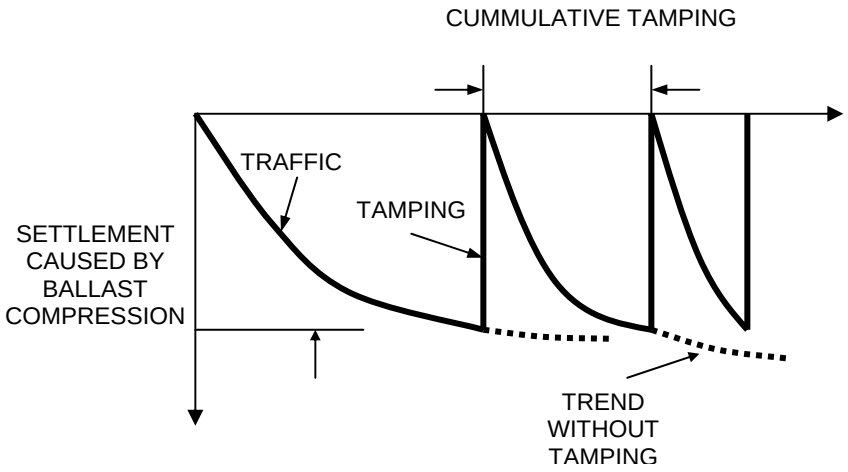

Figure 2.5: SELIG & WATERS (1994): Effect of progressive fouling on length of tamping cycle

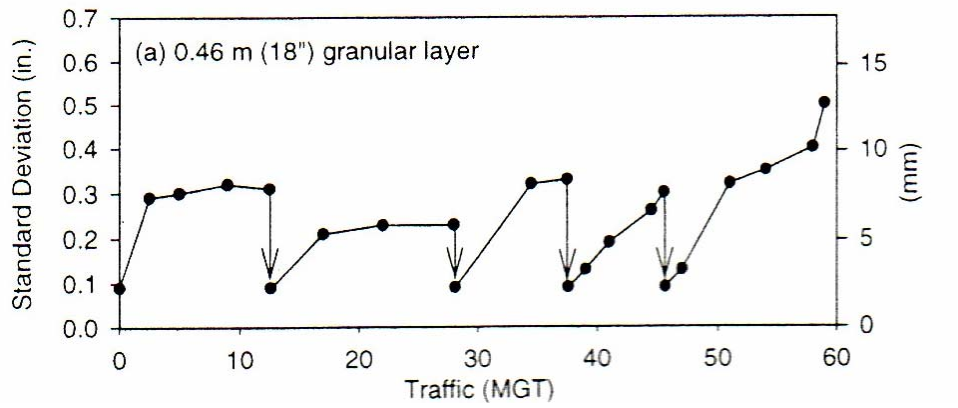

Figure 2.6: LI (2000) Settlement and tamping operation under the standard 0.46m (18") granular ballast. (Arrow indicating surfacing and tamping maintenance)

One of the possible reasons behind the ineffective tamping procedure is the tamping maintenance is aimed at restoring the ballast and not the subgrade where problems may originate (see *Table 2.1*). The ballast acts as a stress distributor where train loadings are better distributed over a larger area of the subgrade. By restoring the ballast to its original thickness, the subgrade is temporarily relieved of concentrated train loadings. However, soft subgrade will continue to undergo large displacements and leading to deterioration of track capacity (SELIG & WATERS 1994). Therefore, in soft subgrade, tamping may not be the best solution to effectively tackle the subgrade failure.

2.3.6 Geosynthetics and other forms of subgrade improvements

Geosynthetics, Hot Mixed Asphalt (HMA), add-mixture stabilisation (cement, lime, fly ash) are sophisticated and expensive methods aimed at improving the performance of the subgrade. Generally, there are two methodologies employed by these methods to increase the life-span of the subgrade:

a) Deviator stress reduction: A layer of stiff load bearing structure can be placed between the ballast and the subgrade to reduce the transmission of the train loading onto the subgrade (redistribution of contact stresses). Various geosynthetics such as geotextiles, geomembranes, geogrids etc and HMA increases the stiffness of the low track modulus and distribute the imposed stress over a larger area of subgrade.

b) Reinforcement by providing tensional strength – Geosynthetics can provide additional tensile strength into the subgrade, very much akin to the tensile

reinforcement bars in concrete beams. Admixture stabilisation methods, on the other hand, increase the overall stiffness and shear strength of the subgrade.

In rail road engineering, geosynthetics are one of the more common subgrade improvement methods and have been used since the early 1970s in North America (FLUET 1986), Germany (MARTINEK 1986) and in Britain (AYRES 1986). Geosynthetics are polymeric products and have four main functions in civil engineering (WHITTLE & LING 2002), and is summarised in *Table 2.2*: Further to the two general methodologies described above, the function of geosynthetics can be further characterised as follows:

Separation

Geosynthetics is used to separate layers of soil (e.g. clay subgrade from the overlying gravel ballast). The layer of geosynthetics prevents intrusion of the aggregate (from the ballast) into soft subgrade, and prevents upward pumping of the fine particles into the ballast which will reduce the drainage and shear strength at the base of the aggregate/ballast.

Reinforcement

Geotextiles and geogrids can be used to reinforce soil masses and finds applications in embankments and retaining walls. The geotextile is laid horizontally within the soil masses and the lateral spreading (straining) of the soil mass (due to self weight, and loads) is resisted by shearing along the soil-geosynthetic interface and the development of tensile stresses with in the reinforcing layers. In the railroad application, the geotextiles are normally placed at the ballast-subgrade interface, where wheel-loading (generating high local stress concentration) are resisted by the geotextiles and redistributed over wider area on the underlying subgrade, thus reducing stress concentration.

Filtration

For areas where build-up of water could be a problem, suitable drainage system have to be provided. However, most sub-surface drainage systems are susceptible to infiltration by fine soil particles, resulting in drain blockage and waterlogged subgrade (which will weakened the subgrade). Geotextiles (with high permeability) offers a cost effective filter wrappings (in comparison with the more expensive graded filter) to the

drainage pipes to prevent infiltration of fine soil particles. This application has been used in Germany with some success (MARTINEK 1986). Nevertheless, clogging of the geotextiles may occur and site specific tests have to be performed.

Containment

Polymeric geomembranes can be manufactured to have very low hydraulic conductivities (1 x 10^{-12} to 1 x 10^{-15} m /sec) and are used as hydraulic barriers in landfills to prevent escape of leachate or infiltration of rainwater. This application is more suitable for landfills rather than the trackbed.

Table 2.2: Types of geosynthetic and functions (SELIG & WATERS 1994)

Type	Functions
GEOTEXTILES Woven Non Woven	Separation Filtration Reinforcement
GEOMEMBRANES	Separation Reinforcement
GEOGRIDS	Reinforcement
GEONETS	Transmission
GEOWEBS	Reinforcement
GEOCOMPOSITES	Combinations

Geosynthetics are, unfortunately, susceptible to high abrasion, elongation, and areas of high stress concentrations. The trackbed provides a hostile working condition for the geosynthetics (due to sharp ballast aggregates and high loading stresses) and many of the geosynthetics installed in North America (during the early 1970s) have failed due to inadequate strength design and drainage problems (RAYMOND 1999)[6].

In general, these techniques are costly to implement, requires great expertise, and even so, work only for certain subgrade problems (and not a general solution for all subgrade problems). Effective use of the geosynthetics and other forms of subgrade improvement can only be achieved through fundamental understanding of the site specific failure mechanism, achieved through good site monitoring.

[6] Investigations and visual examinations of exhumed geosynthetics retrieved from various sites in North America and Canada were presented by Raymond. Design recommendations for geosynthetic were also suggested.

2.4 Instrumentations overview

Instrumentation plays an important role in engineering, as it provides the necessary parameters needed to analyse the performance of a structure during construction and serviceability life. Traditionally, field monitoring used in geotechnical engineering practice are based on hydraulic or mechanical operation of instruments, which are labour intensive (i.e. personnel are needed on-site to obtain and record readings). These instruments generally are reliable and have long-term accuracy, but the absence of automatic measuring capabilities meant that they could not be used for stand-alone remote monitoring. Recent advances in electronics provide the capability for automated data collection, thus paving the way for remote site monitoring without the presence of personnel. Data collected in remote site can be transferred to the central command area through various communication methods. Cellular wireless Internet (provided by giant telecommunication companies such as AT&T, Verizon and etc.) are cost effective and provide rather good coverage around populated areas throughout the United States. Satellite Internet (provided by Starband, Pegasus and etc.) provides complete coverage of the United States and can be used in most remote sites.

Remote monitoring systems have been used in monitoring earth dams and embankments (MÖLLER & LÖFROTH 1999), and concrete faced rockfill dam (POTCHANA *et al*. 1999). These systems are capable of measuring large deformation (settlement) in dams and embankments, and can be interfaced with automatic alarm to sound when the movements reach critical levels. Nevertheless, electronic devices have their limitations, including questionable long-term accuracy, and increased cost as compared the hydraulic or mechanical sensors. Currently, electronic instruments are extensively used in embankments, tunnelling, slope stability and deep excavations. Companies such as Slope Indicator, Geokon, and Roctest produce electronic instruments such as inclinometers, piezometers and extensometer for that purpose. Nevertheless, extensive subgrade monitoring is relatively new and the lack of available commercial products reflects this situation. Often, instrumentation designed for other applications (which are normally unsuitable) are being used for subgrade monitoring. The ideal instrumentation system suitable for railroad applications are summarised below:

a) Remote operation – The instrumentation system should be completely self-sufficient, able to generate its own power and capable of automatically collecting data,

processing and relay it back to the main computer at the main office. The main computer should be able to interact and control the remote on-site terminal.

b) Easy installation – These sensors will be installed below running track with minimal traffic disruption, or usage of heavy machinery. The sensors should be easily installed limited manpower or interference with the rail bed.

c) Low cost – Automated sensors are more expensive than manual sensors. Since problematic sites can stretch for miles, extensive monitoring systems could become expensive very quickly. It is therefore important to keep the unit cost of sensors to enable more extensive monitoring networks.

d) Modular – The system should be adaptable for different applications and different subgrade conditions. The system should be able to accommodate a variety of sensors necessary to characterise the subgrade.

A typical remote monitoring system consists of the following components; a) sensors, b) on-site data acquisition, c) power supply, d) host computer (computer in the main headquarters), and e) communication between the host computer and the on-site data acquisition. The electronic sensors are instruments which convert certain measurements (e.g. pressure, deformation) into electrical signals (e.g. voltages or frequencies). These electrical signals will be converted into digital format understood by computers by the data acquisition system. These data will have to be transmitted back to the host computer by some means of communication (e.g. Internet).

In this master's thesis, a prototype monitoring system is developed comprises of pore pressure and vertical deformation sensors. The following sections review existing methods for monitoring pore pressures and settlements.

2.4.1 Piezometer

Piezometers are sensors that are capable of measuring the fluid pressure in the ground independently from the stresses in the soil skeleton. Piezometers are widely used in geotechnical engineering for measuring pore pressure, determining ground water level and rate of groundwater flow. The simplest form of a piezometer consists of a porous element and a pressure-measuring device embedded into the ground. The porous element is permeable only to the groundwater, enabling pressure transfer from the external groundwater to the inner measuring device while separating the soil stresses.

The pore water pressure exists in two states: positive or negative pressure. Under fully saturated condition, the groundwater is likely to exist under positive pressure when subjected to loading from the trains. However, most railway subgrades lie above the water table, resulting in a partially saturated state. Water levels above the natural groundwater level are maintained by capillary action and exist under negative pore pressure, leading to matrix suction[7]. The state of the pore pressure is particularly important as it affects the design of a piezometer - a poorly designed piezometer may be drained as a result of matrix suction. Existence of partially saturated soils is common in some geotechnical applications, in particular embankment and road pavement engineering where the structures are built above the water table. Special piezometers, known as high air entry piezometers, are used in applications where high matrix suction could pose a problem. The design of high air entry piezometers lies in the selection of the porous stone. Air entry is defined as the critical pressure needed for the air on one side of the porous filter to penetrate the capillary tension of the fluid in the largest continuous pore, thus forcing out the fluid from the porous filter. Therefore, pores in the porous stone must be sufficiently small to enable better capillary pressure developing between the fluid and the pores. Pores of diameter in the range of 0.002 to 0.0005mm may withstand theoretical air entry from 100 up to 600 kN/m^2 (HANNA 1985). In contrast, low air entry piezometers, designed for positive pore pressure (and low negative pore pressure), may have pores of 0.05mm.

The design of commercial piezometers widely differs according to the type of applications. DUNNICLIFF (1988) and HANNA (1985) provide extensive coverage of the

[7] The negative pore pressure causes negative pressure (below the atmospheric pressure) in the subgrade. This negative pore pressure, while detrimental to the piezometer (sucking out the inner fluid), is in fact beneficial to the subgrade as it increases the effective subgrade stresses, leading to more stable subgrades.

existing commercial piezometers. Piezometers, in general, can be categorised according to:

a) Type of installation – borehole installation (traditional Casagrande type), borehole installation (grouting), push-in, etc.
b) High air entry vs. low air entry
c) Type of measurement reading – rising head, pneumatic, vibrating wire, pressure transducer, hydraulic, manometer (which may be manual or automatic reading)

Railroad applications demands special design considerations listed below:

a) Low cost, expendable and easily manufactured. Problem sites requiring monitoring may extend for miles and the sensors installed are not easily retrievable due to heavy ground compaction.
b) Automatic and remote operation ability for remote site applications.
c) Robust, reliable and good long term stability. Typical duration of monitoring varies between a few months to a few years. The piezometer will be subjected to frequent heavy train loadings and disturbance from track maintenance vehicles.
d) Easy installation requiring limited manpower with minimal interference with the roadbed[8].
e) The piezometer should be able to record both positive and negative pore pressure.

2.4.1.1 Casagrande Porous Tube Piezometer

The Casagrande Porous Tube Piezometer, also known as the open standpipe piezometer, is one of the earliest piezometer designed and is still widely used (*Figure 2.7*). A small diameter riser pipe is installed in a borehole. The open tip of the piezometer (filter) is covered by porous sand to facilitate the ease of water flow into the filter. Point measurement in the ground can be made by sealing the top region of the open tip with bentonite seal to isolate the measurement region. The water pressure is measured by using either the water-level indicator probe that is lowered into the borehole, or an in-place pressure transducer. The latter method of measurement is favoured for remote monitoring system, as automatic readings can be obtained. However, there are many disadvantages of the standpipe piezometer which render it unsuitable for railroad application:

[8] Roadbed is defined as the rail and the supporting rail ties, etc

a) Limited installation location. The Casagrande's piezometer requires a vertical borehole to install. It is therefore difficult to install the piezometer under existing tie seat where pore pressure might be the highest.

b) The borehole diameter may be as large as 20cm, which may be difficult to drill and install between tie spacing of about 30cm. In addition, the borehole may be stiffer than the soft subgrade and interferes with the subgrade deformation.

c) Not quite suitable for fine-grained ground like clays, as it may take more than half a year to saturate.

d) Only positive pressures

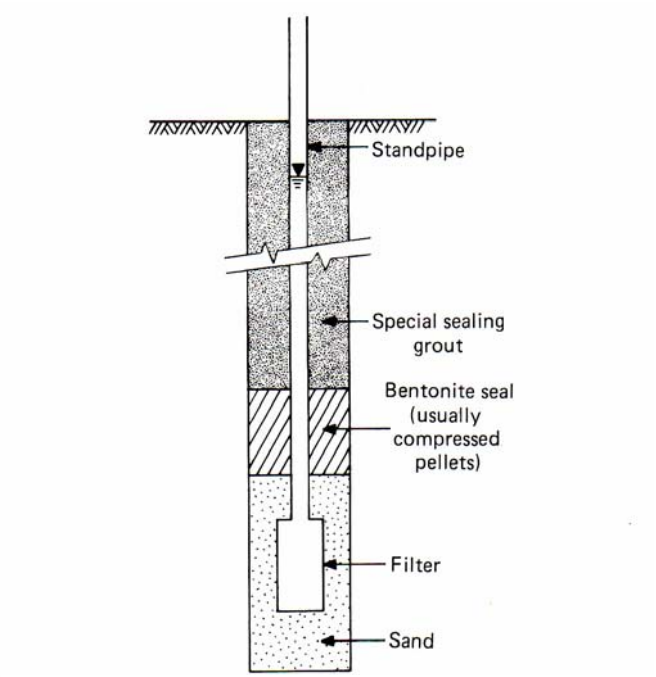

Figure 2.7: Schematic of open standpipe piezometer installed in a borehole (DUNNICLIFF 1998).

2.4.1.2 Push-in Vibrating Wire Piezometer

Push-in piezometers are generally smaller in size and can be easily installed in a small borehole (*Figure 2.8*). The borehole, not necessary vertical, may be drilled by a hand auger or a machine. The push-in piezometer is fitted with AW rods, lowered into the borehole, and is pushed into the ground so that the filter tip is displaced into soil region undisturbed by the augering. Most commercial push-in piezometers are of the vibrating wire type.

Figure 2.8: (Slope Indicator) Small push in vibrating wire piezometers

The vibrating wire piezometer, as the name implies, measure pressure changes by inferring from the frequencies of a vibrating wire. A pre-tensioned wire has a unique natural frequency and any stress changes in the wire causes changes in natural frequencies. Therefore, the stresses in the pre-tensioned wire can be inferred from the frequencies generated by the wire. In the design of a vibrating piezometer, a metallic diaphragm separates the groundwater from the measuring system and a pre-tensioned wire is attached to the metallic diaphragm. Increasing or decreasing pore water pressure causes the diaphragm to extend or relax, causing changes in the wire stress and hence the frequencies. The wire is magnetically plucked by an electrical coil attached near the midpoint between two wire clamps (*Figure 2.9*). The vibrating frequency is picked up by a receiver coil and the frequency for the vibrating wire is given by

$$f = \frac{1}{2L}\sqrt{\frac{\sigma g}{\rho}}$$

where f = natural frequency (sec^{-1})

L = length of the vibrating wire (cm)

σ = stress in the wire (N/cm^2)

ρ = density of the wire material (kg/cm^3)

g = gravity acceleration (N/sec^2)

The frequency output is directly proportional to the root square of wire tension, and is calibrated to measure pore pressure. The advantage of the vibrating wire technology is the output frequency is immune against unwanted noise during data transmission in the long cables. However, the vibrating-wire piezometers are not immune to electrical problems normally associated with electronic instruments. Indeed they are susceptible to zero drifts, offsets, and long term drift (a year or more) due to relaxation of the vibrating wire under permanent tension, slippage at wire clamping points, and corrosion (DUNNICLIFF 1988). Dunnicliff reported that with careful manufacturing, vibrating wires can perform very well in the long run of up to several years. Vibrating-wire piezometers are also susceptible to temperature fluctuations and atmospheric pressures. The complexity of the instrument contributes towards its relatively high unit cost.

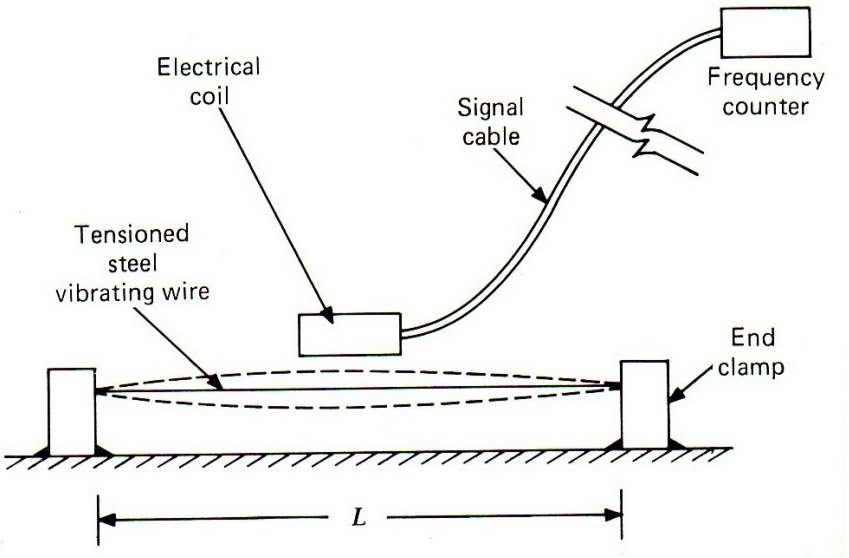

Figure 2.9: DUNNICLIFF (1988). Principle of the vibrating wire.

2.4.1.3 Pneumatic Piezometers

Pneumatic piezometers measure the pore pressure by mechanical means. There are a few types of pneumatic piezometers (DUNNICLIFF 1988), most of which operate as normally closed transducers. Normally closed transducers consist of a flexible diaphragm, connected to a gas supply and gas flow detector (*Figure 2.10*). In order to measure the external pressure, compressed gas (e.g. nitrogen) is introduced into the system. When the pressure of the compressed air equals the external pressure P, the flexible diaphragm is forced away from the vent, and therefore enabling gas to flow into the gas detector. The gas supply is then shut off and the gas will continue to dissipate through the outlet tube until the gas pressure in the system equals the external pressure P. The diaphragm will seal the vent, and the gas pressure in the system can be measured using a pressure gage.

The pneumatic piezometer is a simple, reliable and accurate sensor. However, it is very difficult to automate as it involves automatically turning on and shutting of the gas valves, and detecting very small gas that flows from the outlet tube.

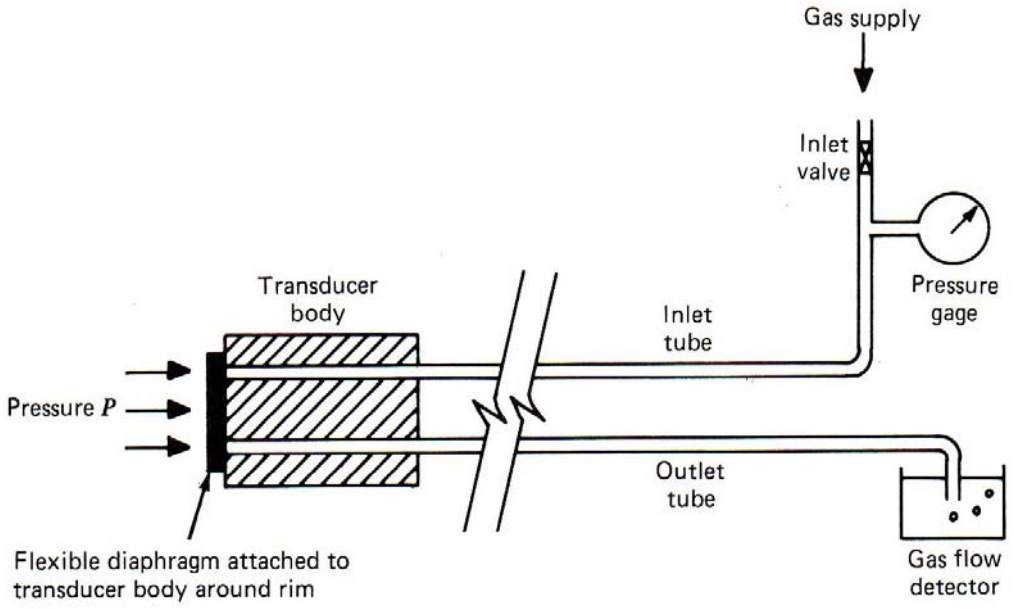

Figure 2.10: (DUNNICLIFF 1988): Pneumatic Piezometers, read under a condition of no gas flow

2.4.1.4 Hydraulic Piezometer

Hydraulic piezometers were first developed at Imperial College, London (BISHOP *et al.,* 1960; PENMAN, 1960), and have been widely used in long term embankment monitoring. The device itself is simple, yet reliable for long term pore pressure measurements. It consists of a twin tube connected to the filter tip at one end and two pressure measurement device (which could be in the form of bourdon gage, manometer, or electrical transducer system) on the other (*Figure 2.11*). The elevation head of the pore pressure is read by taking the average of the two pressure measurements.

The hydraulic piezometer is especially designed to work in highly unsaturated regions. High entry filter tips are normally used and the twin tubing allows for regular flushing to ensure the liquid system always stay saturated. It is possible for water to seep out of the equipment into the partially saturated environment and reduce the accuracy of the readings. However, with proper installation, flushing of the de-aired water is rarely needed.

Even today, the hydraulic piezometer is limited to embankment monitoring. It has certain limitations to be conformed: the routing of the tube must not rise too high above the water table such that it exists in sub atmospheric pressure, and water may become discontinuous (not more than 5m above the water level); and the de-aired water may freeze during winter. It is also not easily automated and personnel are required on-site to flush the system with de-aired liquid.

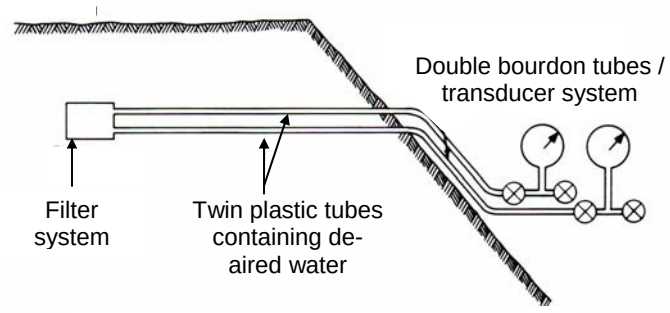

Figure 2.11: (DUNNICLIFF 1988) Schematic of twin-tube hydraulic piezometer installed in fill

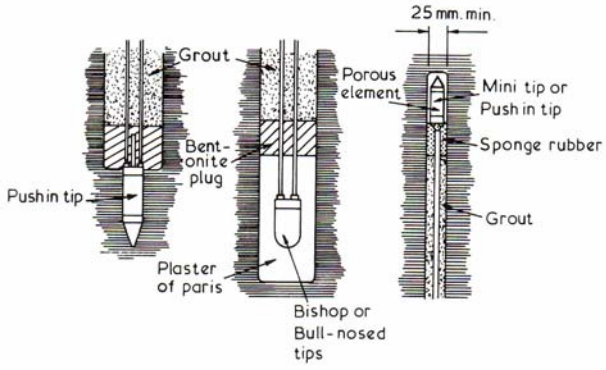

Figure 2.12: (HANNA 1985) Types of hydraulic piezometers in boreholes

2.4.2 Vertical deformation

There exist many methods of measuring the vertical deformation of a soil relative to its starting position. *Table 2.3* shows the various categories and types of instrumentation used in monitoring deformation. In addition to DUNNICLIFF (1988) classification, the instrumentation can also be categorised into manual intensive or automatic operation. The latter dictates the capability of operating in a remote site without the need of human intervention.

In order to capture subgrade movements such as the progressive failure, vertical deformation sensors will have to be placed under the rail seat and distance away from the rail track. In addition, since the soil is undergoing horizontal displacements, the sensors have to be flexible and small enough to be carried with the soil, so that they will not interfere with failure mechanism in the soil. The ideal monitoring vertical deformation sensor would satisfy the following criteria:

a) Low cost, easily produced, and able to operate in a remote location without the help of personnel.
b) Easy installation below existing rail track (where settlements are the largest), robust and will not be damaged by train loading and track maintenance vehicles.
c) Good resolution for small deformation range (say 0 to 8 cm)
d) No interference with the soil failure. Large and stiff sensors are likely to inhibit the ground failure, leading to unrealistic measurements.
e) Good long-term stability (one to five years)

In geotechnical practice, the most commonly used sensors for measuring vertical deformation are extensometers, inclinometers, and liquid settlement gages. This chapter will attempt to introduce some of the commonly used instruments, highlighting the relative advantages and disadvantages with reference to railroad applications.

Table 2.3: Categories of Instruments for Measuring Deformation (DUNNICLIFF 1988)

Category	Type of Measured Deformation					
	↔	↕	⤢	↻	÷	∓
SURVEYING METHODS	●	●	●		●	
Optical and other methods						
Benchmarks						
Horizontal control stations						
Surface measuring points						
SURFACE EXTENSOMETERS	●	●	●		●	
Crack gages						
Convergence gages						
TILTMETERS				●	●	●
PROBE EXTENSOMETERS	●	●	●			●
Mechanical heave gage						
Mechanical probe gages						
Electrical probe gages						
Combined probe extensometers and inclinometer casings						
FIXED EMBANKMENT EXTENSOMETERS	●	●	●			●
Settlement platform						
Buried plate						
Mechanical gage with tensioned wires						
Gages with electrical linear displacement transducers						
Soil strain gage						
FIXED BOREHOLE EXTENSOMETERS	●	●	●			●
Single-point and multipoint extensometers						
Subsurface settlement points						
Rod settlement gage						
INCLINOMETERS	●	●	●	●		●
TRANSVERSE DEFORMATION GAGES	●	●	●			●
Shear plane indicators						
Plumb lines						
Inverted pendulums						
In-place inclinometers						
Deflectometers						
Borehole directional survey instruments						
LIQUID LEVEL GAGES		●				●
Single-point and multipoint gages						
Full-profile gages						
MISCELLANEOUS DEFORMATION GAGES						
Telltales	●	●	●		●	●
Convergence gages for slurry trenches	●					●
Time domain reflectometry	●	●	●		●	●
Fiber-optic sensors	●	●	●		●	●
Acoustic emission monitoring	●	●	●			●

2.4.2.1 Extensometers

Extensometers are used to measure settlements in embankments and deep excavations projects, and most commercially available extensometers have settlement ranges in the order of metres. The extensometer measures settlements through relative movement between a fixed point (connected to a solid and unmovable ground) and a point in the moving ground, measured by devices such as vibrating wire, induction coil, magnetostrictive or Linear Variable Differential Transformer (LVDT). DUNNICLIFF (1988) provides a good overview on the types of extensometers available.

In general, extensometers are not quite suitable for subgrade settlement applications. The settlement and movement in the subgrade occurs at the top 1.5 to 2m. The movement region is too shallow to be measured by a standard extensometer. In addition, the challenge also lies in searching for a fixed datum in the soft subgrade site. It is difficult to install the extensometer under pre-existing ties and rail seats without first removing the rails and the ties.

2.4.2.2 Inclinometers

Inclinometers are one of the most common and popular instruments used to measure both horizontal and vertical deformation profiles. They are extensively used in almost all types of geotechnical projects, ranging from deep excavations, foundations add tunnelling. Inclinometers are able to measure continuous deformation over a large range between 8 to 10 metres. The inclinometer can be installed horizontally to measure the settlement profile over the railtrack.

Early inclinometer design consisted of a flexible borehole casing and a single tilt-sensing probe which is pulled across the length of borehole. The vertical deformation of the ground is found by integrating the tilt angle measured at each point along the length of the borehole with respect to a stable reference point. This is a cheap but labour intensive process. More recent digital inclinometers have replaced the moving probe by a series of electronic tiltmeters spaced at a certain fixed length (*Figure 2.13*).

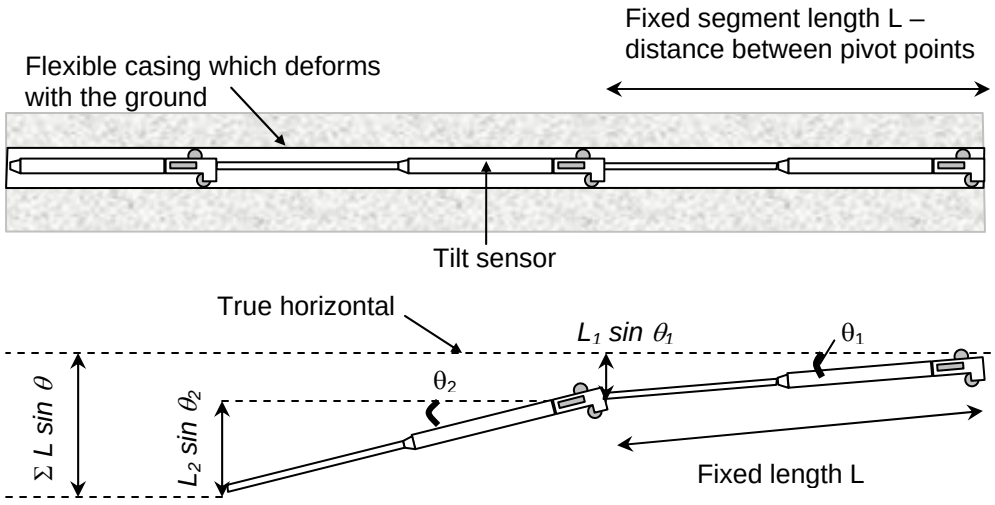

Figure 2.13: Principle of horizontal in-placed inclinometer operation.

The components of inclinometers are:

a) Flexible casing: A flexible casing (ranging from 48mm to 90mm) is installed in the borehole. The flexible casing has lower bending stiffness compared to the surrounding soil and will deform with the ground. The casing contains grooves to guide the wheels of the sensors. The space between the flexible casing and the ground is normally grouted to ensure proper transfer of stress.

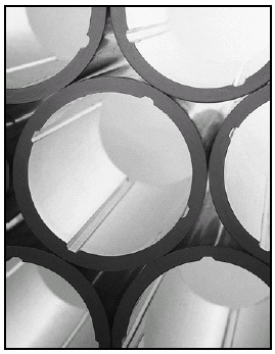

Figure 2.14: Casing

b) Tilt sensor: Each fixed length (L) segment consists of a tilt sensor, a stiff steel rod, and guiding wheels (*Figure 2.15*). The segments are free to rotate against other segments (one or two degrees of freedom), and the tilt sensors measure the relative angles between the segments (*Figure 2.13*). Most commercial inclinometers have the resolution of ±10 arc sec or 0.05mm/m. Since fixed length (L) of most commercially available inclinometers ranges from 0.8 to 1m, a maximum of 3 sensors are packed over the cross section of the rail.

Figure 2.15: Inclinometer (Courtesy of Slope Indicator, Inc, USA)

c) Data acquisition – The readout from the tiltmeters are fed into the data acquisition for further processing.

It is, however, not easy to select a suitable fixed datum in soft subgrade sites and the problem is clearly illustrated in *Figure 2.16*. It is likely that the required reference datum will move with the failure zone and jeopardise the accuracy of the reading. Installation of the inclinometer under the existing track may prove to be rather difficult without first removing the track.

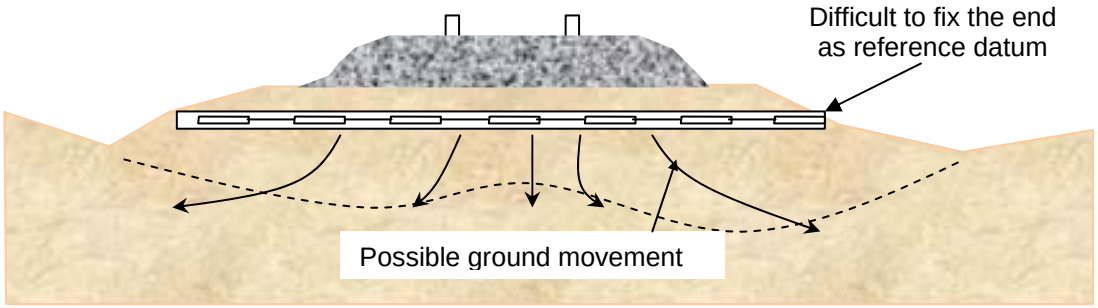

Figure 2.16: Installation of a horizontal inclinometer

Inclinometers are certainly not cheap, costing up to $600 per tilt sensor and up to $800 per segment (including steel rod, swivel joints, cable and guiding wheels). An inclinometer with 5 segments could cost up to $4000 without including cost of installation and data acquisition.

2.4.2.3 Liquid level gage

The liquid level gage instruments use fluid as means of determining the vertical deformation in the ground. A typical liquid level gage consists of an embedded instrument in the soil, connected to a liquid-filled tube, where the change in liquid pressure or liquid elevation can be read from pressure sensors or a manometer. There are many versions of liquid level gage available, but can be roughly separated into the following categories – a) manometers, b) single liquid level gages, and c) multiple liquid level gages. Liquid level gage are popular and widely used in measuring embankment settlement, and the commercially available ranges matches that – up to 10m of water head.

In general, the gages provide a means of measuring relative elevations between two or more points. This means a reference point, preferably fixed physically, will have to be employed. This could be solid ground near the track which is strong and not affected by the transient movement and displacement of the track.

The liquid level gages have the advantage of being flexible and small which facilitate ease of installation. The drawback of the liquid settlement gage is its susceptibility to liquid density changes caused by temperature variations and presence of gas in the liquid filled tube.

2.4.2.3.1 Single liquid level gage – both ends on same level

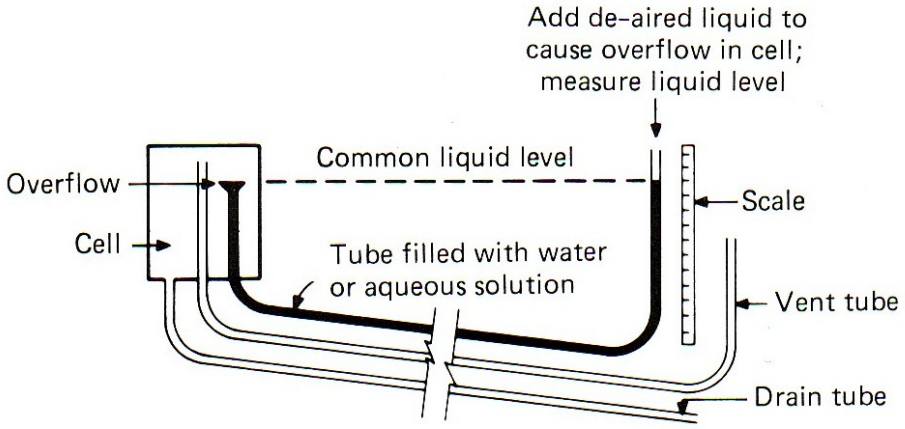

Figure 2.17: (DUNNICLIFF 1988). Schematic of single liquid level overflow gage with both ends at the same elevation.

This is a common levelling device used for measuring settlements in embankments. The cell and the overflow container are installed in the embankment and the measurements are performed from the side. The instrument is described by PENMAN *et al.* (1975) and is shown in *Figure 2.17*. This device, much akin to the manometer principle, allows the user to read the elevation of the buried sensor by determining the common liquid level. The vent tube is used to maintain similar pressure in the embedded container and the atmospheric pressure to enable more accurate reading. As with all liquid gages, this instrumentation is subjected to problems when air is present in the system, leading to inaccurate reading. PENMAN *et al.* (1975) indicates that flushing is necessary before the reading to ensure the liquid is reasonably de-aired.

The advantage of this system is its long-term reliability and ease of use. However, it is not easily automated and requires personnel to flush the system with de-aired liquid.

2.4.2.3.2 Single liquid level gage – Pressure transducer on one end

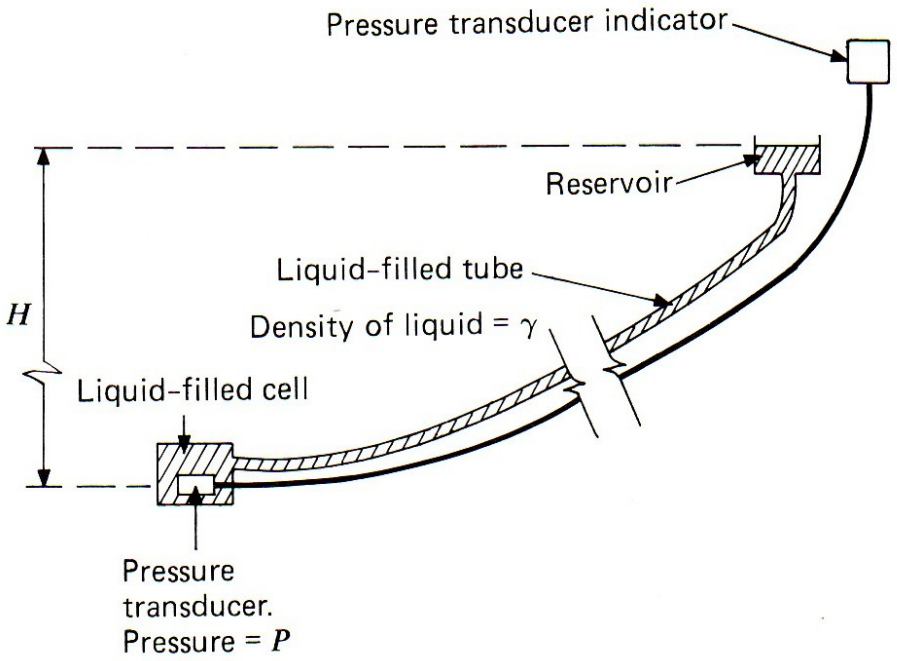

Figure 2.18: (DUNNICLIFF 1988) Schematic of liquid level gage with pressure transducer

This is another variation of the single point liquid level gage with the pressure transducer attached to the embedded end. The pressure transducer can either be a pneumatic, vibrating wire, or a piezoresistive type. The reservoir end is set as a reference point and is physically fixed, while the embedded end is free to move with the ground. The relative distance (H) between the embedded end and the reservoir can be determined from the pressure measurement at the embedded end and the known liquid density. More than one tube can be employed in the device to enable periodic flushing.

The accuracy of the gages is dependent on the two major factors: the pressure transducer must read the pressure head correctly and the liquid must transmit the pressure from the reservoir to the pressure transducer correctly. The transducer could come in the form of absolute or gage pressure. Absolute pressure transducers, as previously mentioned, are influenced by atmospheric pressure, which could vary up to

100mm of silicone head. They are also subjected to variation in temperature which has to be accounted for. Gage pressure transducers are not influenced by atmospheric pressure but are susceptible to corrosion and temperature changes.

The transmission of the static pressure between the reservoir and the pressure transducer is important and is affected by the selection of the diameter of the liquid filled tube (DUNNICLIFF 1988). The upper limit (6mm) is to ensure that any gas in the tube can readily be displaced, and the lower limit (4.3mm) is to ensure that equilibrium is achieved in an acceptably small time (PENMAN 1978).

The instrument can be backpressured to enable any gasses available in the system to go into solution. I.e. – any discontinuous phase will become continuous as the gas goes into solution. However, personnel are needed on-site to backpressure the system and this is not feasible in remote monitoring. Therefore, proper saturation process of the probes has to be done in the laboratory.

2.4.2.3.3 Single liquid level gage – Pressure transducer on one end

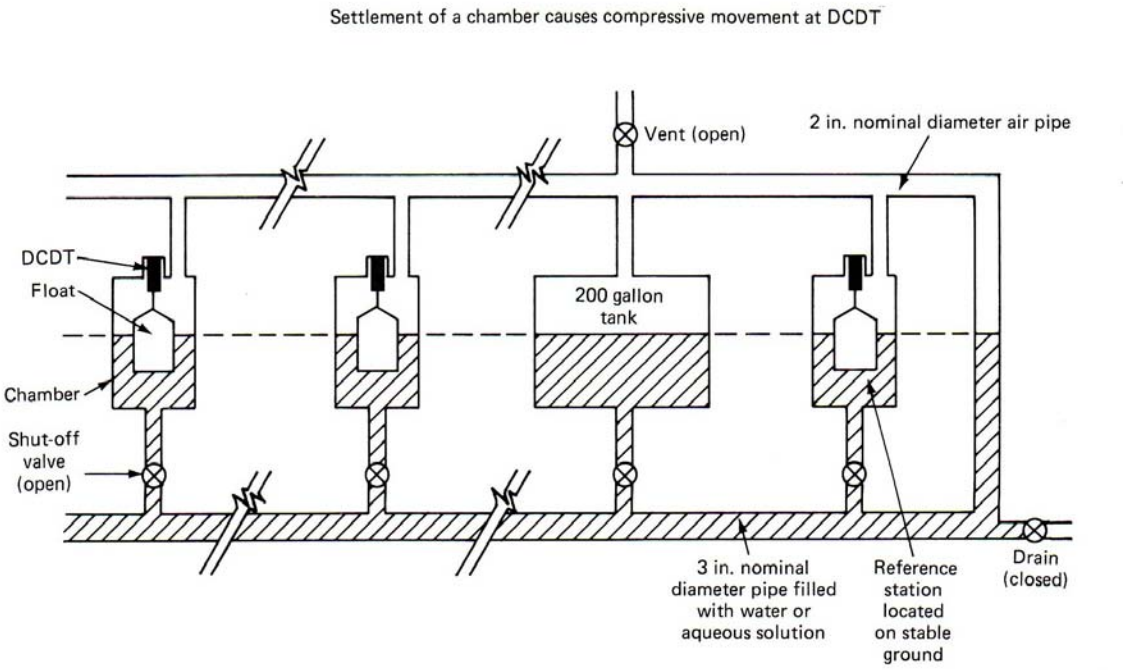

Figure 2.19: Multipoint gage for vertical settlement (Geokon, Inc., Lebanon, NH)

Multipoint gages consist of a series of interconnected liquid-filled chambers which are placed at similar elevation across the ground (*Figure 2.19*). There are multiple designs of the multipoint gages. *Figure 2.19* shows the use of floats and DCDT to measure the movement of the chamber. The system can accommodate up to 11

chambers. Larger diameter pipes (up to 2 inches) are used in the system to enable better filling up of the chamber. While multipoint gages are available commercially, they are not frequently being used as single point gages better preferred. Multipoint gages are more complex in construction and operation; each of the DCDT in the gages has to be placed in the same elevation (not always easy to install, especially under an existing railway track), and a loss in one of the chamber could lead to failure of the whole system.

2.4.3 Data Acquisition System

The transducers produce analog signals which is not recognised by computers. The analog signals are converted into digital signals by A/D converter found in all data acquisition systems (DAQ). For geotechnical field work, there are two common types of DAQ systems:

a) Standalone data logger.

Modern field standalone data loggers are able to support many channels of analog, digital and frequency signals without the presence of an on-site computer. Some data loggers have wireless communication capability to enable remote data transfer to the main computer. Field standalone data loggers are normally environmentally robust and can withstand the rigours of field data gathering. They are cost effective and are widely used in field data gathering. However, most standalone data loggers have the best resolution of 16 bit.

Figure 2.20: Standalone data logger (Iotech Logbook 360)

b) Computer based (laptop and desktop)

These DAQ systems are plugged into the computer either through USB or PCMCIA slot. Computer based DAQ are capable of reading analog, digital and frequency signals, and may have higher resolution (up to 22 bit) than the standalones. They are small, convenient and easy to set up both in the field and in laboratories.

Figure 2.21: Laptop based data acquisition (Iotech DAQ 55)

2.4.4 Remote Data Communication

Once the remote monitoring system has been established, data needs to be transmitted back the main headquarters (e.g. MIT). Selecting and setting up data communication, especially from remote areas is a challenge and the available choices are often limited to the availability of existing communication infrastructure. The Internet provides a cost effective method of communication and is widely available. However, most infrastructures provided by the Internet Service Provider (ISP) are found only in reasonably populated areas such as cities and towns, and have very few services, if any, at remote areas. Generally, are three main methods of connecting to the Internet: a) Modem Internet, b) Wireless Internet, and c) Satellite Internet (*Figure 2.23*). The important considerations involved in selecting the method of communications include:

a) Communication service availability.

   The choice of communication is often limited by the availability of the communication infrastructures which may not be readily available in remote areas.

b) Cost

   The cost per byte of data transmission varies between type of connection and between ISP. The total cost of the system consists of installation cost, hardware, and monthly service plan.

c) Energy usage

   The system set-up for each type of communication requires different energy usage. For example, the energy consumption of the satellite dish may be as high as 50W,

which is quite significant if the monitoring system was to be powered by a portable power supply.

Once the Internet connection is set up, the main computer can communicate with the remote terminal in the site with a suitable remote control software which is available commercially (eg NetOp, PcAnywhere by Symantec), and allow complete control of the remote terminal from the main terminal. The user is able to transfer data from the remote site into the main computer via the Internet, starting a new set of readings or changing the reading acquisition configurations.

2.4.4.1 Modem Internet

The computer is connected to the Internet via a modem, a telephone line, and a subscription service from an ISP. The modem Internet is commonly used by residential establishments and small companies, has relatively cheap hardware and subscription costs, and is widely available in cities and towns in the United States. The bandwidth of a modem is limited to 56 kbps, which is considerably slow compared to 2mbps of a DSL (Digital Subscriber Line). However, it would be sufficient for applications that require low data transfer rate. Unfortunately, the cable modem may not be readily available in very remote areas, thus reducing the flexibility of deploying the monitoring system in terms of location. The modem Internet requires both the telephone line and the availability of an ISP in that vicinity in order to enable Internet connection.

In addition to the modem Internet, there is another Internet connection service known as the DSL (Digital Subscriber Line) which offers very fast connection (up to 1.5Mbps) and is able to accommodate more than one computer. DSL would be more suitable for applications which require large bandwidth and data transmission. DSL uses the same telephone wire, but unlike the modem Internet, DSL is a distance-sensitive technology – the further is the computer from the DSL service provider (with typical limit of five kilometres), the connection speed decreases dramatically. This is because DSL transmit frequencies in the telephone cable that is not compatible with the small amplifiers known as loading coils (used to amplify conventional telephone signals along the telephone line to prevent the signals from damping). The major drawback of the DSL is that it is not widely available, even within major cities.

2.4.4.2 Cellular Wireless Internet

Cellular wireless Internet uses the mobile phone technology to transmit the data from the computer to the Internet. Major mobile phone companies such as T-Mobile, Verizon, Cingular and Nextel offer the wireless Internet option. These companies now act as ISPs, converting the signal transmitted from the mobile phone into the form compatible with the Internet. The typical speed connection speed is 40 to 60 kbps, which is slower than the cable modem. Cellular Wireless Internet cost more than the modem Internet (but cheaper than Satellite Internet) but has the advantage of greater location flexibility and the user is not constraint by the need to telephone lines. Due to high demand, the coverage of cellular wireless Internet is expanding very quickly all over the United States.

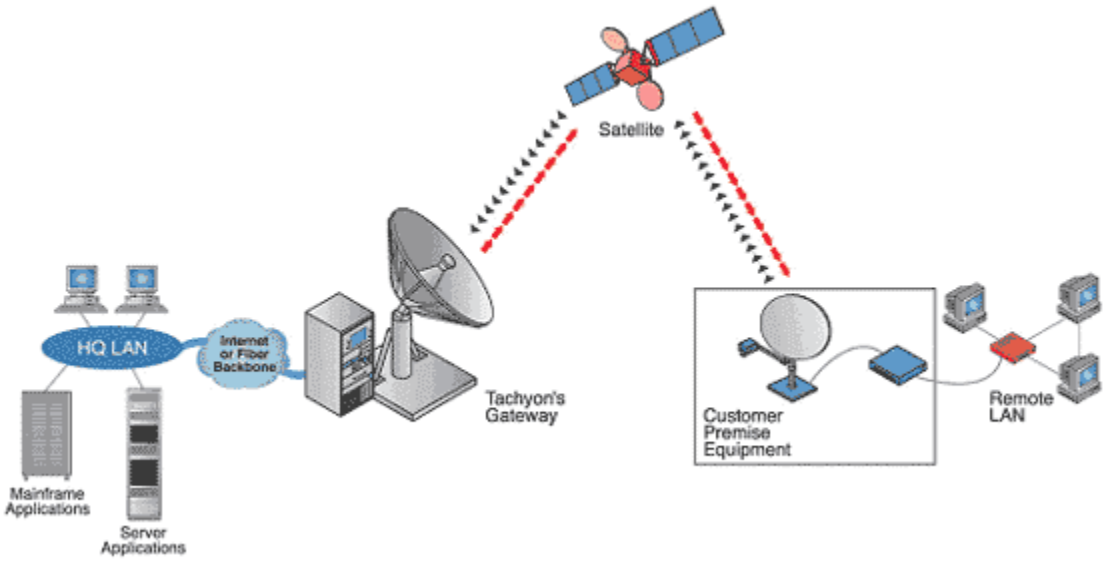

Figure 2.22: Satellite Internet communication infrastructure (courtesy of Tachyon).

2.4.4.3 Satellite Internet

The major advantage of the satellite Internet is its location flexibility; the satellite Internet can be used anywhere in the United States which has a clear view of the southern sky (because the geosynchronous communication satellites are orbiting in the equator). The remote computer is connected to the Internet via the mini satellite dish (at the remote terminal), space borne satellite, and the receiving satellite dish at the provider's premises *Figure 2.22*. The service provider acts as an ISP, converting the signal received from the ground satellite dish into the conventional Internet signals. The equipment in the remote terminal consists of a 0.8 m diameter mini satellite dish, two

modems for uplink and downlink respectively, and coaxial cables between the modem and the dish. The typical upload speed is 50kbps, with download speed ten times of that, placing the data transmission capabilities equal to the modem Internet. The satellite Internet, with its more sophisticated equipment, is costlier than modem Internet and cellular Internet, but provides unrivalled location flexibility. The disadvantages are the satellite reception and connection is highly affected by the weather, and consumes enormous amount of power (50W). Some of the companies providing this service (in the United States) are Starband, Tachyon, Pegasus, Earthlink and American Satellite.

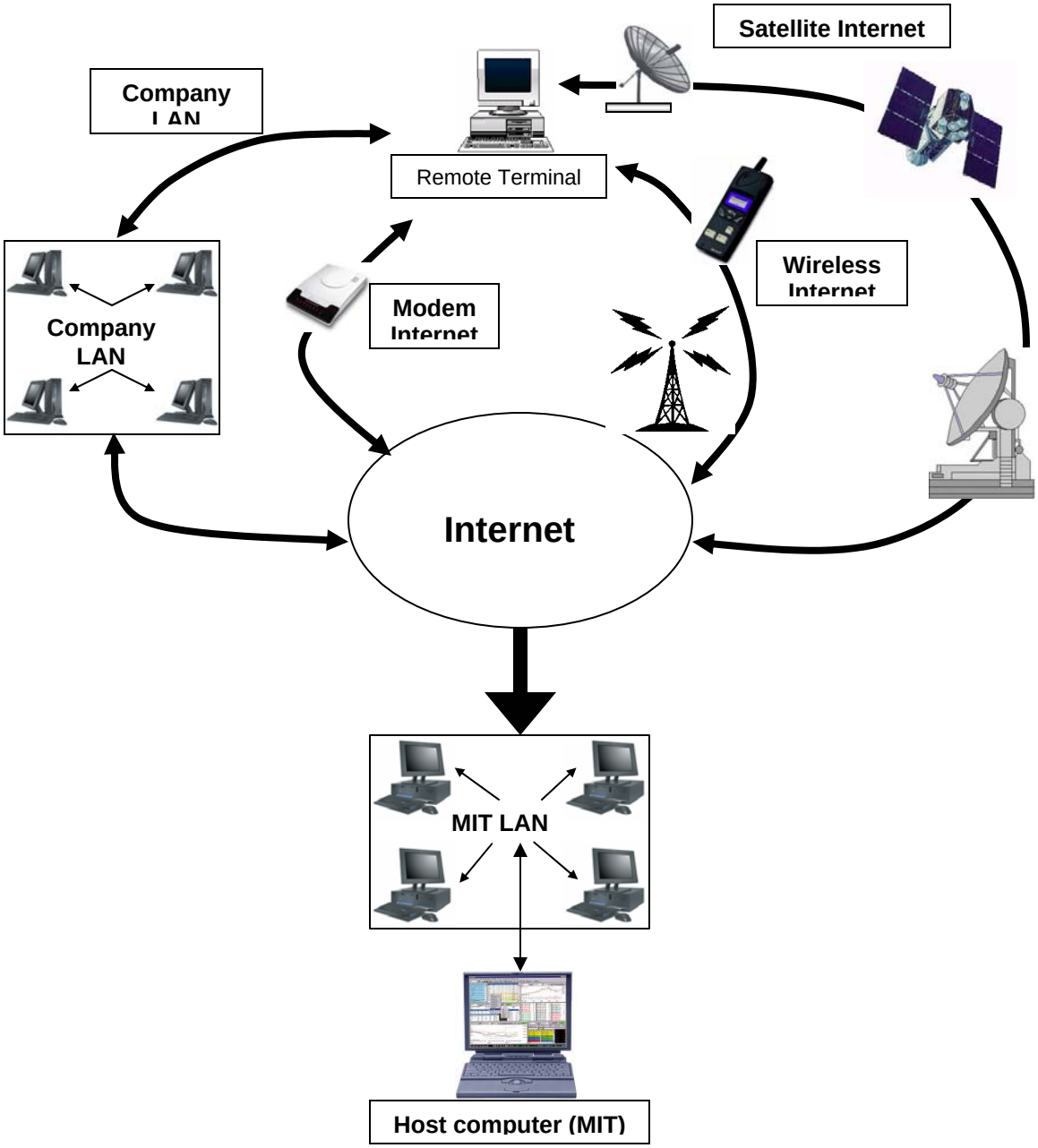

Figure 2.23: Schematic diagram showing possible communication methods between the remote system and host system at MIT.


III
Equipment
Development

Chapter 3: Equipment Development

3.1 Introduction

A low-cost remote monitoring system aimed at characterising the rail track foundation problems is presented in this Chapter. In this first phase of development, the prototype monitoring system consists of a piezometer and five vertical deformation sensors. More measuring capabilities (horizontal deformation and total stresses) will be included in subsequent phases of the research. The main requirements of the sensors are listed as follows:

a) Unmanned operation and environmentally robust.
b) Easy installation process
c) Low cost and ease of production to enable extensive monitoring.
d) Robust and minimal interference with train traffic and maintenance programs
e) Good long-term measurement stability
f) Resolution and accuracy

Existing commercial products are not suitable for railroad subgrade monitoring (since they are not designed for railroad applications) due to inappropriate design and size, unsuitable resolution and accuracy, or relatively high costs. There is now a clear need to design and fabricate new piezometers and vertical deformation sensors for diagnosing rail subgrade problems. The proposed sensor system has been tailored to meet the resolution, accuracy and requirements suitable for railroad applications.

The design methodology of a monitoring system consists of the following phases:

1) Conceptual design and fabrication

   Identify the parameters to be measured and the corresponding resolution.
   Design of the probes and overall monitoring system

2) Laboratory Evaluation

   The sensors are calibrated in the laboratory and performance of the complete monitoring system is evaluated under laboratory conditions.

3) Field Testing

The monitoring system will be evaluated for robustness and long-term stability at the bridge approach site of the FAST loop at TTCI, Pueblo, Colorado, USA, while being subjected to well defined HAL train loadings.

3.2 The monitoring system

The prototype monitoring system consists of three segments; a) Embedded sensors consisting of 1 piezometer and 5 liquid settlement probes, b) On-site data acquisition system, and c) Client computer system which is able to control and receive data from the on-site data acquisition system through the internet and remote connection (*Figure 3.1*). Each piezometer and the liquid settlement probe consists of a piezoresistor pressure transducer and a thermistor, capable of measuring pore pressure or deformation at resolution of 0.05kPa and 0.5mm respectively. The on-site data acquisition consists of an USB-based Iotech DAQ 55 data acquisition module connected to an on-site laptop. The laptop is wired to the TTCI Local Area Network via a directional wireless antenna transmitter. Commercially available remote control software, Symantec PcAnywhere 10.5v remote control software enables the computer at MIT to access the data acquisition system at TTCI. The physical location and installation of the system is discussed in Chapter 5.

Since TTCI requires that the data acquisition system be placed at 19m from the sensors, an intermediate junction box is used. The junction box also houses the reservoir for the liquid settlement probe. Currently, TTCI provides the necessary power supply and the Internet for establishing the remote connection. The power supply is supplied from the main grid at TTCI, with solar power and batteries to provide emergency power backup.

Good grounding plays an important role in ensuring low electrical noise during the data collection and transmission. All power and signal wires are insulated from the environmental effects by BX cables that act as a Faraday cage. The BX cables and drain wires from the signal cables are electrically connected to the junction box (main ground), and all charges are drained into the ground via a three metre copper rod. The signal ground (connected to the low end of the power supply) is earthed separately.

.

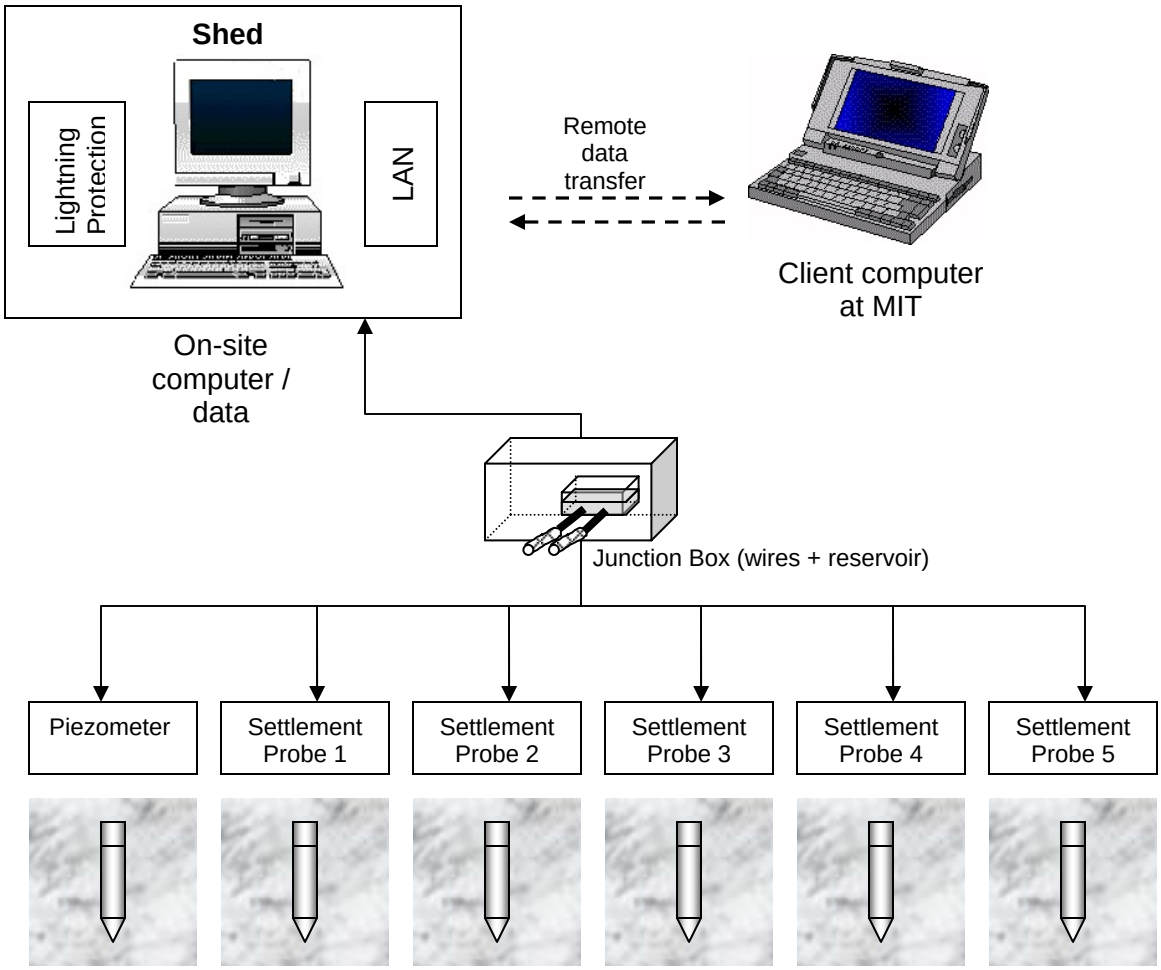

Figure 3.1: The prototype monitoring system consisting of one piezometer and five settlement probes.

3.3 Piezometer Probe

3.3.1 Introduction

The piezometer is a small pushed-in type stainless steel probe, measuring at only 27 x 187 (diameter x length) mm, designed to measure the pore water pressure in the subgrade. The piezometer is connected to the junction box via 10m cable encased in strong steel BX sheath, which protects the cable from train loadings and electrical interference.

Figure 3.2: Piezometer

A small porous stone is located just above the sharp conical tip (designed to facilitate push-in installation) to enable pressure transfer between the pore pressure in the ground and the pressure transducer in the probe via silicone oil medium. This piezometer measures only positive pore water pressure but will not drain under negative pressure found in subgrades. The absolute pressure transducer is a silicon piezoresistive sensor, and is selected over the widely used vibrating-wire transducer due to its simpler design, smaller size and cheaper cost. The piezometer has a range and laboratory resolution of 220 kPa and 0.01kPa respectively. The train loading induced pore pressure in fine-grained material is estimated to apply pressure up to 100 kPa.

The piezometer design is designed to be low cost (expendable after usage[9]), and has high flexibility during installation. The relatively small diameter of the probe enables it to be pushed into the ground through the hole in a small hollow stem, hand operated auger. In order to ensure good connection between the porous stone and the soil, the probe must be further pushed into the undisturbed soil zone (about 2cm). The

[9] The total cost of the piezometer (raw materials alone) is $55; $18 for the pressure transducer, $15 for the thermistor, and $22 for the rest of the components. In comparison, the typical commercially available vibrating-wire piezometer with the same size and resolution costs about $500. However, the piezometer is expected to take 10 man-hours to manufacture, and less if bulk manufacturing is performed.

piezometer can be installed in a borehole of any orientation, thus achieving great flexibility and can be installed in critical areas such as under the rail ties.

3.3.2 Conceptual design

The piezometer consists of 3 main sections: a) The pressure transfer mechanism – external pore water pressure is transferred to the internal measuring system via silicone fluid in the fluid chamber, through a carborundum porous stone; b) The measuring system consisting of an absolute MPX2200A pressure transducer and a thermistor, encapsulated in epoxy which provides physical protection, and c) Outer stainless steel body that houses and protects the delicate measuring system, and data cables connecting the piezometer to the data acquisition. The data cable is protected from train loadings and insulated from background electrical noises by aluminium BX sheath.

The pore pressure is measured by a pressure transducer contained in the piezometer housing. The pressure transducer is connected to the outside of the piezometer by a chamber via internal conduits in the conical headpiece to a porous filter ring (this prevents soil particles from entering while allowing free transmission of fluid pressure). This filter separates the measurement pore pressure from the effective stress in the soil. Low viscosity 20 PaS silicone oil is used as the internal fluid. The detailed description of each component is given in Section *3.3.3*.

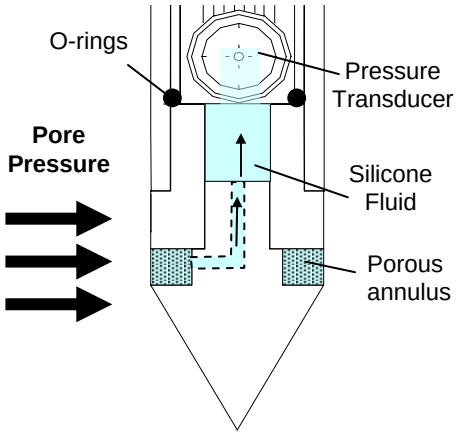

Figure 3.3: Pore pressure measurement

The design of the pressure transfer mechanism and the measuring system forms the major part of the piezometer design. The accuracy of the measured pore pressure depends on three major factors: a) the time response of the system, b) pressure transfer efficiency, and c) measuring accuracy of the pressure transducer.

The time response refers to the time taken for the piezometer to register the full changes in the external pore pressure and is determine by: volume change required to deflect the diaphragm of the pressure transducer, compressibility of silicone oil, and expansion of the steel body (HENDERSON 1994). For long-term monitoring applications (with sampling rate of once every hour), the pore pressure response is not a critical issue (critical measurements are limited to less than 0.1 seconds).

The efficiency of the pressure transfer can be increased by ensuring full saturation in the porous filter, inner chamber of the piezometer, and the port of transducer. The relative relationship between the pressure response of a piezocone and the effects of partially saturated porous stones (varying from S = 30% to 100%) has been investigated by RAD & TUMAY (1985). Partially saturated porous stones delay the time response of the pressure change (in this example here is 0.1 seconds), although the full magnitude of the pressure change is eventually reached (*Figure 3.4*). These data use water in the pressure sensor rather than the silicone oil in the current design. Since silicone has higher viscosity (20 PaS) than water (0.98 PaS), it is highly likely that a slower time response is expected for silicone oil medium. Nevertheless, this delay in response measurements will not be critical for this application where long-term measurements are important, in an event of imperfect field saturation. This piezometer measures only positive pore pressure but the inner silicone oil will not drain under negative pressure.

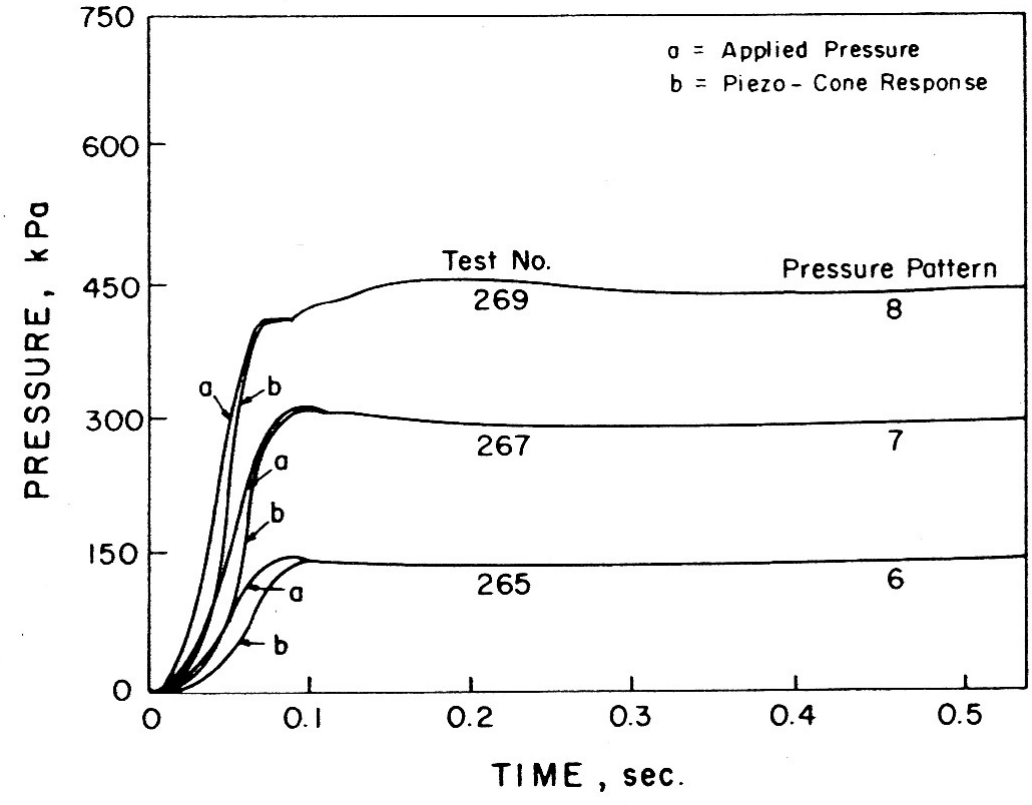

Figure 3.4: Pore pressure response of partially saturated piezocone to step pressure using water as the medium of pressure transfer (Rad & Tumay 1985).

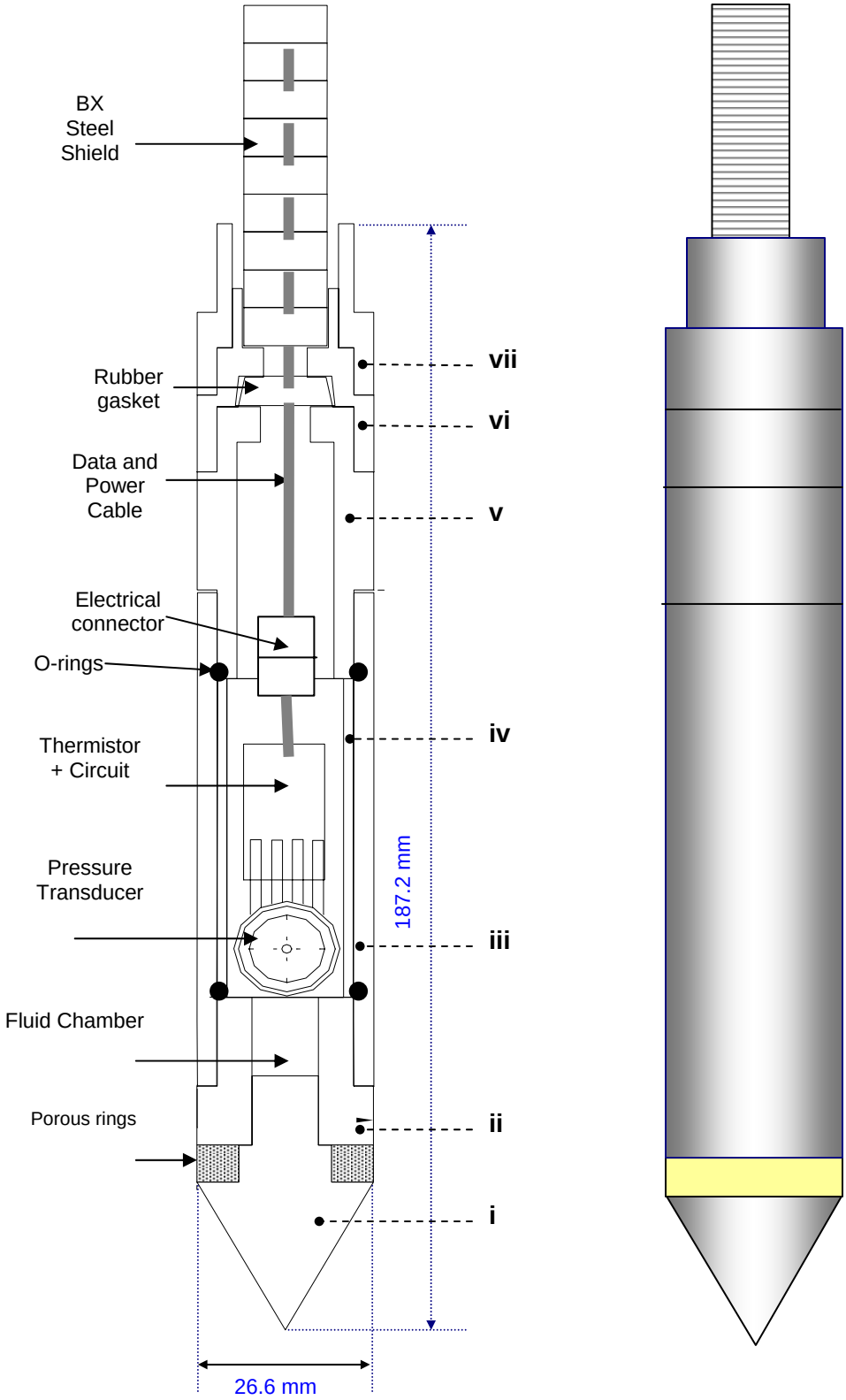

Figure 3.5: Design of the piezometer probe

3.3.3 Components of Piezometer

3.3.3.1 Body

The body is made of Stainless steel grade 304 and has good corrosion resistance, strong enough to withstand the train loadings and yet soft enough for machining. The piezometer has seven major components (as labelled in *Figure 3.5*) which are detachable to enable easy assembling. The components are labelled from i to vii (see *Figure 3.5*)

Component (i) Conical Head

A conical head contains a series of internal conduits to enable fluid connection between the porous stone and the fluid chamber. The porous stone is held in place between the side of the conical piece and component ii. The sharp cone tip (at 62° from the horizontal) helps to facilitate easy push-in installation.

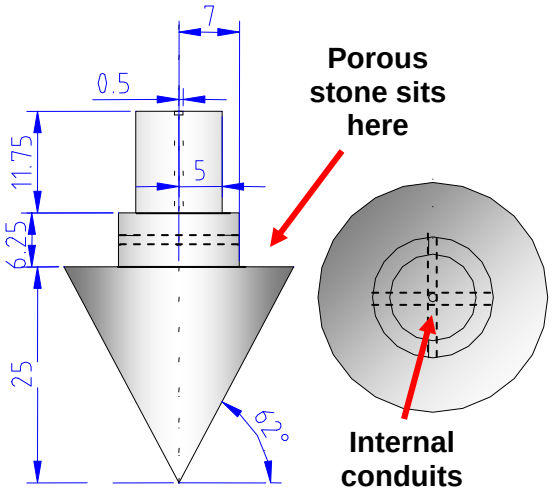

Figure 3.6: Component i

Component (ii), (iii), (iv), and (v)

Component iv is probably the most important component as it contains the pressure transducer and the thermistor (encased in epoxy). For portability, the pressure transducer is not soldered onto the 6m cable, but to a 5 pin female connector. During assembly, the male connector (connected to the 6 m of cable will be attached to the female connector.

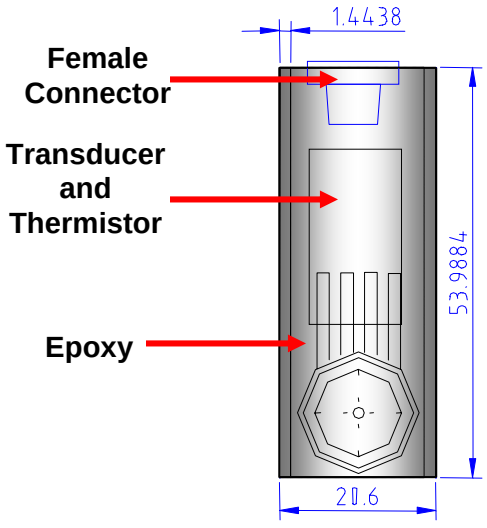

Figure 3.7: Component iv.

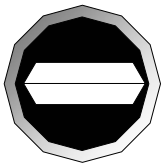

Component iv is protected by the outer body (component iii) and is held in place by two components (ii and v). Component ii and v are screwed into the outer body in a clockwise and anticlockwise manner respectively. The tolerance spacing between the three components is limited to 0.5mm to ensure component iv is tightly held into position.

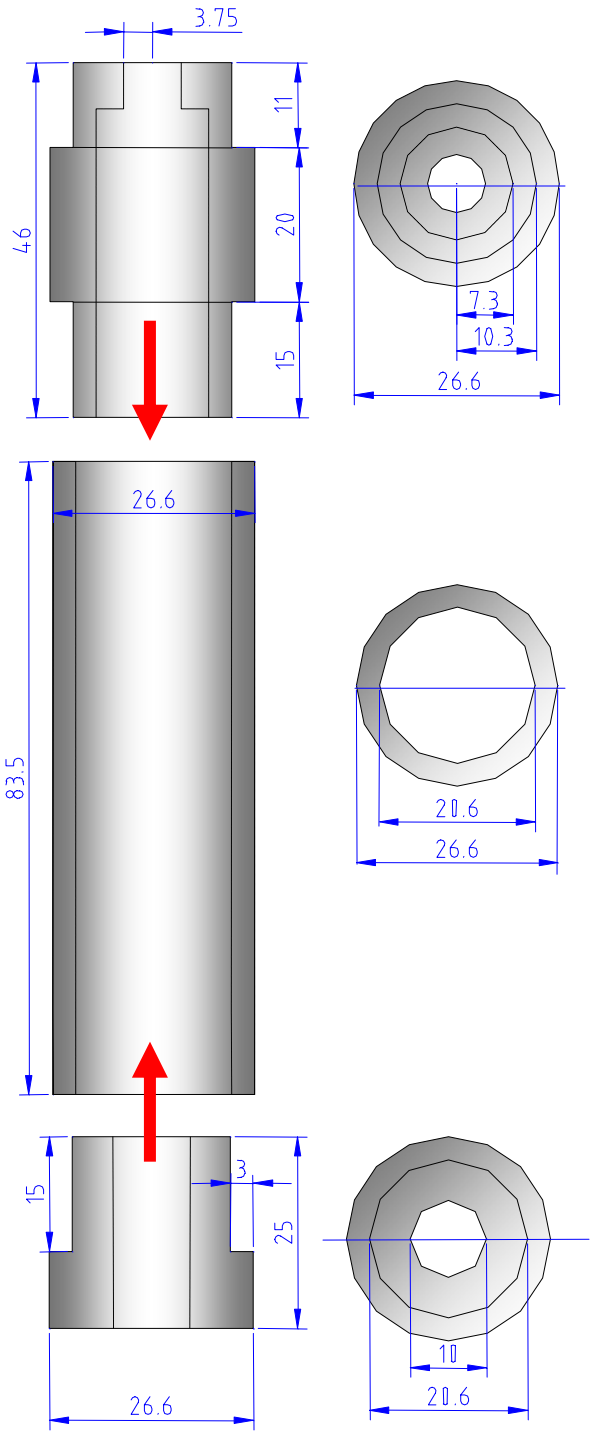

Figure 3.8: From the bottom: Component ii, iii and v.

Component (vi)

Component (vi) serves two functions: a) groove to accommodate the BX cable, and b) containing the chamber to hold the rubber sealing. The former function is elaborated under component vii. The latter functions as a sealing to prevent water from entering the chamber containing the electrical connection. See sealing (Section *3.3.3.2*) for more information.

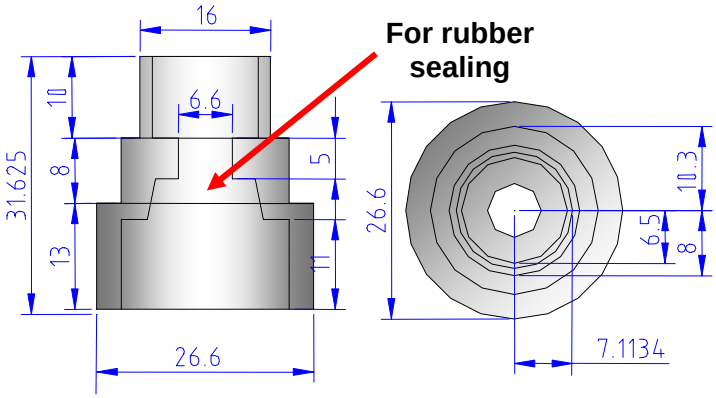

Figure 3.9: Component vi)

Component (vii): BX gripper

The BX cable has to be rigidly secured onto the probe (able to withstand high train loading) and the BX gripper is designed for that purpose. It is used in conjunction with component vi, which has a groove for inserting the BX cable. A compressible polyester hollow cylinder is pulled over the end of the BX cable, increasing its effective diameter so that it is now bigger than the diameter of the groove. Component vii is screwed into component vi, thus forcing and compressing polyester and the BX cable into the groove. The compressed polyester provides very high friction which will grip the BX cable and, hopefully, withstand the rigours of train loading.

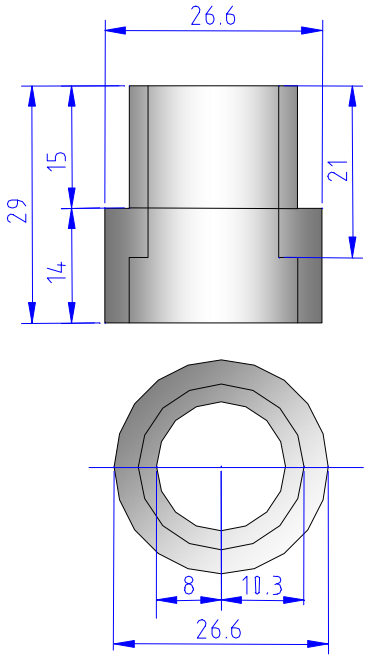

Figure 3.10: Component vii) BX gripper

3.3.3.2 Sealing

The piezometer contains sensitive electrical devices (the chamber which is bounded by component iii) and has to be sealed from the external groundwater. The chamber contains the electrical connection between the transducer and thermistor (component iv) and the 6m of cable. There are two fluid paths (or ways of infiltration) into the chamber i) from the BX cable connection, and ii) from the side of the probe (*Figure 3.11*). The fluid path through the BX cables is sealed by means of a rubber gasket compressed between components ii and iii. The fluid path through the middle of the probe (between components iii and v) is sealed by an o-ring.

The fluid path iii between component ii and iv is sealed by an o-ring. This prevents groundwater from infiltrating the silicone oil chamber and vice versa.

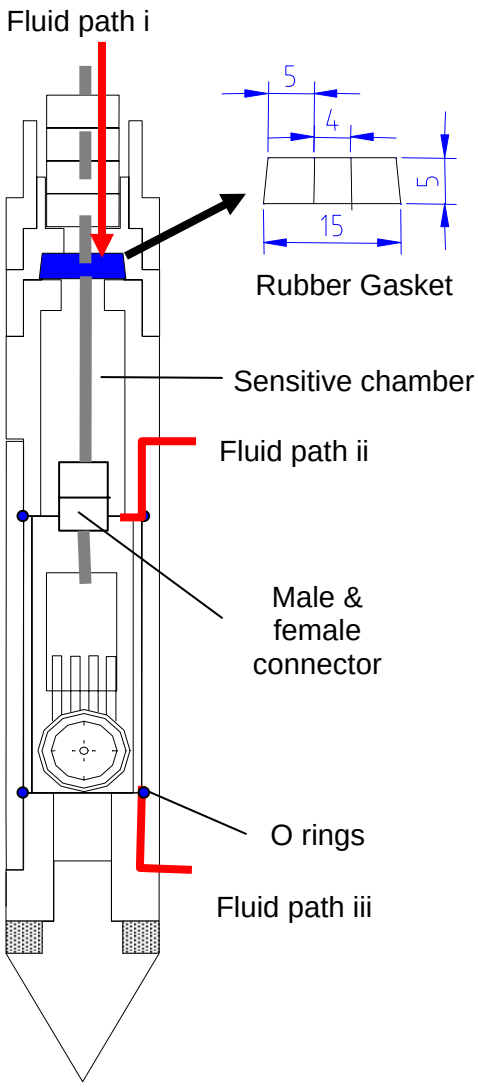

Figure 3.11: Fluid path and sealing of the piezometer

3.3.3.3 Porous Filter

The porous filter separates the internal silicone fluid from external soil pore fluid, while enabling fluid pressure transfer. It is machined from carborundum porous stone. The porous stone, measuring 6 millimetres thick, is held in place by the conical head and a metal shaft which is screwed onto the main body.

3.3.3.4 Data cable and BX cable

Selection of the data cable is bounded by three main requirements: a) 3 pairs of individually shielded wires; b) physical constraints limit the cable to approximately 4mm outside diameter; c) the system must operate within site temperature of –20 to 50^{0}C. Three pairs of wires are needed for power supply, transducer and thermistor output.

Since the output of the transducers is in the milivolt ranges (1mV causes uncertainly of 5 kPa or 271mm for piezometer and settlement probe respectively) and the data cable will run at lengths in excess of 25 metres, providing proper insulation from electrical noises during the data transmission is of paramount importance. Individually shielded pair of wires with drain wires should be sufficient in providing good noise insulation.

Belden 89503 has three pairs of 24 AWG wires (each pair has a 24 AWG drain wire and individually shielded by Aluminium Foil-Polyester Tape (Bedfoil)), and is wrapped by flame resistant Fluorinated Ethylene Propylene (FEP) jacket. The external diameter is 4.3mm and has an operating temperature rating of –70 to 200^0C, well above the required in-situ temperature. The resistance of the cable is sufficiently small - 24.1Ω / 305m, measured at 25°C.

The data cable is protected from train loading and noise-insulating Faraday cage by a steel 5/16" BX sheath, with internal and external diameter of 7.7mm and 12.7mm respectively. The data cable is inserted into the BX cable by means of the "fish" method, described as follows: a 50ft, thin metal rod (soft enough to negotiate the curves in BX cable and yet rigid enough to stand on its own) is inserted through the BX cable, exiting on the other end. The data cable is tied to the end of the exited BX cable and the metal rod is now pulled such that the data cable will be pulled into the BX cable.

3.3.3.5 Pressure Transducer

The pressure transducer is of one of the most important components in the piezometer. Selection of the pressure transducer is based on the following criteria:

- Range and resolution of at least 150 kPa and 0.1 kPa respectively. The train-induced pore pressure can be estimated to lie within the range of 100 kPa, given that the typical dynamic train-induced subgrade stresses are about 100 kPa (SELIG & WATER 1994).

- Absolute vs. gage pressure transducer. The pressure measured by the transducer is relative to two points – the applied pressure and reference point. The reference point for a gage and absolute transducer is the atmospheric pressure and vacuum respectively (for this application). The gage transducer, being vented to the

atmosphere, has the advantage of not being affected by the atmospheric pressure[10] variation. However, keeping the gage transducer (buried 10m in the ground) vented to the atmosphere presents a design challenge. The absolute pressure transducer, on the other hand, eliminates the technical and logistical difficulties of venting the transducer, but is highly affected by changes in the atmospheric pressure.

- Sensitivity to temperature and atmospheric pressure variation. Atmospheric temperature and pressure variation present a major source of problems for all sensors based on absolute pressure measurements. Pressure transducers with temperature compensated circuits are less susceptible to the temperature variation and the errors can be easily quantified within the compensated range.

- Cost – Pressure transducers currently range in cost from USD$18 to USD$500, and dictate the overall cost of the piezometer. The stark difference between the costs is manifested in terms of the type of transducer, complexity, robustness, and long-term stability.

- Inert to silicone oil.

Two types of pressure transducers have been investigated for the suitability of this application: a) Omega PX-26 gage pressure transducer and b) MPX2200A absolute pressure transducer. Omega PX-26 gage pressure transducer is "characteristically" more suitable for this application than MPX series transducers. It has better (range of 210 kPa and output of 100mV), port design (allows for easy epoxying) and is relatively low-cost ($35). However, there is a caveat; the PX-26 is only available in the form of a gage transducer where the 'wet side' and 'dry side' of the transducer are exposed to silicone oil and atmospheric pressure respectively (*Figure 3.13*). Attempts were made to transform the gage Omega transducer into an absolute version by sealing the back port with epoxy. Since the back chamber was not sealed in vacuum, the trapped air (in the chamber) expands and contracts with temperature and affects the diaphragm in the pressure transducer. This induces artificial pressure difference: increases in temperature cause expansion of air in the back chamber and exert more pressure in the diaphragm, thus causing reduction of the measure applied pressure, and vice versa (*Figure 3.13 b*).

[10] The atmospheric variation causes up to 100mm of change in silicone oil head.

This phenomenon is acceptable and can be accounted for through temperature calibration. However, at temperatures above 40°C, the pressure in the back chamber causes air leaks around the diaphragm and hence relieves the high pressures in the back chamber (*Figure 3.13*). Further physical examination shows that the diaphragm was clearly designed to seal from the direction of principal stress application (σ_{WET}). Therefore, gas leakage through the diaphragm occurs when $\sigma_{heat} > \sigma_{WET}$. In conclusion, PX-26 gage transducers cannot be sealed to simulate absolute transducers.

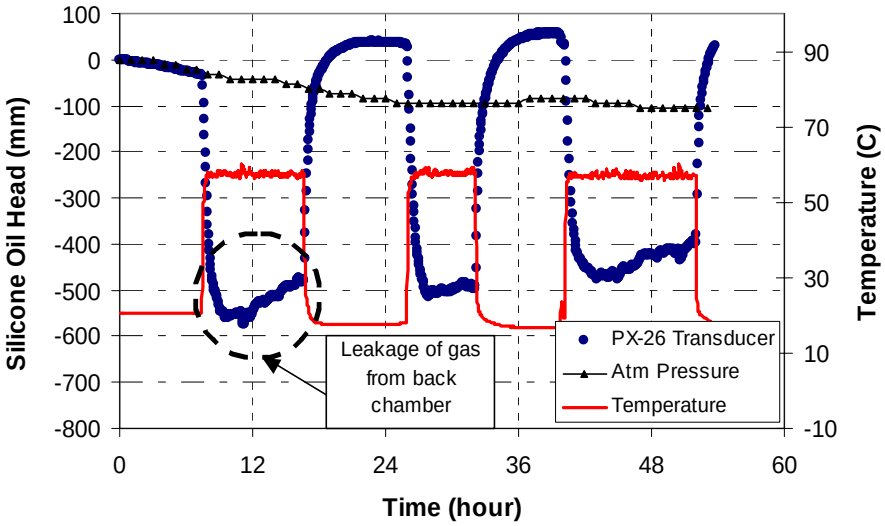

Figure 3.12: Temperature Stability Omega PX-26 gage pressure transducer.

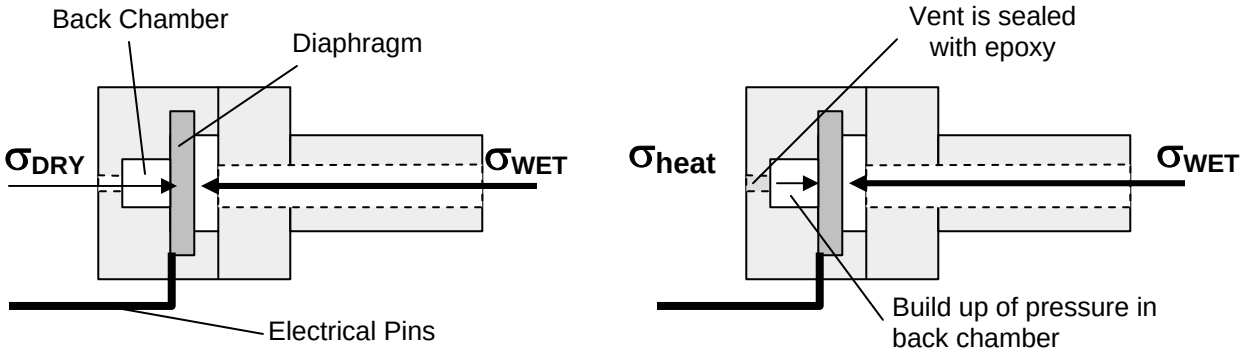

a) Original gage transducer

b) Sealed pseudo absolute transducer

Figure 3.13: a) and b) shows the main schematic diagram of the Omega PX-26 transducer, without the outer shell.

The MPX2200A, on the other hand, is an absolute pressure transducer although it has lower resolution of 10^{-3} kPa (compared with 10^{-5} kPa for PX-26), and comes in a flat cylindrical design with metal cap[11] (*Figure 3.14*). MPX2200A transducer comprises a strain gauge (implanted in a monolithic silicone piezoresistor), which generates output voltage approximately proportional to the applied pressure (marked as absolute die in *Figure 3.14*, Fig b). A layer of silicone gel die coat physically separates the strain gauge from the atmospheric pressure, while enabling pressure transfer. It has pressure capacity of 200 kPa (29psi), input voltage of 10V, full-scale span of 40mV, giving a theoretical resolution of 1.5 x 10^{-3} kPa (22 bit data acquisition with range of ±62.5mV) at a cost of $18 per transducer. The transducer contains temperature compensated circuit that moderates temperature within the range from 0^{o}C to 85^{o}C. The manufacturer suggested the offset of pressure when temperature is cycled from 0^{o}C to 85^{o}C relative to pressure held at constant 25^{0}C is about 1% of full-scale reading (or 2kPa). However, Motorola has no test record of the long-term compatibility of the silicone gel die coat with silicone oil.

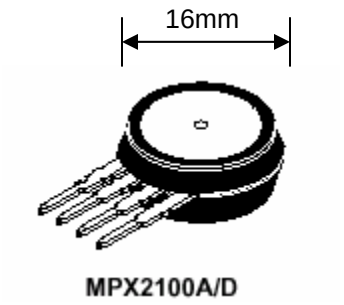

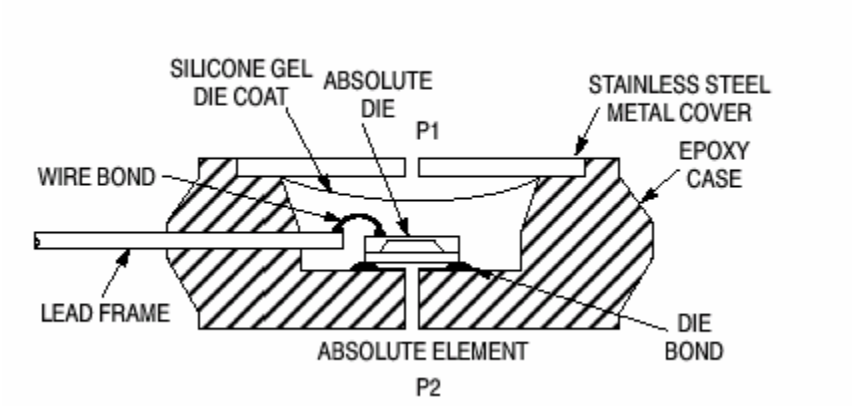

(b) Cross Section of the transducer

Figure 3.14: Motorola MPX2200A and MPX2100A pressure transducers. (Courtesy of Motorola)

[11] MPX2200A comes in a flat cylindrical design with metal cap, which is harder to encase in epoxy compared with the PX-26 port design.

Table 3.1: Manufacturer Specification for MPX2200A (Motorola).

Characteristics	Symbol	Min	Typical	Max	Unit
Pressure range [1]:	Pop	0	-	200	kPa
Supply Voltage [2]	V_S	-	10	16	Vdc
Supply Current	I_O	-	6.0	-	mAdc
Full Scale Span [3]	V_{FSSS}	38.5	40	41.5	mV
Offset[4]	V_{OFF}	-1.0	-	2.0	mV
Sensitivity	$\Delta V/\Delta P$	-	0.4	-	mV/kPa
Linearity [5]	-	-1.0	-	1.0	$\%V_{FSS}$
Pressure Hysteresis [5] (0 to 100 kPa)	-	-	+0.1	-	$\%V_{FSS}$
Temperature Effect on Full Scale Span[5]	TCVFSS	-1.0	-	1.0	$\%V_{FSS}$
Temperature Effect on Offset [5]	TCVoff	-1	-	1.0	mV
Input Impedance	Z_{in}	1300	-	2500	Ω
Output Impedance	Z_{out}	1400	-	3000	Ω
Response Time[6] (10% - 90%)	t_R	-	1.0	-	ms
Warm – Up	-	-	20	-	ms
Offset Stability [7]	-	-	±0.5	-	$\%V_{FSS}$

OPERATING CHARACTERISTICS (VS = 10 Vdc, TA = 25°C unless otherwise noted, P1 > P2)

1. 1.0 kPa (KiloPascal) equals 0.145 psi.
2. Device is ratiometric within this specified excitation range. Operating the device above the specified excitation range may induce additional error due to device self–heating.
3. Full Scale Span (VFSS) is defined as the algebraic difference between the output voltage at full rated pressure and the output voltage at the minimum rated pressure.
4. Offset (Voff) is defined as the output voltage at the minimum rated pressure.
5. Accuracy (error budget) consists of the following:
   - Linearity: Output deviation from a straight line relationship with pressure, using end point method, over the specified pressure range.
   - Temperature Hysteresis: Output deviation at any temperature within the operating temperature range, after the temperature is cycled to and from the minimum or maximum operating temperature points, with zero differential pressure applied.
   - Pressure Hysteresis: Output deviation at any pressure within the specified range, when this pressure is cycled to and from the minimum or maximum rated pressure, at 25°C.
   - TcSpan: Output deviation at full rated pressure over the temperature range of 0 to 85°C, relative to 25°C.
   - TcOffset: Output deviation with minimum rated pressure applied, over the temperature range of 0 to 85°C, relative to 25°C.
6. Response Time is defined as the time for the incremental change in the output to go from 10% to 90% of its final value when subjected to a specified step change in pressure.
7. Offset stability is the product's output deviation when subjected to 1000 hours of Pulsed Pressure, Temperature Cycling with Bias Test.

3.3.3.6 Thermistor

The thermistor provides a reliable way of measuring the atmospheric and probe temperature. The Omega 44005 thermistor, measuring only 0.24mm in diameter is comfortably fitted together with the transducers in the probe and the junction box (*Figure 3.15*). The thermistor is made of #32 tinned copper wires, and has a working temperature range of –60 to 150^{O}C. The resistance of the thermistor is a unique function of temperature, and a Wheatstone bridge is used to amplify the relatively small resistance change (*Figure 3.16*).

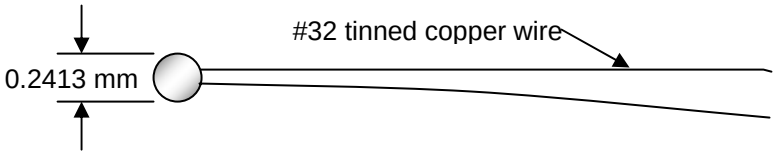

Figure 3.15: Omega 44005 thermistor

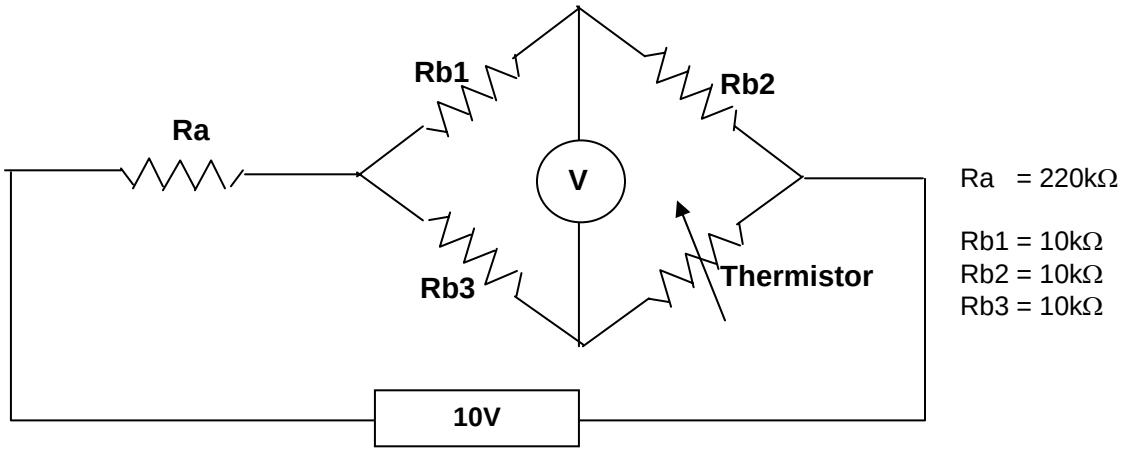

Figure 3.16: Schematic diagram of Thermistor configuration.

The unique resistance vs. temperature curve of the thermistor is provided by the manufacturer. The corresponding variation of voltage measured over the Wheatstone bridge and temperature is plotted at *Figure 3.17*. The fitted equation can be written as

$$T = 0.5 \exp(0.335 \times mV/V) + 1.5 \times (mV/V) - 0.5 \quad \text{.....Equation 3-1}$$

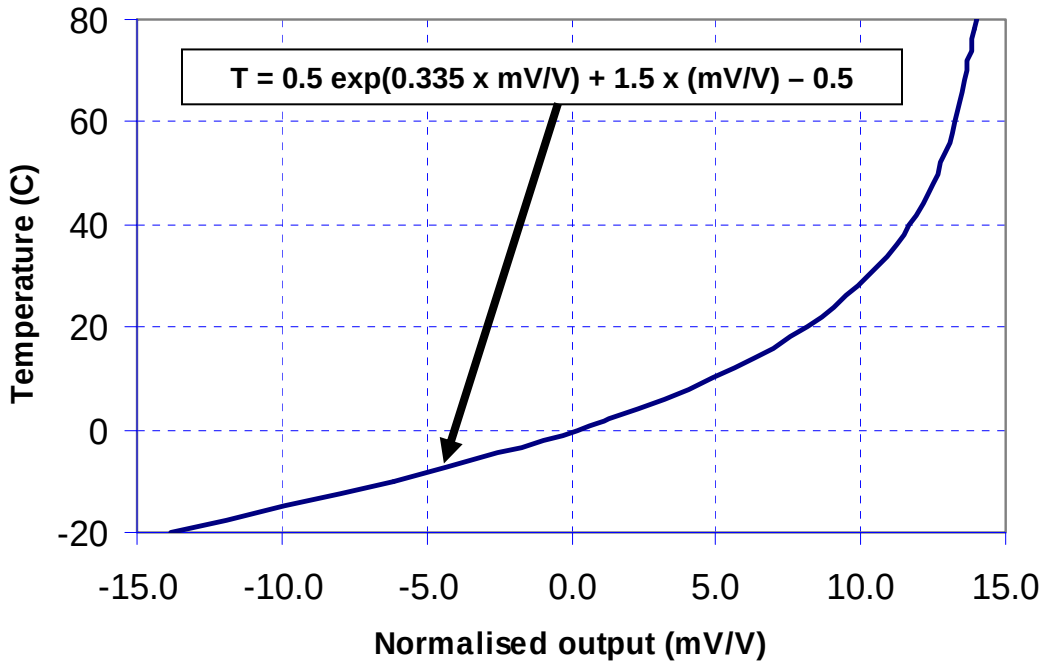

Figure 3.17: Variation of voltage (mV/V) output across the Wheatstone bridge versus the change in temperature.

3.3.3.7 Silicone Fluid

There is no one single fluid which is ideally suited for the piezometer. In practice, the commonly used fluid is de-aired water mixed with some ethylene glycol (antifreeze mixtures). However, the de-aired water is prone to evaporation in dry areas (such as the Colorado deserts). Instead, a non-volatile silicone fluid is used as the pressure transfer medium between the external water pressure and the internal measuring system.

The silicone oil is a clear, colourless polydimethylsiloxane and is formed from multiple chains of $(Si\text{-}CH_3\text{-}CH_3\text{-}O)_n$ (*Figure 3.18*). The number of the $(Si\text{-}CH_3\text{-}CH_3\text{-}O)$ chains dictates the mass, density and the viscosity of the silicone oil. The Dow Corning

230CST silicone oil has low viscosity of 20PaS (or 20 Centistokes) and density of 94g/cc at 25^{O}C. Silicone oil, with its large molecular structure, is generally inert to most field conditions; relatively stable between temperatures of –20^{0}C and 50^{0}C and does not evaporate in dry weather.

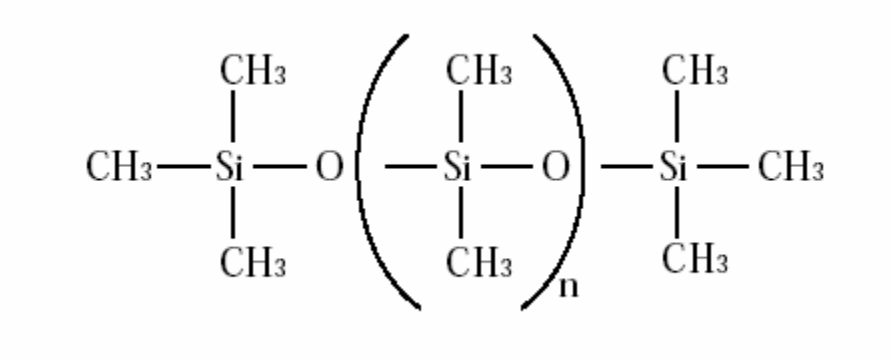

Figure 3.18: Molecular structure of polydimethylsiloxane silicone oil

The viscosity of the silicone fluid dictates the fluidity and the pressure transfer time response of the medium. Silicone fluid with viscosity of 20PaS has viscosity twenty times that of water (0.98PaS at 25^{O}C) and responds more slowly to pressure changes the water (see also Section *3.3.2*). The real time response for the piezometer using silicone oil is not known but is not expected to exceed a few seconds (i.e. this is not critical in the current application with a sampling rate of one measurement per hour).

The density of the silicone fluid is a function of ambient temperature; a 75^{0}C change in temperature results in 10% change in the density of silicone oil (*Figure 3.19*). The density-temperature effect is small for the piezometer as the ground temperature is close to constant (varying only be a few degrees Celsius throughout the four seasons in a year). However, the converse is true for the settlement probe since part of the silicone fluid is exposed to the atmospheric temperature. (see *Section 3.4.2.10*).

The silicone fluid is generally inert, non-corrosive, relatively stable and is only susceptible (will be chemically broken down) to hydrogen fluoride (not likely to be encountered in field monitoring). However, the long term performance and compatibility with Motorola transducers has not been investigated by the manufacturer.

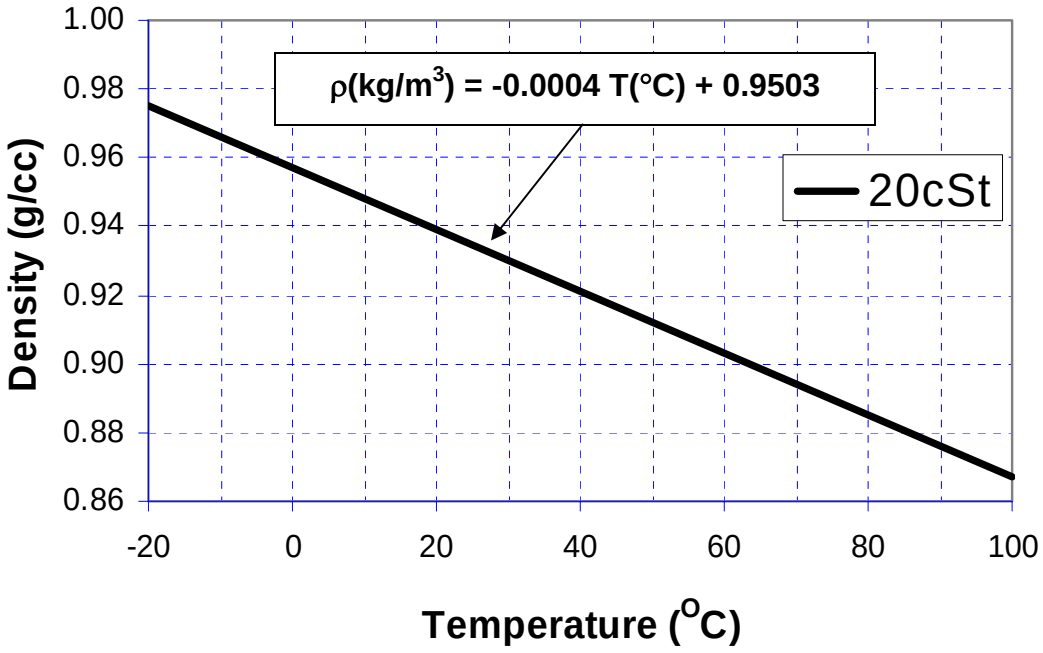

Figure 3.19: Density vs. Temperature graph for 20cSt silicone oil.

The importance of using fully saturated (or deaired) piezometer and settlement probes are accentuated in *Section 3.3.2* and *3.4.2.9*. However, atmospheric gasses are soluble in silicone oil and may slowly diffuse into the equipment. Some of the soluble gasses are shown in *Table 3.2*.

Table 3.2: Solubility of gasses in silicone oil.

Solubility of Gases	
Gas	**Ml gas/ml liquid @25 °C**
Nitrogen	0.16 – 0.17
Carbon Dioxide	1.00
Air	0.16 – 0.19
Hydrogen	0.11 – 0.12

3.3.3.8 Assembling the electronic components

The transducer, thermistor and the Wheatstone bridge are wired together as shown in *Figure 3.20*. The transducer and thermistor are connected in parallel to the 10 V power supply. Three pairs of wires are used in total: a pair (black and red) to provide 10V power, a pair (white and green) to receive transducer output readings, and a pair (two blues) to receive the thermistor output readings. The wires are soldered at the connection point to ensure good signal connection. However, the MPX series transducers are sensitive to heat and the soldering temperature should not exceed 260^{O}C for more than 10 seconds, to avoid damage to the delicate electrical components of the transducer (Motorola 2003).

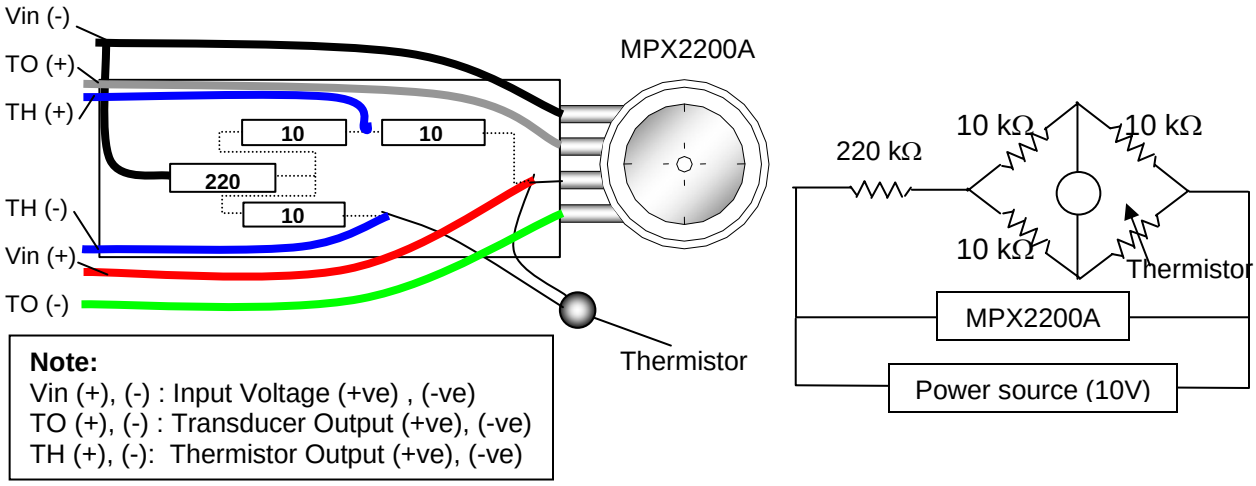

Figure 3.20: Transducer, Thermistor and Wheatstone bridge configuration.

The electrical components are inserted into a hollow cylinder (component iv in *Figure 3.7*) and encapsulated with epoxy. The epoxy provides two important functions: a) to hold the electronic components in the steel cylinder and to protect them from vibrations and shock, and b) to provide electrical insulation from water and silicone oil. The general purpose Stycast 2651 epoxy and catalyst 9 from Emerson & Cuming is suitable for this application.0

The recommended practice for preparing the epoxy is as follows:

Weigh (up to 0.01 gram resolution) the required amount of Stycast 2651 liquid. Now, weigh the Catalyst 9 exactly 7% of the mass (or 11.5% by volume) of the Stycast 2651 and thoroughly mix the two components with a rod. It is important to mix the two components according to the exact specified ratio in order to achieve the ideal epoxy properties and strength (Stycast Manual).

Once the components are mixed, there are about 45 minutes of working time before the epoxy hardens. Place the liquid epoxy in the vacuum chamber for 10 minutes to remove entrapped air bubbles. Do not exceed 10 minutes or else the individual components will start to separate.

Carefully pour the epoxy into the steel cylinder and allow 16 hours (if at room temperature of 24°C) for the epoxy to set. The recommended hardening temperature is, in fact, 45°C (although not entirely necessary and is not followed here). At higher temperature, the viscosity of the epoxy reduces, and the epoxy is able to flow between tight spaces in the electronic board and provide better encapsulation. In addition, the hardening time will be reduced to just 5 hours.

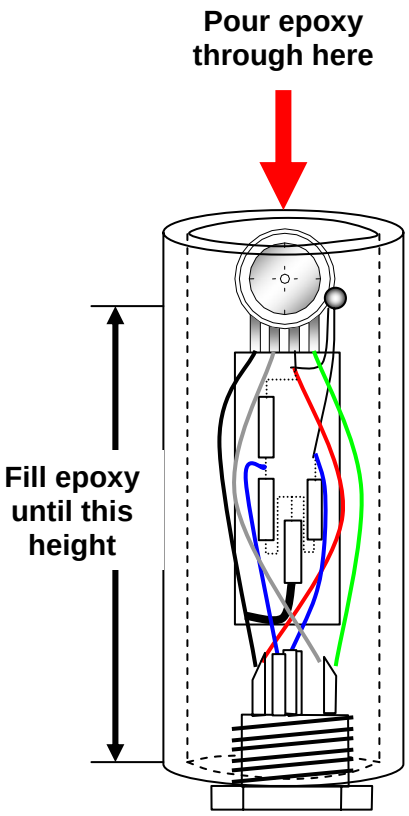

Figure 3.21: Epoxying the transducer element

3.3.3.9 Saturation

The saturation process is achieved by saturating three components: porous stones, deaired liquid, and the pressure transducer. The porous stone is saturated by immersing into a silicone oil bath and placing it in an ultrasound chamber for at least 24 hours. The silicone fluid is deaired by means of a vacuum chamber. The pinhole in the pressure transducer is saturated by injecting silicone fluid by using a hypodermic syringe. During installation, it is important to ensure that the fluid chamber is properly filled with silicone fluid. This is done by immersing the fluid chamber under a pool of silicone oil (achieved by using a plastic reservoir) and closing the conical head while ensuring no air is trapped at the underside of the component (*Figure 3.22*). This plastic reservoir technique is portable and saturation can be performed on site relatively easily (using pre-saturated stones).

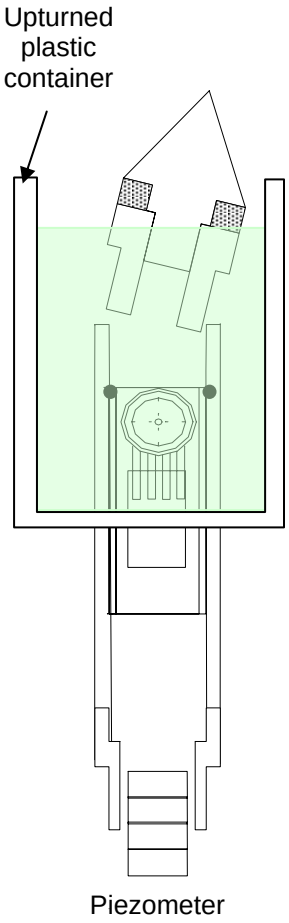

Figure 3.22: Saturating the piezometer.

3.4 Liquid vertical settlement probe

3.4.1 Introduction

The vertical settlement probe is a single point liquid settlement probe with a fixed reservoir head on one end and a pressure transducer (hydraulically connected to the reservoir via small tubing) embedded in the ground. The liquid settlement probe offers a viable way of measuring the vertical deformation in terms of ease of installation, accuracy, and location selection. The measurement of the vertical deformation is made by measuring the changes of fluid pressure in the sensor end relative to a fixed fluid-head datum. The principle is demonstrated in *Figure 3.23*, whereby any increase in the vertical settlement results in an increase of fluid pressure measured by the transducer at the sensor end, therefore enabling calculation of the settlement if the density of the fluid is known (i.e. $H = P / \gamma_s$ (γ_s – unit weight of the silicone oil)). The liquid settlement probe has the advantage of being small, easy to install, and cost effective. In addition, once the head datum is fixed, the probe can be installed at virtually any depth and orientation, thus achieving high flexibility for sensor placement and installation. Unlike plate settlement sensors, (where a relatively large area of soil has to be excavated), this settlement probe can be easily installed through a 3 cm diameter hole made by a hand auger. The settlement probe is designed to share similar parts with the piezometer in order to reduce manufacturing costs.

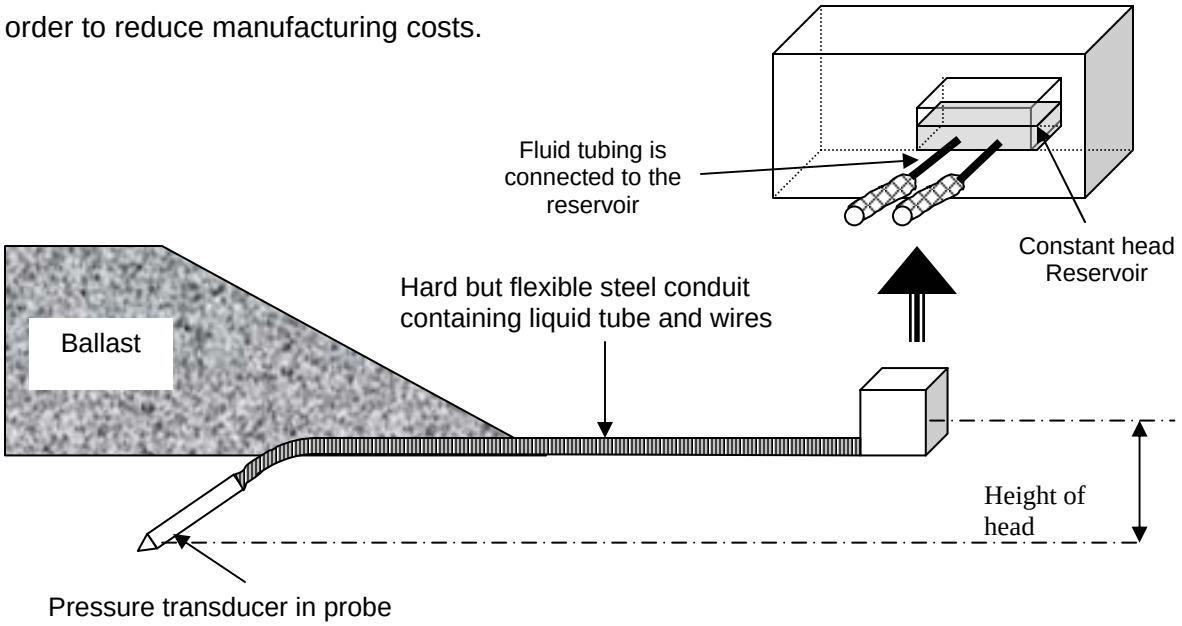

Figure 3.23: Liquid settlement probe.

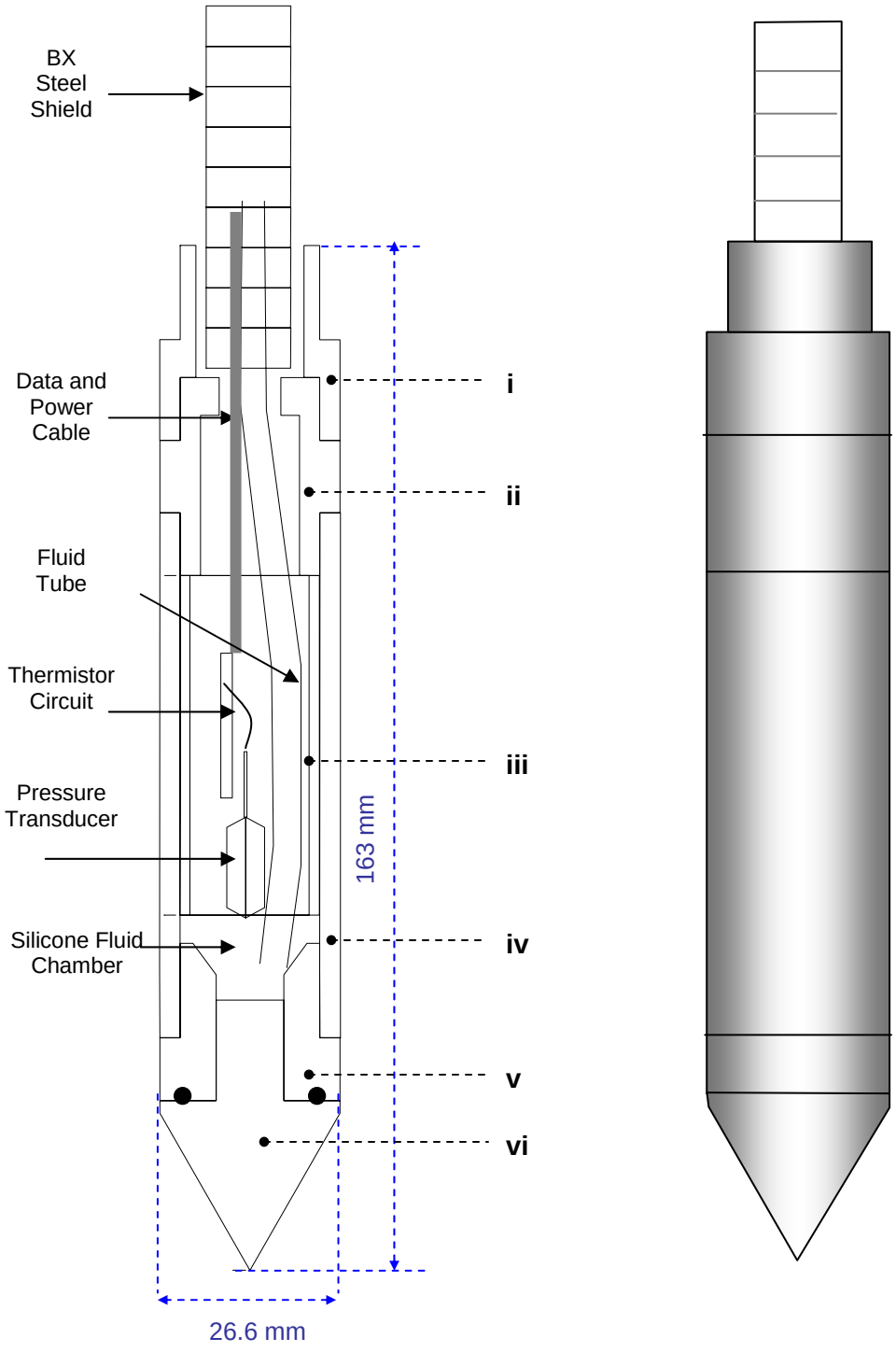

Figure 3.24: Design of Settlement Probe (to scale)

3.4.2 Conceptual design and components

The settlement probe is made of four main sections: a) Measuring system consisting of absolute MPX2100A pressure transducer and a thermistor, both encapsulated in epoxy (to provide physical protection), b) Fixed fluid reservoir datum (for reference pressure), c) Liquid tubing and silicone oil to transfer the pressure from the reservoir to the pressure transducer, and d) Outer stainless steel body that houses and protects the delicate measuring system, and data cables connecting the piezometer to the data acquisition. The delicate data cable and tubing is protected from train loadings and background electrical noises by an aluminium BX sheath.

3.4.2.1 Body

The body of the settlement probe is similar to the piezometer. It is made of 304 Stainless Steel and has six major components (as labelled in *Figure 3.24*).

Component (i) Conical Head

The conical head has a sharp tip angled at 56° to aid push-in installation and is attached to component ii. The o-ring groove is located at the "shoulder" of the conical head to keep the o-ring in place to provide sealing for the chamber.

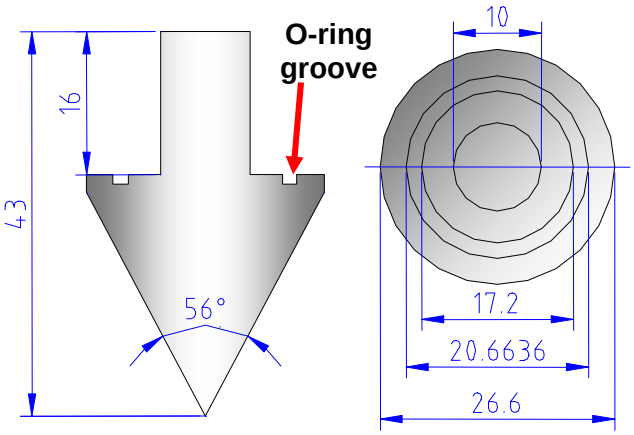

Figure 3.25: Component i: Conical head

Component (ii)

Component ii and component v help to keep component iv (electronic sensor) in position. It also holds on to the conical head (component iii). The conical head is detachable to aid the process of saturation.

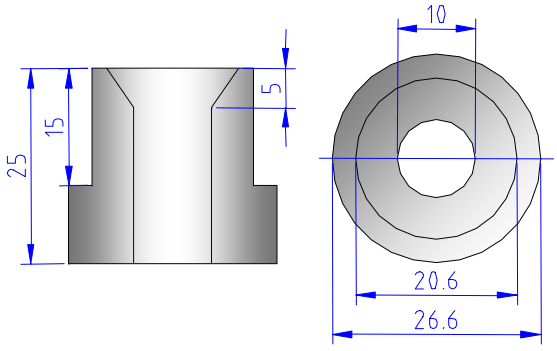

Figure 3.26: Component ii

Component (iii)

The steel body is similar to body of the piezometer (Section *3.3.3.1*)

Component (iv)

The pressure transducer and the thermistor is contained in component iii and held by epoxy. The tubing goes through the epoxy to reach the fluid chamber near the conical head. Care has to be taken to ensure that the tube is positioned close to the centre of the cylinder so that the end of the tube is not blocked by the side walls of component v.

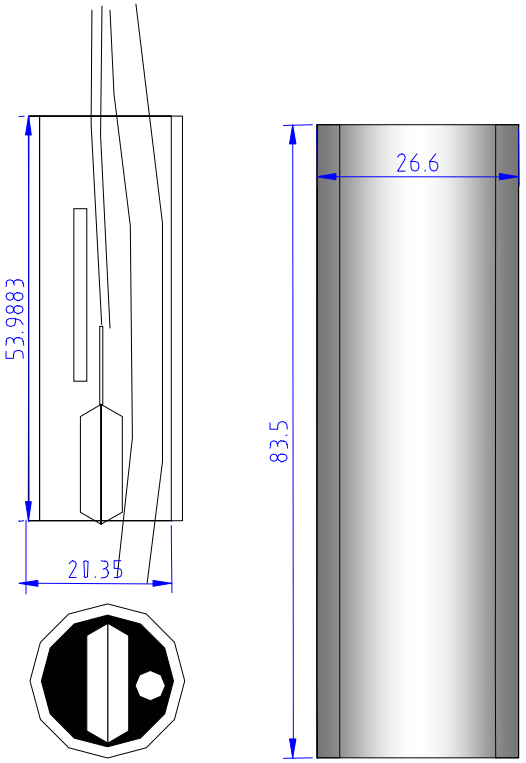

Figure 3.27: Left (component iv) and right (component iii)

Component (v)

Component (v) works in tandem with component vi to grip the BX cable. Unlike the piezometer, no rubber sealing is required because there is no electrical connection in the chamber because the 6 metres of cable are directly connected to the electronic circuit board.

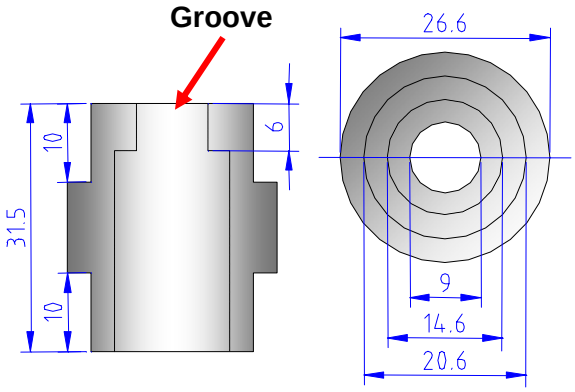

Figure 3.28: Component v

Component (vi): BX gripper

The principal of the BX gripper is similar to component vi in the piezometer (Section 3.3.3.1). The BX cable and the compressible polyester are placed into the groove of component v. The gripping action on the BX cable is obtained when component vi is tightly screwed into component v.

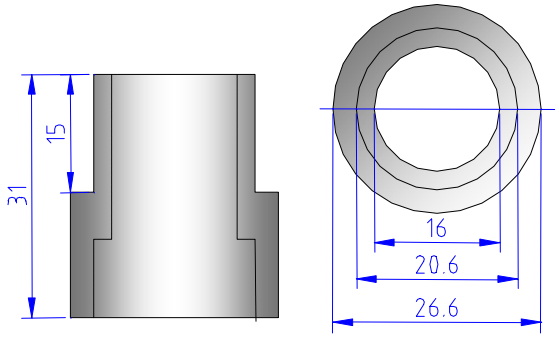

Figure 3.29: Component vi: BX gripper

3.4.2.2 Sealing

The sealing of the silicone fluid chamber represents the critical part of the probe design: faulty sealing could lead to draining of the silicone oil and affect the performance of the system. Sealing is done by means of rubber O-rings between component (v) and (vi) and silicone sealant to block paths along the component (iii) and (iv) interface. The O-ring size 017 (21 mm diameter and 1.9 mm thick) is used and is obtained from McMaster-Carr.

3.4.2.3 Tubing

The tubing is used to connect the reservoir to the pressure transducer in the embedded probe. 4 mm Nylon 11 tubing with internal diameter of 2.7 mm and external diameter of 3.97 mm is used for the settlement probe. The tubing is tough (Rockwell R: 78), has tensile strength of 66500 kPa and has working temperatures range of –10°C to 93°C. It is also chemically stable to silicone oil and is impermeable to air (i.e. prevents air from diffusing into the silicone oil).

3.4.2.4 Cable and BX cable

Belden 89503 cable has three pairs of 24 AWG wires (each pair has a 24 AWG drain wire and individually shielded by Aluminium Foil-Polyester Tape (Bedfoil)), and is wrapped by flame resistant Fluorinated Ethylene Propylene (FEP) jacket. The external diameter is 4.3mm and has an operating temperature rating of –70 to 200^0C, well above the required in-situ temperature. The resistance of the cable is sufficiently small - 24.1Ω / 305m, measured at 25C. The data cable is protected by a steel 5/16” BX sheath, with internal and external diameter of 7.7mm and 12.7mm respectively.

3.4.2.5 Transducer and Thermistor

Motorola MPX2100A absolute pressure transducer (Section *3.3.3.5*) and Omega 44005 thermistor (Section *3.3.3.6*) is used to measure the silicone head pressure and temperature in the probe respectively. In order to protect the transducer, thermistor and its Wheatstone bridge circuit, these components are encased in epoxy (Stycast 2651; Catalyst 9). The Motorola MPX2100A absolute transducer has pressure capacity of 100 kPa (14.5psi), input voltage of 10V, full-scale span of 40mV, and calibration of 2.5

kPa/(mV/V). An absolute pressure transducer is used to eliminate the uncertainty and logistical difficulty of ensuring that a gage transducer is properly vented to the atmosphere. MPX2100A utilises a strain gauge (implanted in a monolithic silicone piezoresistor), which generates output voltage proportional to the applied pressure. A temperature compensated circuit is also built into the transducer and works well for temperature range 0^{o}C to 85^{o}C. The full specifications for MPX2100A are given in *Table 3.3*.

Table 3.3: Manufacturer Specification for MPX2100A (Motorola).

The manufacturer specification of the transducer is given in the table below:

Characteristics	Symbol	Min	Typical	Max	Unit
Pressure range [1]:	Pop	0	-	100	kPa
Supply Voltage [2]	V_S	-	10	16	Vdc
Full Scale Span [3]	V_{FSSS}	38.5	40	41.5	mV
Offset[4]	V_{OFF}	-2.0	-	2.0	mV
Sensitivity	$\Delta V/\Delta P$	-	0.4	-	mV/kPa
Linearity [5]	-	-1.0	-	1.0	$\%V_{FSS}$
Pressure Hysteresis [5] (0 to 100 kPa)	-	-	+0.1	-	$\%V_{FSS}$
Temperature Effect on Full Scale Span[5]	TCVFSS	-1.0	-	1.0	$\%V_{FSS}$
Temperature Effect on Offset [5]	TCVoff	-1	-	1.0	mV
Input Impedance	Z_{in}	1300	-	2500	Ω
Output Impedance	Z_{out}	1400	-	3000	Ω
Response Time[6] (10% - 90%)	t_R	-	1.0	-	ms
Warm – Up	-	-	20	-	ms
Offset Stability [7]	-	-	±0.5	-	$\%V_{FSS}$

OPERATING CHARACTERISTICS (VS = 10 Vdc, TA = 25°C unless otherwise noted, P1 > P2)

1. 1.0 kPa (kiloPascal) equals 0.145 psi.
2. Device is ratiometric within this specified excitation range. Operating the device above the specified excitation range may induce additional error due to device self–heating.
3. Full Scale Span (VFSS) is defined as the algebraic difference between the output voltage at full rated pressure and the output voltage at the minimum rated pressure.
4. Offset (Voff) is defined as the output voltage at the minimum rated pressure.
5. Accuracy (error budget) consists of the following:
   - Linearity: Output deviation from a straight line relationship with pressure, using end point method, over the specified pressure range.
   - Temperature Hysteresis: Output deviation at any temperature within the operating temperature range, after the temperature is cycled to and from the minimum or maximum operating temperature points, with zero differential pressure applied.
   - Pressure Hysteresis: Output deviation at any pressure within the specified range, when this pressure is cycled to and from the minimum or maximum rated pressure, at 25°C.
   - TcSpan: Output deviation at full rated pressure over the temperature range of 0 to 85°C, relative to 25°C.
   - TcOffset: Output deviation with minimum rated pressure applied, over the temperature range of 0 to 85°C, relative to 25°C.
6. Response Time is defined as the time for the incremental change in the output to go from 10% to 90% of its final value when subjected to a specified step change in pressure.
7. Offset stability is the product's output deviation when subjected to 1000 hours of Pulsed Pressure, Temperature Cycling with Bias Test.

3.4.2.6 Reservoir

The reservoir is comprised of 230 x 120 x 90 mm or (9” x 5” x 3.5”) Rubbermaid clear plastic container capable of accommodating up to 5 settlement probes. The side of the reservoir is fitted with Swagelok fittings to enable easy attachment and detachment of the tubes. The quick connect fittings are generally expensive (costing up to USD$30 a piece) and an alternative cheaper method can be used. An effective sealing can be achieved by using a male connector (with O-ring fittings, Male SAE/MS straight thread, 3/16), a ferrule and rubber o-ring to seal up the tubing (*Figure 3.30*). The ferrule, as oriented in the diagram, is pressed against the o-ring seal as the female connector is tighten against the male connector, thus providing sealing. This connection will not, however, work if the tubing is under tension as it will easily slide off the connection. The male connector is attached to the reservoir wall by a female connector. The in-built o-ring in the male connector provides sealing against the reservoir wall. The reservoir is exposed to the atmosphere (not sealed) and the fluid pressure is subjected to the atmospheric pressure.

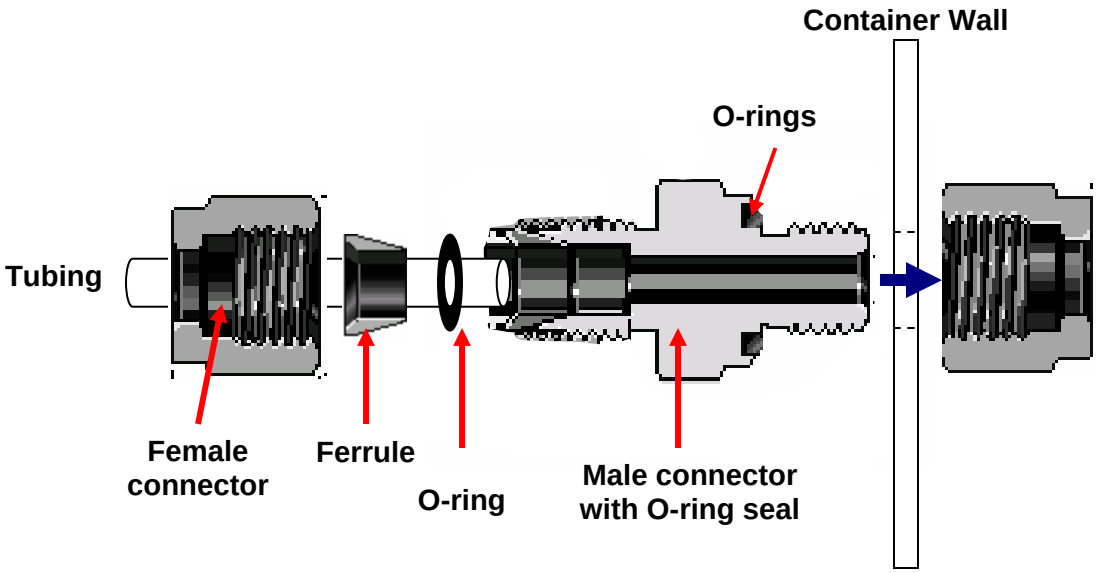

Figure 3.30: Quick connect mechanism for the reservoir

3.4.2.7 Assembling the electronic components

The transducer and the thermistor are assembled in a similar manner to the electronic setup for the piezometer (*Figure 3.20*). The six metres of data cable is connected to the transducer circuit board (and not through a connector as used in the piezometer design). The tubing is inserted into component iii together with the transducer circuit board before encapsulating the section in epoxy.

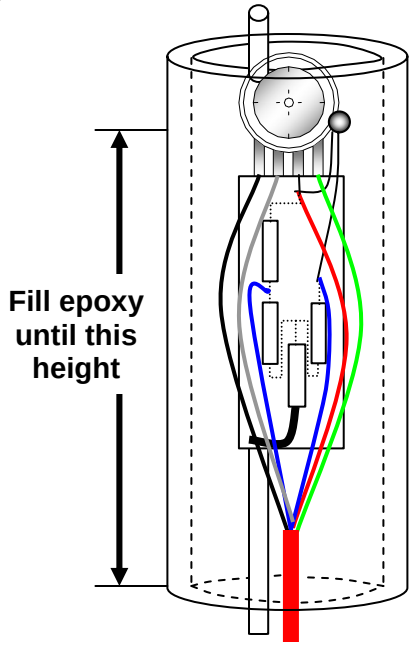

Figure 3.31: Assembling the electronic components for settlement probe

3.4.2.8 Silicone oil

The silicone oil is used as the pressure transfer medium between the reference datum above ground and the embedded probe. The important properties of silicone oil are discussed *Section 3.3.3.7*.

3.4.2.9 Saturation of the settlement probe

The saturation of the settlement probe is very important, as any discontinuity in the tube due to bubbles will affect the measurements. The settlement probe relies on the ability of the silicone fluid to transfer the pressure from the reservoir to the transducer in the probe. Pockets of gasses in the liquid tube may affect the pressure transfer and effectively block a small tube (Penman 1978). At each gas/water meniscus, surface tension causes the gas bubbles to be at a slightly higher pressure than the water. When the pressure is applied on one end of the tube, the gas/water menisci yield to attempt to oppose the direction of the applied pressure, and effectively reduce the magnitude of the

applied pressure. For example, 1000 gas bubbles in a liquid filled tube can resist pressure of up to 100kPa (DUNNICLIFF 1988).

There are three processes which air could enter the system: dissolved gas in the liquid, diffusion through the tubing itself (certain types of gasses and tubing), and through the end of the tube. The first process can be addressed by removing air from the silicone fluid by means of a vacuum chamber before filling up the settlement probe. When the deaired silicone fluid is transferred to the settlement probe, agitation must be avoided to prevent reintroduction of air into the system. Experiments performed by HAYWARD (1959) show that Nylon 66 wall tubing is impermeable to gas, and is therefore recommended for use in the settlement probes. Finally, gasses may enter the system through the open end (which is the reservoir for this particular case) if the silicone fluid is exposed to air for a period of time. *Table 3.2* shows the solubility of gasses in silicone oil, and carbon dioxide is one of the major gasses which are highly soluble in silicone oil (1mg of carbon dioxide dissolves in 1mg of silicone oil). If the dissolved gasses diffuse inside the tubing, this will cause discontinuity (forming bubbles) in the liquid and will influence the settlement readings.

During installation, the saturation process can be performed by removing the conical head (i) and allowing de-aired silicone fluid to flow from the reservoir, through the tubing and the probe. The conical head is then tightly closed after allowing deaired silicone oil to flush through the system for a few minutes. The pin-hole in the transducer is saturated by using a hypodermic needle in the field.

3.4.2.10 Temperature effects

The temperature affects the settlement reading in two ways: a) it affects the transducer's offset readings, and b) it changes the density of the silicone oil in the probe, tubing and reservoir. The former is an inherent problem of all electronic transducers and is addressed in *Section 4.3.2*. The latter develops when a section of the fluid tubing is exposed to differential temperature between the ground and varying atmospheric temperature. This cause non-uniform fluid density along the course of the tubing and must be accounted for. The high latent heat capacity of the ground ensures that the ground temperature remains oblivious to the daily temporal fluctuations of temperature as experienced by the atmosphere (*Figure 3.32*). As shown in the figure, the ground temperature remains at a constant $11^{O}C$ to $13^{O}C$ while the atmospheric temperature

cycles between 5^{O}C and 30^{O}C. With such dramatic changes in the temperature, error corrections can amass up to 2.5cm.

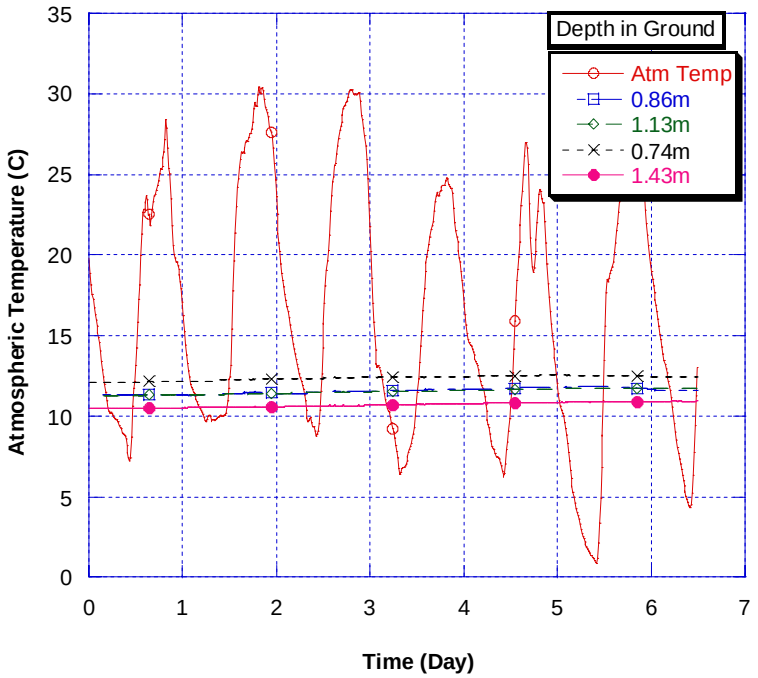

Figure 3.32: Variation of ground and atmospheric temperature with time (from TTCI field data)

3.5 Junction Box

The junction box serves as an intermediate connection point between the data acquisition and the installed sensors, and houses the reservoir for the settlement probes. It is a 17” x 10” x 4” aluminium enclosure, protected from the environment by an outer plastic shell. The reservoir for the silicone oil is a 230 x 120 x 90 mm or (9” x 5” x 3.5”) Rubbermaid plastic container and snugly fits in the steel enclosure.

The junction box can accommodate up to 7 probes and one reservoir transducer (16 differential channels). Wires from the data acquisition are permanently soldered onto the underside of the soldier turrets. Wires from the probes are easily connected on to the screw head at the top side of the soldier turret. This arrangement facilitates easy on-site connection and the wires arrangement is shown in *Figure 3.34*.

3.5.1 Electrical Grounding

The electrical grounding design warrants special consideration, since a poorly designed electrical system generates noise that drowns useful measured data. There are two different grounds used in the system: a) common electrical ground, and b) analogue ground. The single common electrical ground, as its name implies, drains all unwanted electrical charges into the ground. The electrical ground, consisting of a grounded 3m copper rod, is attached to the junction box. All the steel BX cables and internal cable drain wires are electrically connected to the junction box where excess charges are subsequently drained. The steel BX cables and the external steel wall of the junction box act as a Faraday cage, protecting the inner sensitive data cables from environmental noises. The analog ground, on the other hand, sets the zero voltage potential for the low-end of the power supply. This prevents differential voltage floatation which will affect the output in the sensors. The grounding system is neatly summarised in *Figure 3.33*.

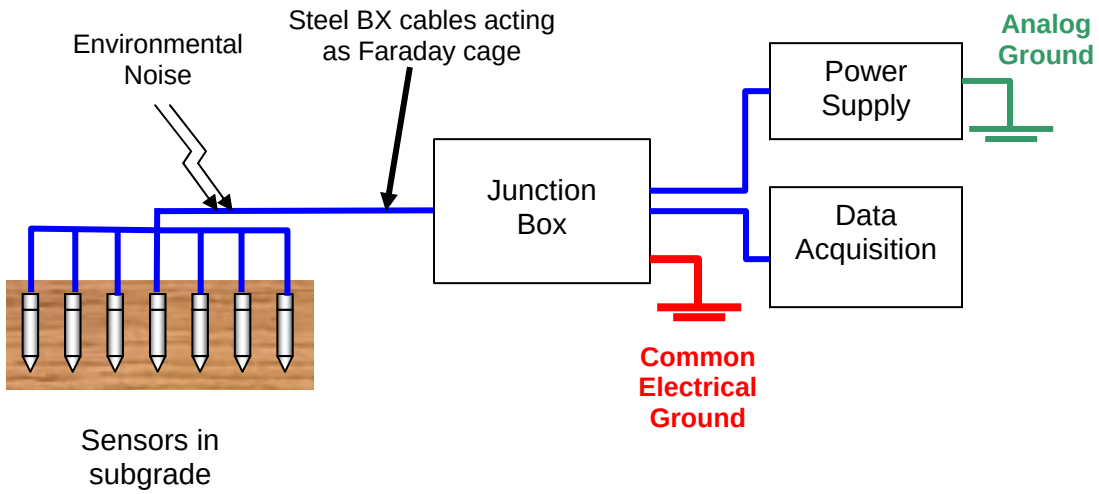

Figure 3.33: Schematic of the electrical grounding.

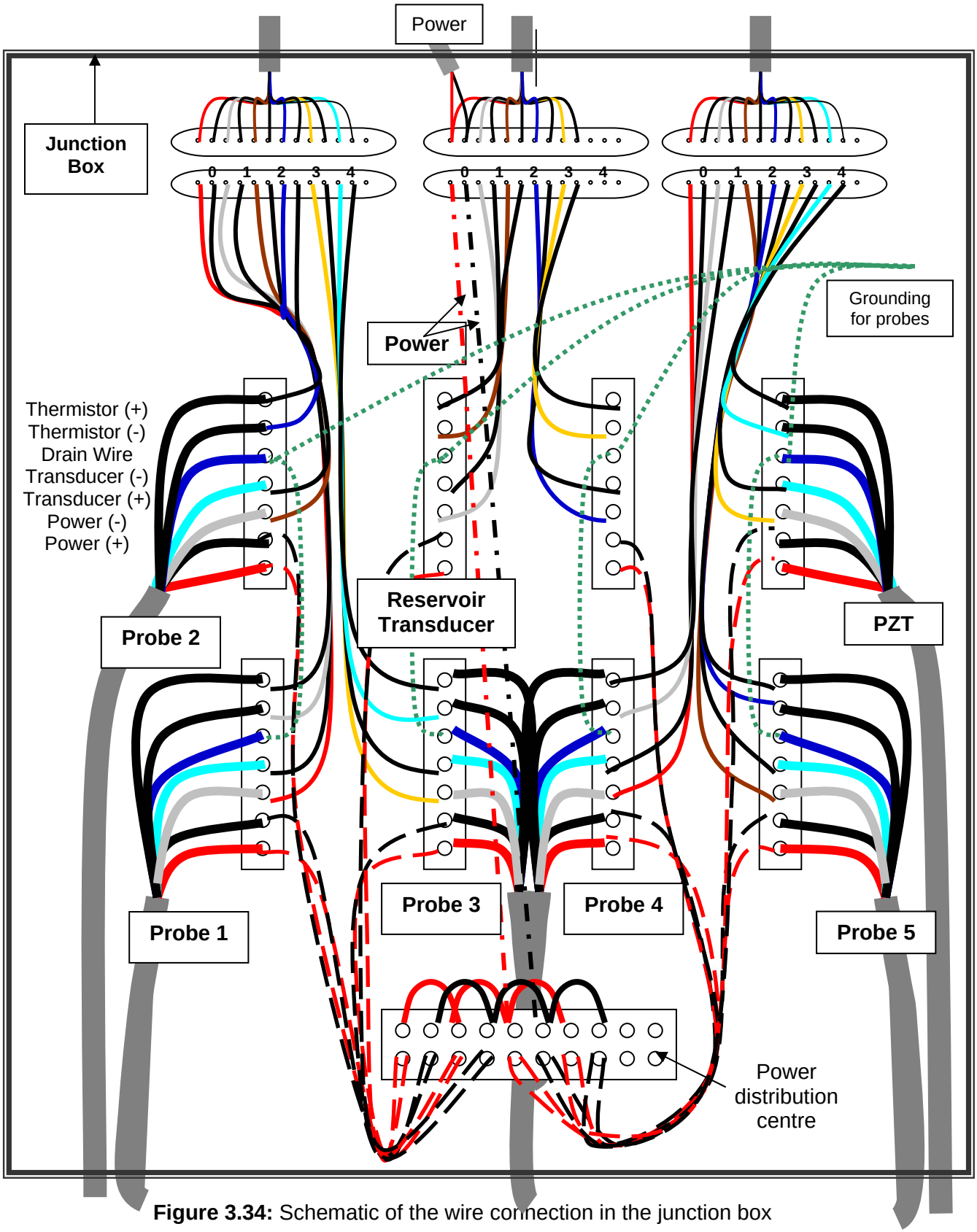

Figure 3.34: Schematic of the wire connection in the junction box

3.6 Data acquisition system

The data acquisition system consists of an Iotech DAQ 55 and a laptop computer. The DAQ 55 is an external data acquisition module and is easily linked to the laptop the Universal Serial Bus (USB). The DAQ 55 (*Figure 3.35*) has been selected because it is portable (182 x 92 x 45mm), lightweight, high resolution (22 bit), and stability of 0.00003 mV and 0.001mV respectively and has relatively low cost ($1800).

Figure 3.35: Iotech Personal DAQ 55 connected to the expansion module (Courtesy of Iotech, DAQ 55)

A single DAQ 55 provides five differential channels for the sensors, which is insufficient for the required 15 differential channels of the monitoring system. However, combining the DAQ 55 and the PDQ2 expansion module will increase the channels to 25 differential channels. If necessary, the data collection capability of the monitoring system can be greatly expanded by connecting up to 100 DAQs through a hub, thus providing more than 2500 differential channels (*Figure 3.36*). The hub is easily connected to the laptop via a single USB cable for further processing. Each of the modules requires 2.5W power input (including expansion sets). This becomes a critical issue in remote monitoring system where a self-sustaining power supply is needed.

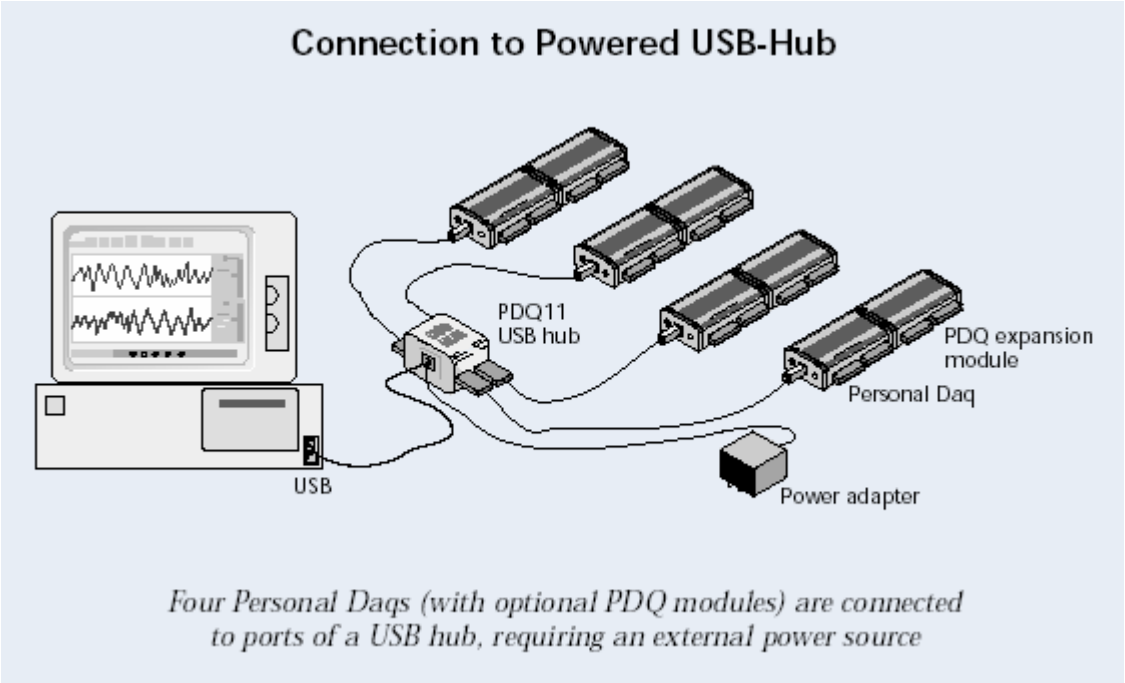

Figure 3.36: More PDQs can be connected to a USB hub, thus increasing the data acquisition capacity of the system. (Courtesy of Iotech, DAQ 55)

The DAQ 55 is a 22-bit data acquisition and has a selection of inputs ranging from ± 31mV to ± 20V (see *Table 3.4*). The MPX series sensors have maximum output voltage of 40mV. The settlement probe requires a minimum resolution and stability of 0.1mm and 1mm respectively; the piezometer needs 7.5 x 10^{-5} kPa and 7.5 x 10^{-3} kPa. The requirements can be accommodated by taking sampling rate of 610ms and voltage range of ± 62.5 mV. The corresponding resolution and noise (claimed by Iotech) of the DAQ 55 is 0.00003mV (0.085 mm) and 0.001 mV (2.54 mm) respectively (*Table 3.5*). The thermistor will require voltage range of ± 156 mV at sampling rate of 610 ms. Each channel can be independently programmed to have different sampling rate and resolution.

Table 3.4: Sampling integration rate and resolution. (modified from Iotech)

Measurement Duration (per channel)	Maximum Sample Rate (Samples/sec)	Resolution (Bits RMS) (-4V to +4V range)
610 ms	1.6 / sec	22
370 ms	2.7 / sec	22
310 ms	3.2 / sec	22
130 ms	7.7 / sec	21
110 ms	9.2 / sec	21
40 ms	25 / sec	19
20 ms	48 / sec	17
12.5 ms	80 / sec	15

Table 3.5: Iotech recommendation of the inherent system noise in DAQ 55.

Programmable Voltage Ranges	RMS Noise (μV) Typical					
	610 ms	370 ms	130 ms	40 ms	20 ms	12.5 ms
± 20V	120	120	120	120	270	1600
± 10V	35	35	35	75	190	740
± 5V	7	7	10	60	95	370
± 4V	4	4	5	20	60	340
± 2.5V	4	4	4	15	30	150
± 1.25 V	2	2	3	9	20	110
± 1V	2	2	3	15	20	75
± 625 mV	3.5	3.5	4.5	10	15	50
± 500 mV	1	1.5	2	15	15	40
± 312 mV	3	3	4	8	10	30
± 250 mV	1	1	2	8	8	25
± 156 mV	2.5	4	4	8	8	20
± 125 mV	1	1	1.5	7	7	20
± 62.5 mV	**1**	**1**	**1.5**	**6**	**5**	**9**
± 31 mV	1	1	1.5	6	5	7

The DAQ 55 comes with Personal DaqView software which enables easy channel and reading setups. The Personal DaqView can be expanded and modified to include user-defined features by using DASYlab®.

3.7 Remote Control System

The remote control capability is provided by the PC Anywhere 10.5 remote control software and can be established if there is a good link (via the Internet) between the on-site computer and the computer at MIT. The host computer (the on-site computer which is being controlled) bestows its full operational control to one or more client computers (computer at MIT) and the collected data can be transmitted from the host to the client computer. Files such as the collected data and programs can be transferred in both directions between the host and the client computers. The host and the client computers are identified by their unique IP addresses, provided by TTCI and MIT respectively.

Security and unwarranted system tapping remain an important concern towards providing a secure and reliable remote control link. There are two levels of security barrier incorporated into the system. The first level of authentication consists of prompting host and client computer passwords. If necessary, different levels of access based on ones responsibilities can be granted to different users. The second level of security involves limiting the remote connections to specific IP addresses. The TTCI computing network provides access only to computers which are involved in the research.


Laboratory
Testing

Chapter 4: Laboratory Testing

4.1 Introduction

The monitoring system, consisting of electronic sensors and data acquisition has been calibrated and evaluated in the MIT Geotechnical Laboratory before the field installation at TTCI, Colorado. In general, the monitoring system can be characterised by four different measures:

1. Data acquisition (Iotech DAQ 55) stability and resolution
2. Motorola Transducer stability and resolution (for both MPX2200A for piezometer and MPX2100A for settlement probe)
3. Complete probe stability and resolution (piezometer and settlement probe)
4. Temperature sensitivity of the probes

4.1.1 Noise and signal management

The noise characterisation for the data acquisition and the pressure transducers are summarised in *Table 4.1*. The data acquisition can be characterised in terms of resolution and system noises; the pressure transducers in terms of sensitivity, linearity, hysteresis, drift, and noise. Temperature fluctuation causes shifts of the offsets in the transducers and can be reduced by applying temperature corrections. Noise arises from changes of atmospheric conditions and interference can be minimised by good cable shielding and grounding. During data analyses, random fluctuations in the data can be further reduced by using techniques such as averaging and filtering.

Table 4.1: Noise characterisation in the measuring system.

Data Acquisition	Resolution	Smallest quantifiable change in the sensors readout scale. Function of sampling integration rate – longer the integration rate, better the resolution (bits).
	System noise	Shunted error band (environmental influences etc)
		Drift (shift of the offset over time – causes systematic error)
Pressure transducers	Resolution	Infinite in theory, limited only by the resolution of the data acquisition. Often, the sensitivity and noise governs the operating characteristics of the transducer rather than its resolution.
	Sensitivity	Calibration factor – how much voltage output for a given change in the measurand. It is expressed in terms of cm/mV/V and kPa/mV/V for settlement probe (MPX2100A) and piezometer (MPX2200A) respectively.
	Linearity	How close the output of the transducer with respect to the change in measurand approximates a straight line.
	Hysteresis	Cycling between the maximum and minimum of the measurand may cause the readings to follow different paths
	Drift	Changes of initial offset over time. Drift could be a result of creep in the measuring diaphragm, relaxation of the electrical connections, heating and etc.
	Noise	Electrical noises
		Environmental noises (lightning, temperature fluctuations, etc)
		Imperfect wire connections and soldering

4.2 Data acquisition

During the course of laboratory testing and calibration, two types of data acquisition are being used: the MIT Geotechnical Laboratories Central Data Acquisition, and the Iotech Personal DAQ 55. Most of the laboratory characterisation of the pressure transducer and the complete probe was performed by using the Central Data Acquisition, as the Iotech DAQ 55 was only selected at a much later stage. In this section, the inherent resolution and stability of the Iotech DAQ 55 will be investigated.

4.2.1 Iotech Personal DAQ 55

The Iotech Personal DAQ 55 and the expansion module PDQ2 have been selected as the field data acquisition unit (see *Section 3.6*). The calibration of the DAQ 55 has been performed by the manufacturer prior to shipment. Calibration should be performed at least once per year to ensure good accuracy and the method of calibration can be found in the Iotech User's Manual. The system stability can be characterised by two main components: drift and static noise. The DAQ 55 unit has in-built automatic

calibration function to reduce the former. The calibration function, aimed at reducing drift, can be executed between the sampling readings (*Figure 4.1*).

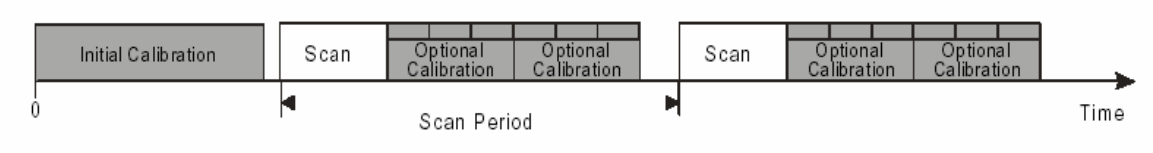

Figure 4.1: Automatic calibration for the DAQ 55.

The latter refers to the inherent system stability of the DAQ 55. Iotech (2001) reports that the channel with range of ± 62.5 mV integrated at 610ms (22-bit) will provide stability of 0.001 mV (2.5mm equivalent of silicone oil head), which is suitable for the settlement probe and the piezometer. A separate laboratory noise test was performed to independently evaluate the suggested inherent noise. Two ± 62.5 mV channels (each on DAQ 55 and PDQ2 expansion module) are shunted (by connecting the high to the low differential channel using a wire) and the system is evaluated at a constant room temperature of 24^{o}C. The data is sampled at 1-minute interval with integration time of 610 milliseconds. This yields results with an average standard deviation of 0.34mm (0.0016 mV), or 17 bit stability and resolution of 22 bit (0.008 mm intervals) (*Figure 4.2*). The upper noise band corresponds to ± 0.006 mV, which is close to the 0.01 mV specified by Iotech. There is no discernable difference in stability between the DAQ 55 and PDQ2 expansion module.

The temperature effects on the DAQ 55 are investigated. The following data (*Figure 4.3*) is obtained after installation of the monitoring system in the field (in the trailer), where DAQ 55 is subjected to atmospheric temperature cycles between 8°C and 28°C. Two channels on the PDQ2 expansion module are shunted. The standard deviation of the noise is 0.0019 mV (0.41 mm) with upper noise band of 0.006 mV (1.6mm). Although there is a slight decrease in the system stability, there is really no apparent temperature induced noises (systematic error that follows the temperature trend). The slight increase in noises could be attributed to the wiring and environmental noise on the field instead.

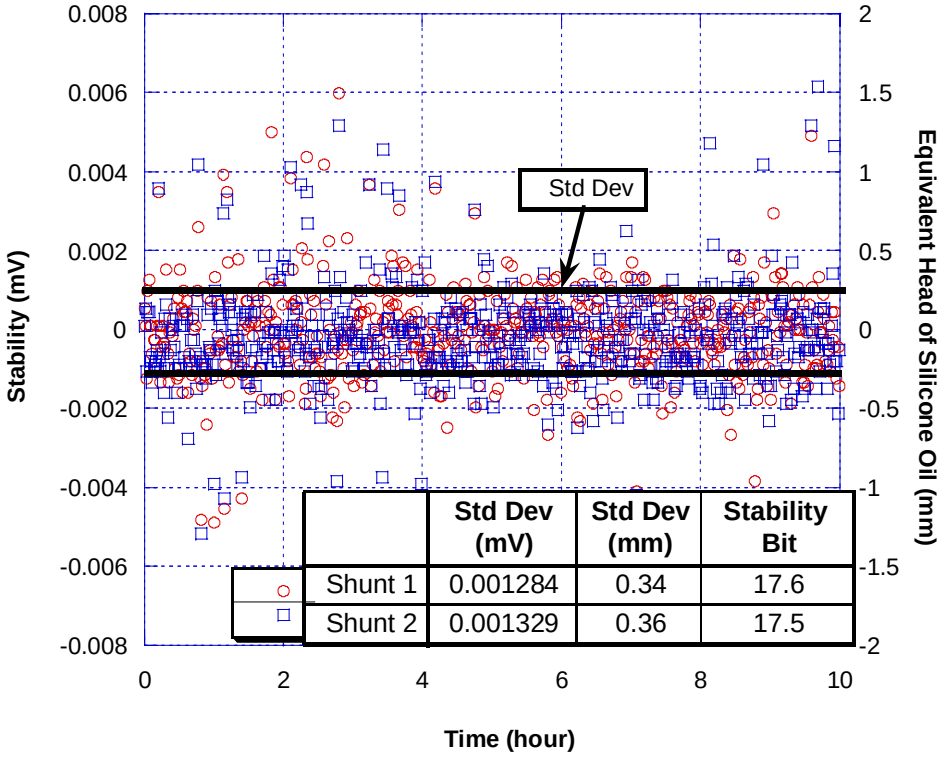

Figure 4.2: Laboratory Stability of DAQ 55 at 24^0C

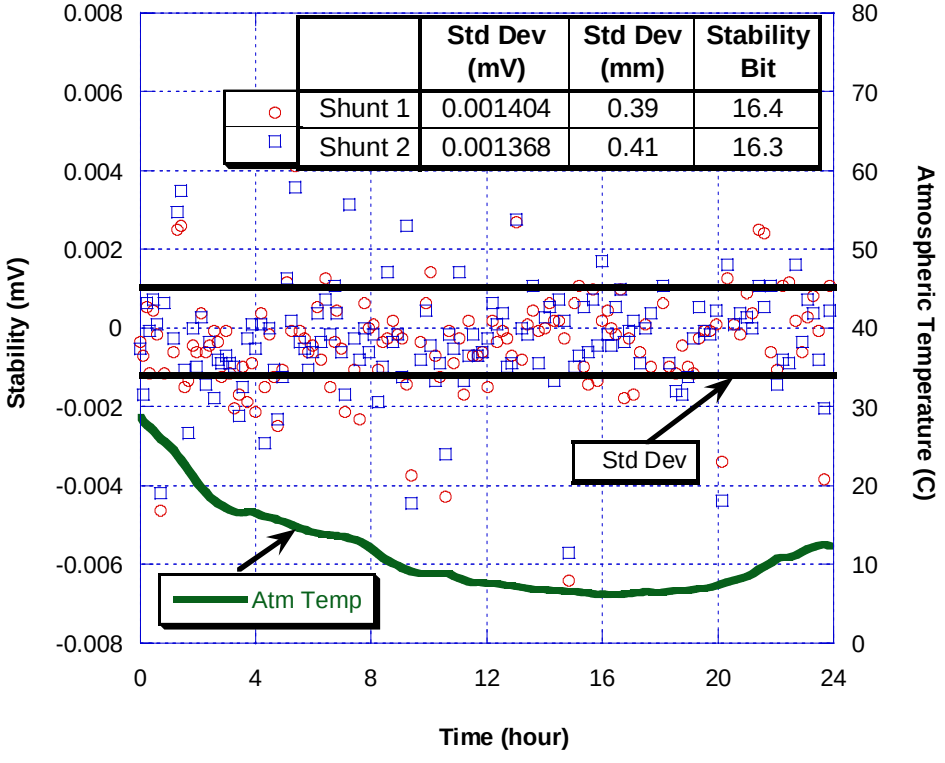

Figure 4.3: Influence of temperature on the stability of the IOTECH DAQ 55

4.2.2 Central Data Acquisition

The MIT Geotechnical Central Data Acquisition has been used to collect data during some of the sensor calibrations. At the heart of the central data acquisition is a HP3497A noise-integrating analog-to-digital converter connected to a 486 microprocessor PC driven by Windows NT software (EASYDAT developed at MIT by GERMAINE and LADD). This system has a 5½ digit-integrating analog-to-digital converter with auto-ranging amplification to four voltage scales (100mV; 1, 10, 100V). The system has the ability of simultaneously monitoring 140 channels at maximum sampling rate of 1Hz (Da Re 2000). The system is capable of measuring up to 0.001mV on the 100mV range, which corresponds to 0.25mm silicone oil stability and 0.000188 kPa for the MPX2100A and MPX2200A respectively.

4.3 Motorola MPX pressure transducer

The laboratory testing and calibration for the MPX2100A and MPX2200A is described. The transducers will be tested individually (not connected to the thermistor or epoxy) for stability, drift and temperature calibration (*Figure 4.4*). The low power line is grounded to provide a zero voltage reference point.

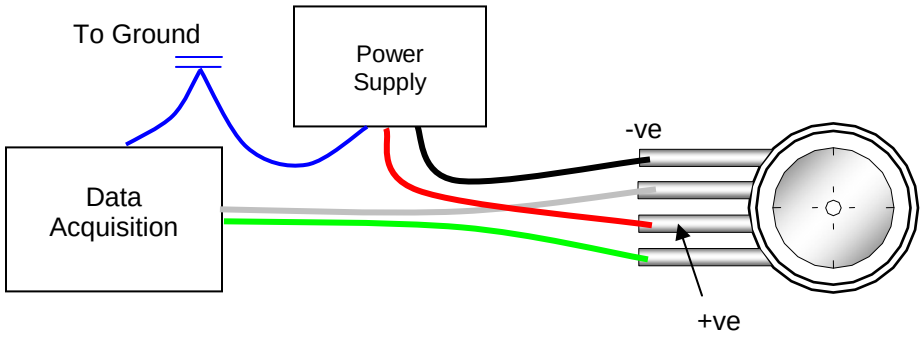

Figure 4.4: Configuration of stability and temperature testing for MPX series transducers

4.3.1 Stability

The stability of the MPX2100A and MPX2200A absolute pressure transducers are tested in the laboratory using the central data acquisition system. Three pressure transducers (two MPX2200A and on MPX2100A) are connected to the 10V input voltage and data acquisition (*Figure 4.4*). The low end (or negative point) of the power supply is

grounded to provide a constant zero voltage reference point, thus preventing unnecessary electrical drift in the system. Since the output from the transducers are proportional to the input voltage (between 0 and 16V), the readings are presented in a normalised form: mV/V_{Input}.

The output readings from the three transducers are shown in *Figure 4.5*. The MPX2100A and MPX2200A have average milivolt output of 4 mV/V and 2 mV/V respectively and are plotted using two different axes of similar scale; the first for MPX2200A and the second for MPX2100A. The offsets for the two MPX2200A transducers are different (due to manufacturing imperfections) although the shape of the stability curve is similar. The MPX2100A has calibration factor that is half that of MPX2200A, resulting in stability curve which has gradient twice that of MPX2200A.

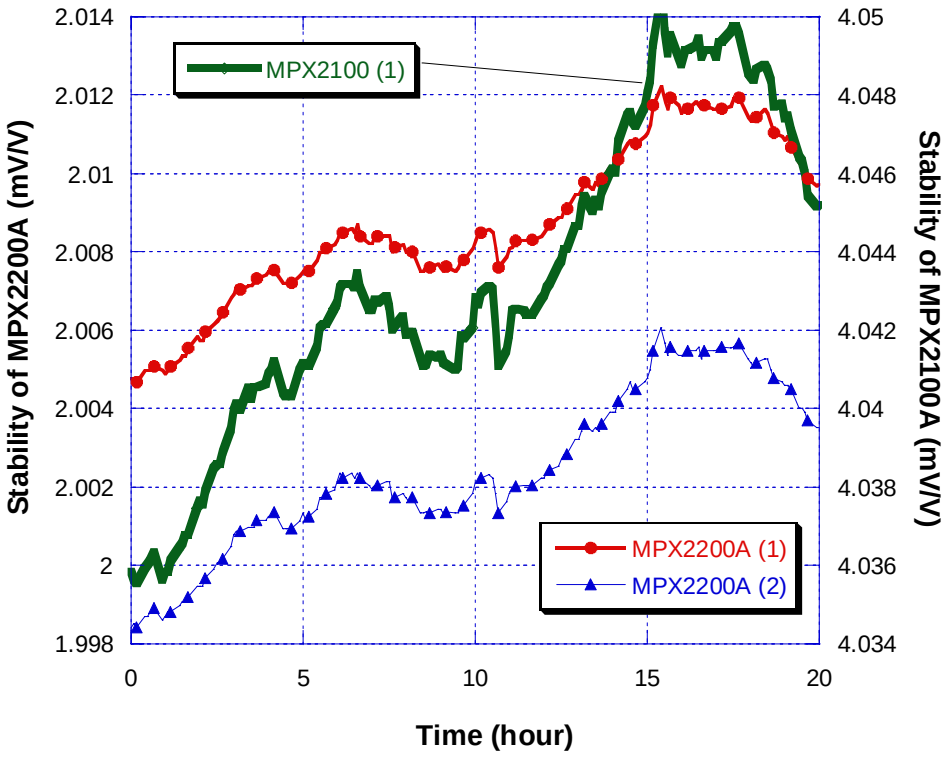

Figure 4.5: Stability of the pressure transducers in mV/V

Given such varieties in output voltages between the transducers, it is useful to convert the readings into the equivalent head of silicone oil using the manufacturer suggested calibration factors, and match the offset of each transducer to enable comparisons between the pressure transducers.

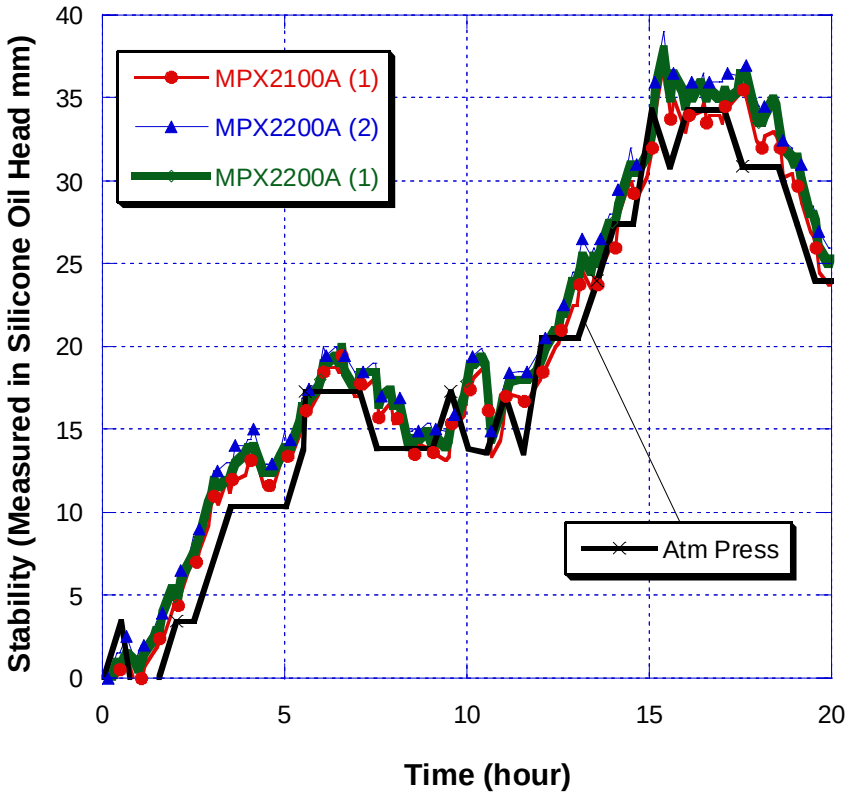

Figure 4.6: Stability of three different pressure transducers (two MPX2200A and one MPX2100A)

Figure 4.6 shows the stability results from the three pressure transducers: two MPX2200A and one MPX2100A (using manufacturer's calibration of 50 kPa/(mV/V) and 25 kPa/(mV/V) respectively). The data trend from the three transducers fluctuates in a synchronised manner between 14mm and 30mm over a period of ten hours. The observed trend is a result of direct expose to the atmospheric pressure, as represented by the black line in *Figure 4.6*. The atmospheric pressure is obtained from a local weather station (www.wunderground.com).

The absolute stability (defined as the variation in reading without the influence atmospheric pressure) can be found by subtracting the output of two pressure transducers. *Figure 4.7* shows absolute stability of the pressure transducers, with noise band of 1 to 1.5 millimetres (ideal absolute stability is undoubtedly zero). The method of subtracting the two pressure transducers together will double the noise band (combining noise band of individual transducers). The central data acquisition has resolution of 0.25mm and 0.5mm for MPX2100A and MPX2200A respectively, which is evident in *Figure 4.7*. The resolution can be improved by using DAQ 55. The transducer has very good short term stability (< 1 day). .

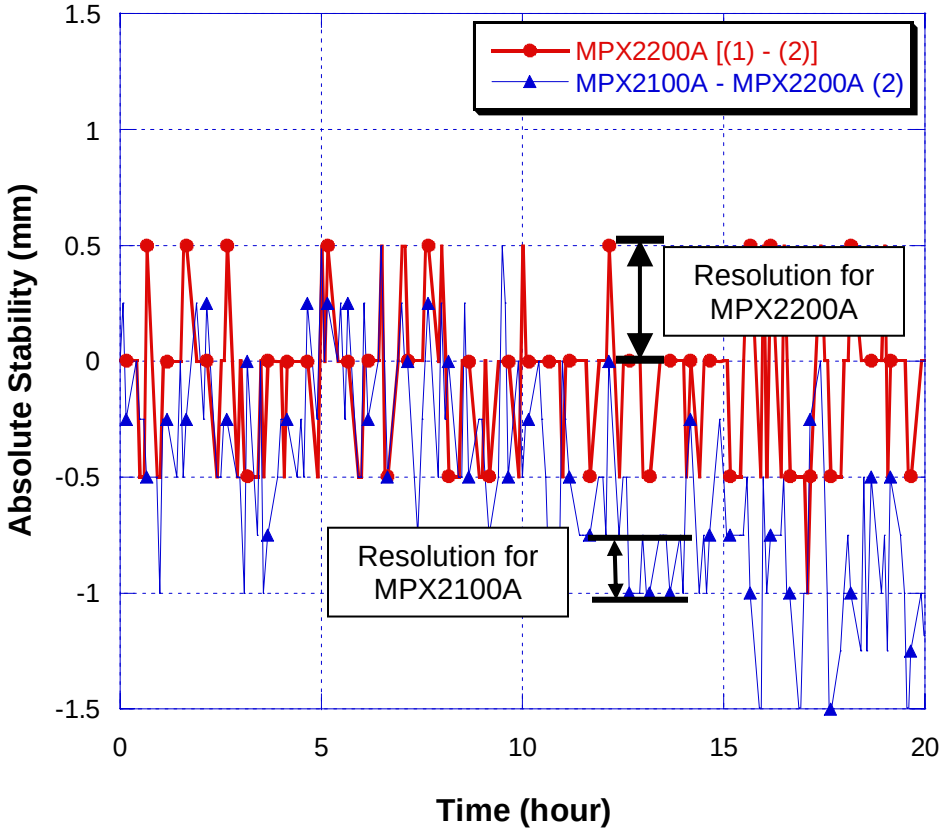

Figure 4.7: Absolute stability of the transducers (normalised by MPX2200A (2)).

4.3.2 Temperature Calibration

All electronic sensors are susceptible to temperature fluctuations, and the MPX series transducers are of no exception. The MPX transducers has a built-in temperature compensation circuit of up to 1% full scale (106 mm for MPX2100A and 2kPa for MPX2200A) for temperatures between 0°C to 85°C.

In order to evaluate these effects, an MPX2100A pressure transducer is placed in a temperature-controlled oven and the temperature is varied between 24°C and 54°C. The output from the transducer is compared with the local atmospheric pressure obtained from the weather station (*Figure 4.8*). As the temperature in the oven is stepped up from the room temperature, the (uncalibrated) readings from the pressure transducer start to deviate from the atmospheric pressure and closely follow the trend of

the temperature. The reading deviation can be as high as 70mm for temperature change of 30°C.

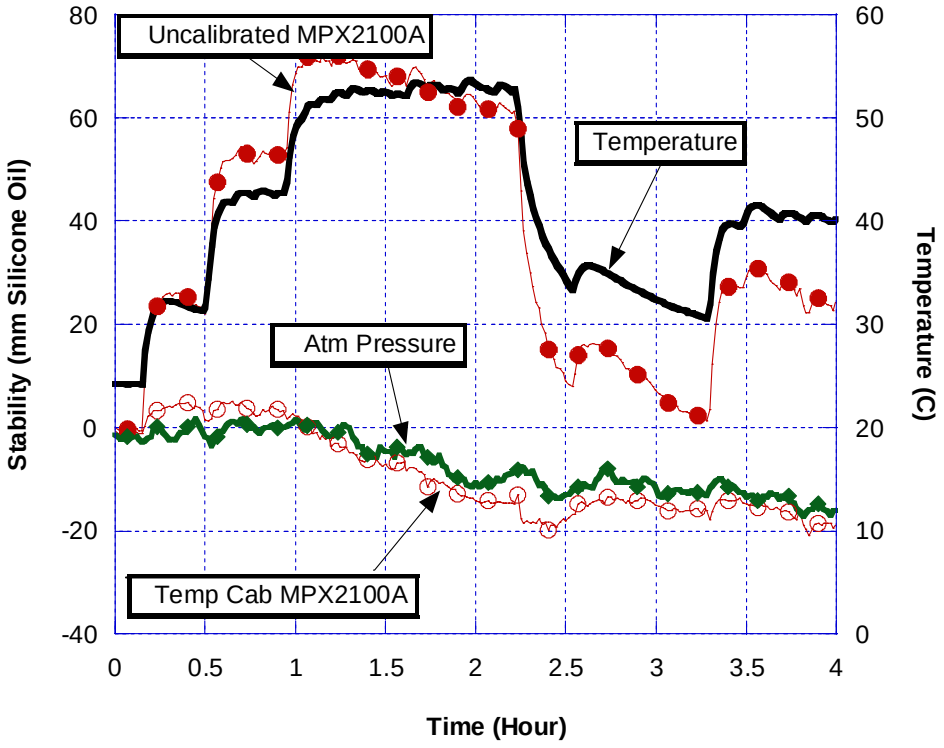

Figure 4.8: Effect of temperature on the MPX2100A

Since the temperature causes changes in the offset values and not the calibration factor, it is possible to quantify the temperature effects. There exists an almost linear relationship between the temperature-induced pressure and the temperature, as shown in *Figure 4.9*. A linear regression equation can be fitted to the data, yielding:

$$\Delta H \text{ (mm)} = -2.6913 \text{ (T)} - 64.983 \qquad \text{(Equation 4-1)}$$
$$\text{with } R^2 = -0.9944$$

where mm = changes of the stability offset in millimetres and T = temperature in °C.

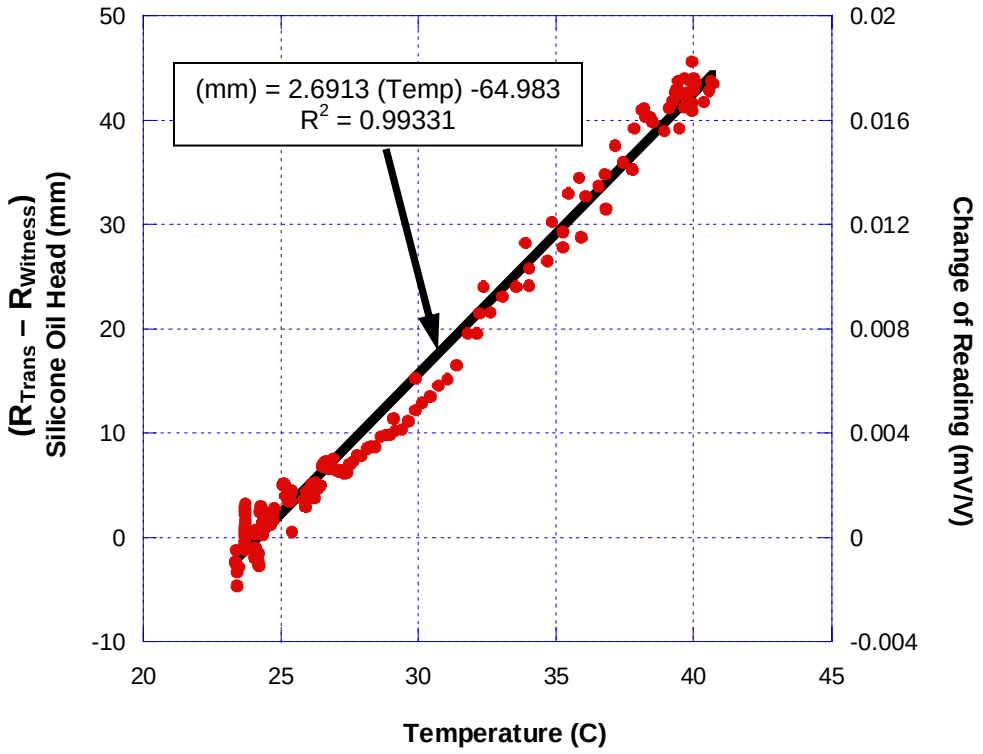

Figure 4.9: Temperature Calibration for MPX2100A (exposed to air)

Now, the temperature corrected readings are plotted in *Figure 4.8* and closely follow the atmospheric pressure with error of ± 2mm. It can be used as follows:

$$Reading_{Corrected} = Output_{(Uncorrected)} - Temperature\ Calibration \qquad (\text{Equation 4-2})$$

4.4 Settlement Probe

The accuracy of the settlement measurements depends on four parameters: a) calibration of the settlement probe (including silicone oil), b) influence of temperature on the pressure transducer, c) influence of the temperature on the silicone oil in the tube (between embedded probe and the reservoir), and d) proper saturation and site installation. Two types of calibration will be performed; pressure calibration and temperature calibration.

4.4.1 Pressure calibration

Motorola suggested that the calibration factor for MPX2100A is 25 kPa/(mV/V) or 2857 mm/(mV/V) (exposed to air). Since the transducer is now used in conjunction with

the silicone oil, it has to be recalibrated for this trend. The calibration process is performed on all five settlement probes which are completely assembled, saturated, and connected to the reservoir. The reservoir is fixed at 950 mm above the ground level.

The calibration process is performed by stepping up the probe at an interval of 10 centimetres (measured with a ruler) and the output signals from the transducer are recorded. Once the probe reaches the level of the reservoir transducers, it is stepped down (at 10 centimetres interval) until the probe reaches the starting location (*Figure 4.10*). The process of stepping up and down is repeated at least twice for statistical significance. The probes are also elevated to an elevation of 200 millimetres above the reservoir to test the performance against negative head.

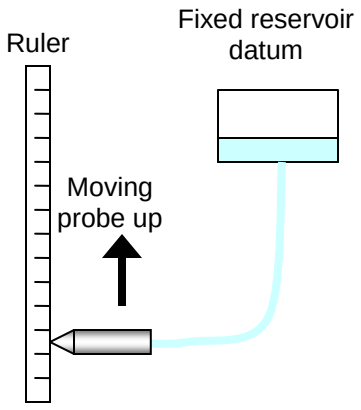

Figure 4.10: Calibration process

The results from the calibration test are shown in *Figure 4.11*. The calibration factor for the settlement probes ranges from 26.4 kPa/(mV/V) to 25.3 kPa (2683 to 2812 mm/(mV/V)), as opposed to the Motorola specified calibration of 25 kPa/(mV/V) (2857mm/(mV/V)). The offset values greatly differ between 3.93 and 4.05 mV/V. The variation of calibration in the pressure transducers arises from inherent differences from manufacturing, the influence of silicone oil and soldering of connections. Removing the effects of the offsets, the relative calibration factors between the 4 settlement probes are clearly seen (*Figure 4.12*). All the settlement probes responded well to the negative head, forming a linear calibration relationship in the negative region (with the exception of Probe 2).

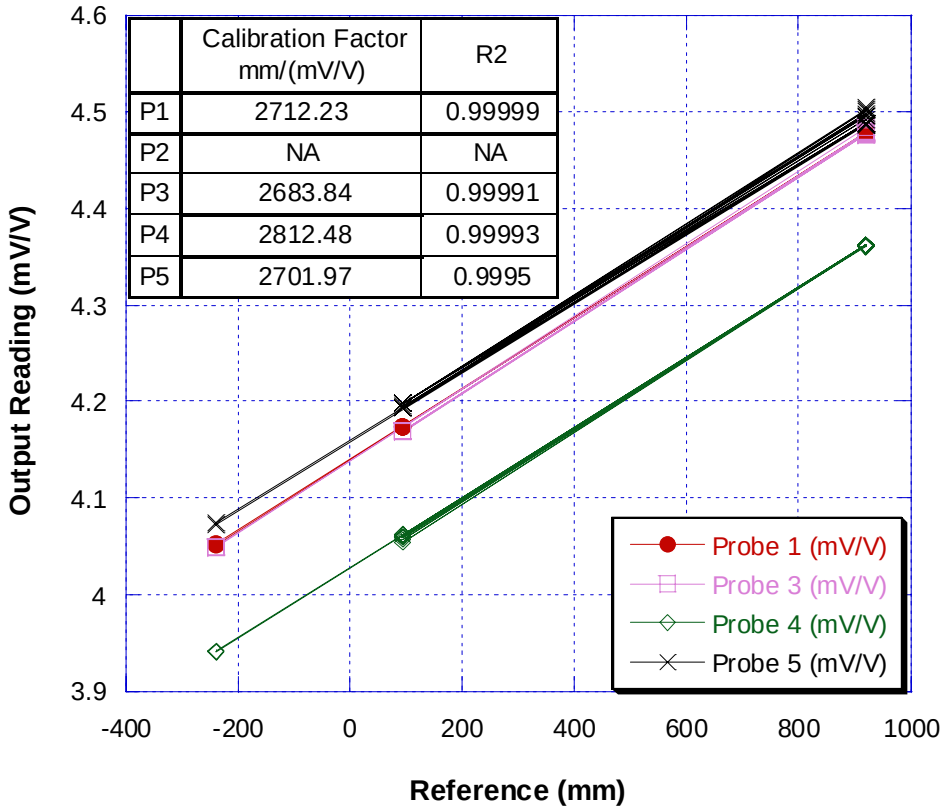

Figure 4.11: Calibration of the settlement probes (including silicone oil)

The next question to be addressed is: How important is the variation in the transducer calibration? *Figure 4.12* shows the sensitivity of the transducer calibrations, matched at a reference mV/V. For a hypothetical settlement change of 40mm, the maximum uncertainties due to calibration variation are 1.9 mm (4.8% error), which is fairly insignificant when compared to electrical noises and changes in atmospheric pressure. Probe 2 is not working properly but was not rebuilt due to time constraints in preparing for field installations.

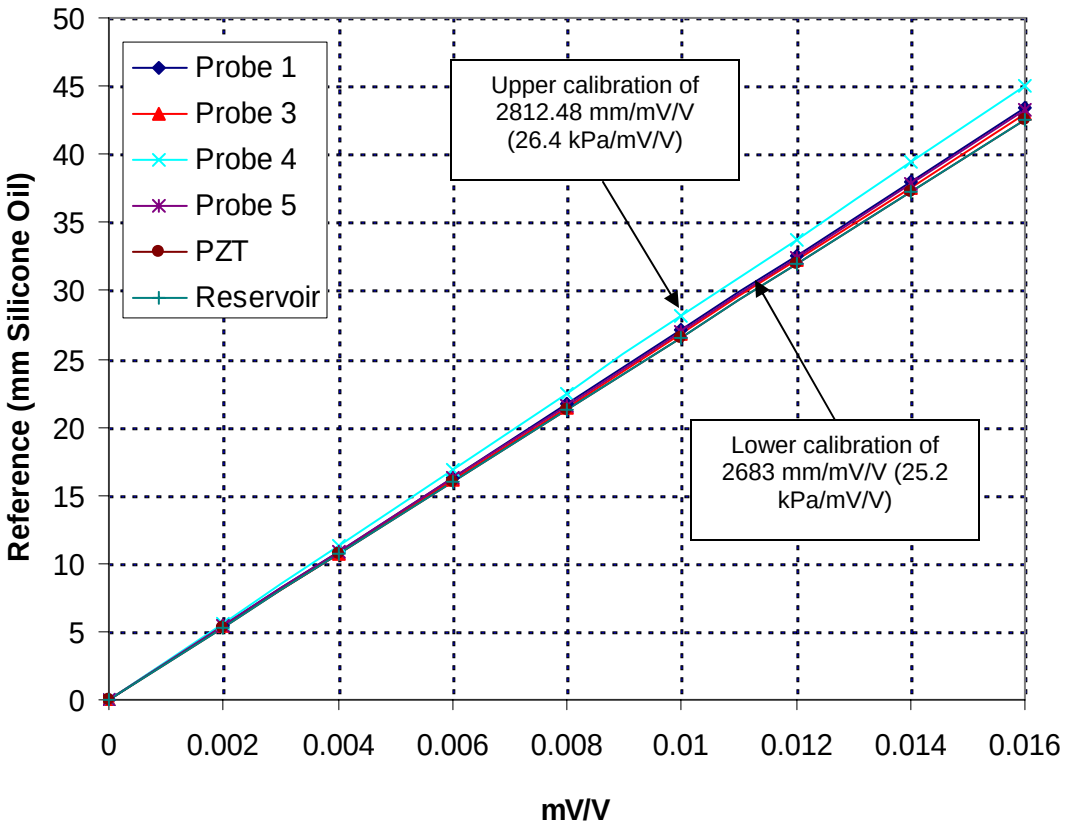

Figure 4.12: Calibration of the settlement probes (matching at the origin)

4.4.2 Temperature Calibration

Temperature fluctuations affect the output readings from the pressure transducers. Two types of temperature calibrations are important here: a) temperature calibration with the pressure transducer, and b) density changes of the silicone fluid.

4.4.2.1 Pressure Transducer, Temperature Calibration

Laboratory temperature calibration tests are performed for the five settlement probes and the influence of temperature cycles on the probe (consisting of transducer encapsulated in the epoxy and silicone oil in the chamber) are investigated. The fully assembled settlement probes (saturated and connected to the reservoir) are placed in the temperature-controlled oven and the temperature is cycled between 23^{O}C and 65^{O}C. The temperature cycling is repeated four times and the output from the probes is recorded. The experimental configuration consists of two temperature zones: a) head of the probe immersed in the oven, and b) the rest of the system exposed to constant room temperature of 23°C (*Figure 4.13*).

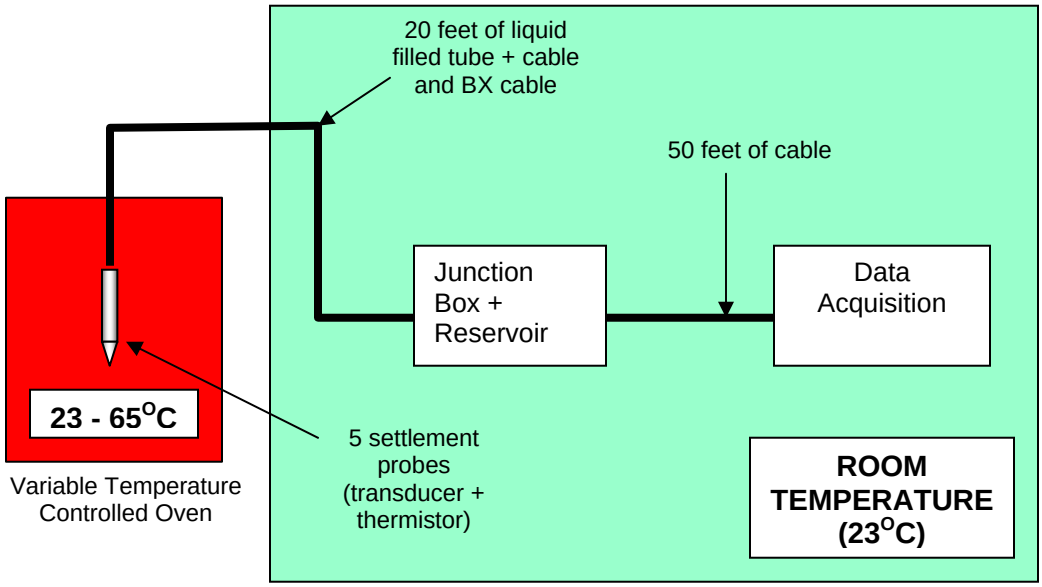

Figure 4.13: Temperature calibration equipment set up for the settlement probes.

The results from the temperature calibration tests are shown in *Figure 4.14* and are plotted with temperature-induced pressure against the temperature. Linear regression curve is used to represent the relationship between the pressure and temperature for ease of computation. The temperature calibration varies between different transducers, necessitating individual temperature calibration for each probe. There are currently no data available for probe 1 due to problems in the data acquisition channel and there was not enough time to perform further testing before the field tests.

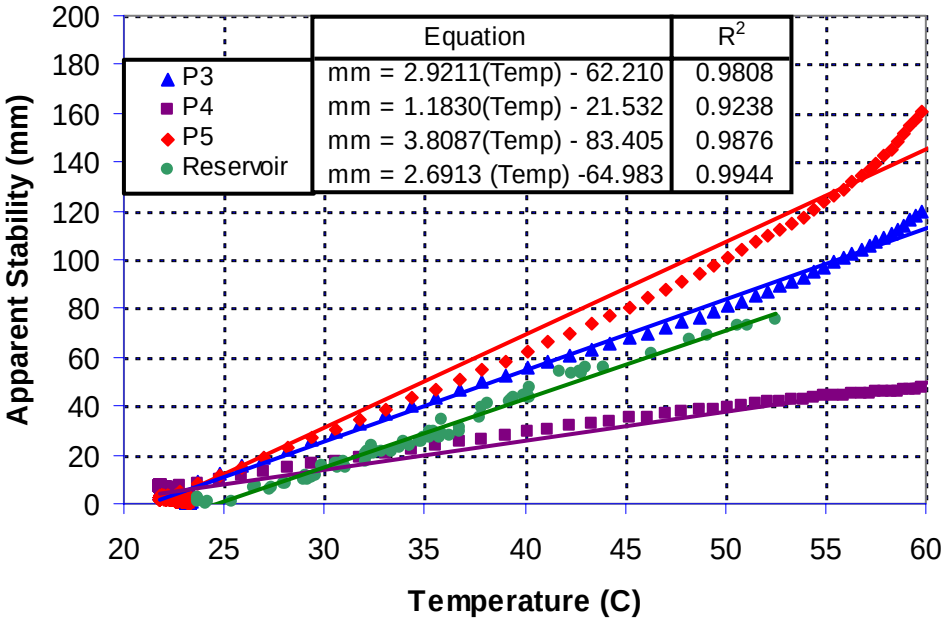

Figure 4.14: Temperature Calibration for P3, P4, P5 and RES

4.4.2.2 Silicone Oil, Temperature Calibration

In addition to the temperature calibration in the transducers, temperature fluctuations also affect the density of the silicone oil, which in turn affects the pressure exerted on the transducer in the embedded probe. Any increase in temperature causes reduction in density of the silicone oil and reduction of pressure exerted on the pressure transducer. As a result, the settlement probe will register an artificial heave in the ground when there is no movement occurring.

The field condition consists of two temperature zones: a) the relatively constant ground temperature of 11°C – 15°C, and b) variable atmospheric temperature. The embedded probe and tubing will be subjected to the ground temperature whereas the exposed tubing and reservoir will be subjected to the atmospheric temperature, leading to temperature density effect error (which, can be estimated analytically. The two temperature zones can be modelled by a two temperature blocks and the density of the silicone oil is assumed a function of temperature (*Figure 4.15*).

Constant model

The simplest model is assuming that the temperature of the system is equal to the temperature of the ground. The silicone oil head can be determined from the following formula:

$$H\ (mm) = P\ (kPa) / \rho\ (kg/m^3) / g\ (ms^{-2}) \qquad \text{(Equation 4-3)}$$

and, from *Figure 3.19*

$$\rho\ (kg/m^3) = -0.0004\ T\ (°C) + 0.9503 \qquad \text{(Equation 4-4)}$$

Variable model

The constant model cannot adequately describe the influence of the differential temperature between the atmosphere and ground. A two-parameter temperature model, with each parameter representing the atmospheric and ground temperature respectively, can better estimate the head. The density of the silicone oil is assumed to change according to the ambient temperature, as shown in *Figure 4.15*.

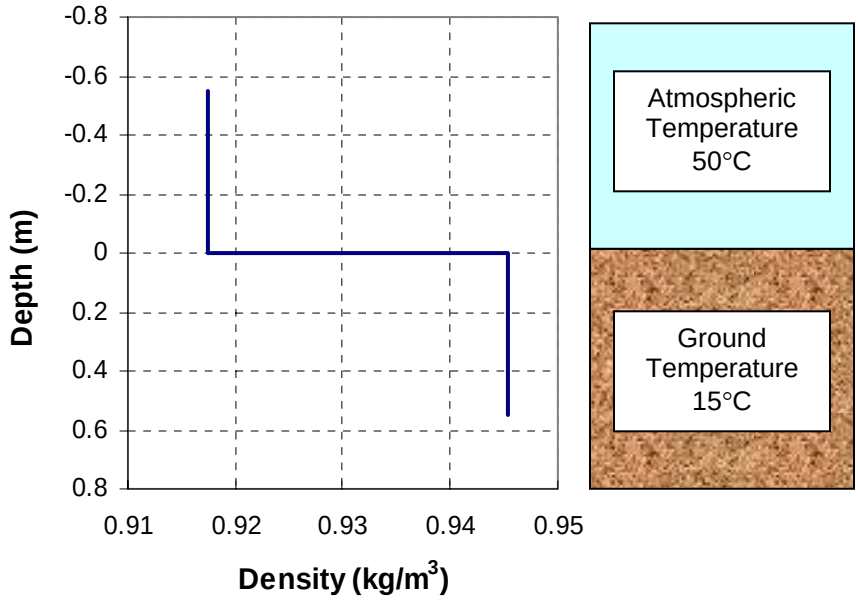

Figure 4.15: Profile of density changes between the ground and atmospheric temperature

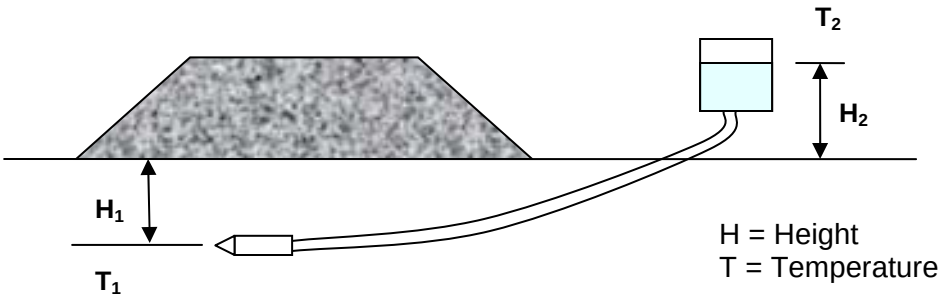

Figure 4.16: Principle of variable model temperature-density correction

The depth of embedment of the probe and ground temperature can be represented by H_1 and T_1 respectively (*Figure 4.16*). Similarly, the elevation of the reservoir above ground and the temperature can be represented by H_2 and T_2 respectively. The average density (ρ) of the silicone oil can be computed:

$$\rho_{AVE} = (\rho_{(T1)} \times H_1 + \rho_{(T2)} \times H_2) / (H_1 + H_2) \quad \text{(Equation 4-5)}$$

And the silicone head is

$$\text{Head (mm)} = \text{Pressure (kPa)} / \rho_{AVE} \text{ (kg/m}^3\text{)} / 9.81 \quad \text{(Equation 4-6)}$$

The density changes can be minimised by reducing the exposed height H_2 of the tubing to the atmosphere and would be completely eliminated if the junction box were to be buried in the ground. The length of the horizontal tubing will not influence the density changes. *Figure 4.17* shows the influence of differential temperature on the density of the silicone oil, with ground temperature set at 10°C. No doubt, this graph will vary as ground temperature changes, which is often not the case in the field

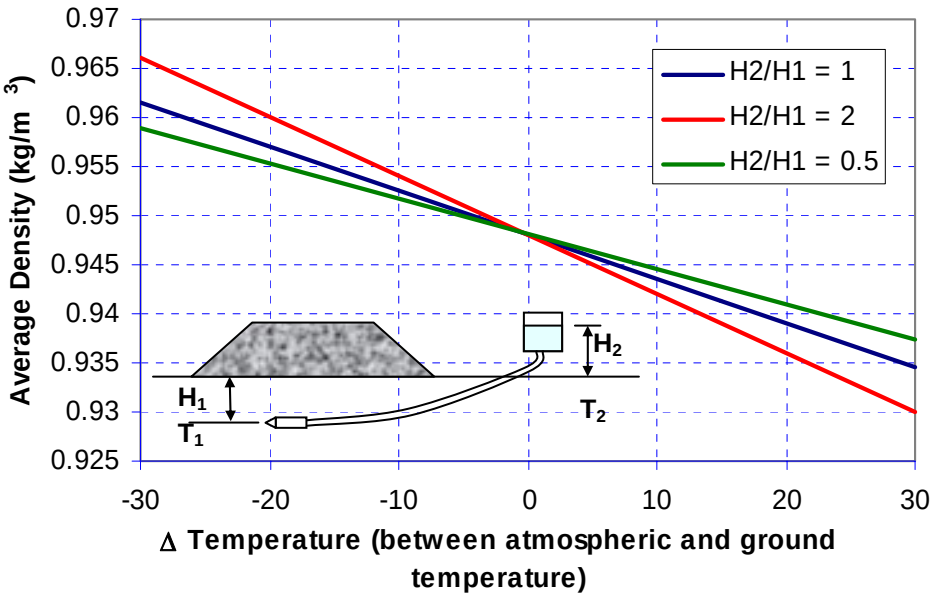

Figure 4.17: Influence of the differential temperature on the density changes of the silicone oil (with ground temperature set at 10°C).

4.4.3 Noise evaluation

The stability of the 5 settlement probes and the reservoir pressure transducer (termed RES-P) subjected to no movements at constant temperature of 24°C is investigated next. *Figure 4.18* shows the response of the five settlement probes with time. The "apparent" settlement experienced by the probes resulted from the changes in atmospheric pressure. An independent measure of the atmospheric pressure obtained from the weather station in Cambridge (www.weatherunderground.com) is shown in the figure. The minor differences in the atmospheric pressure between the probes and the weather station are due to local location pressure variations.

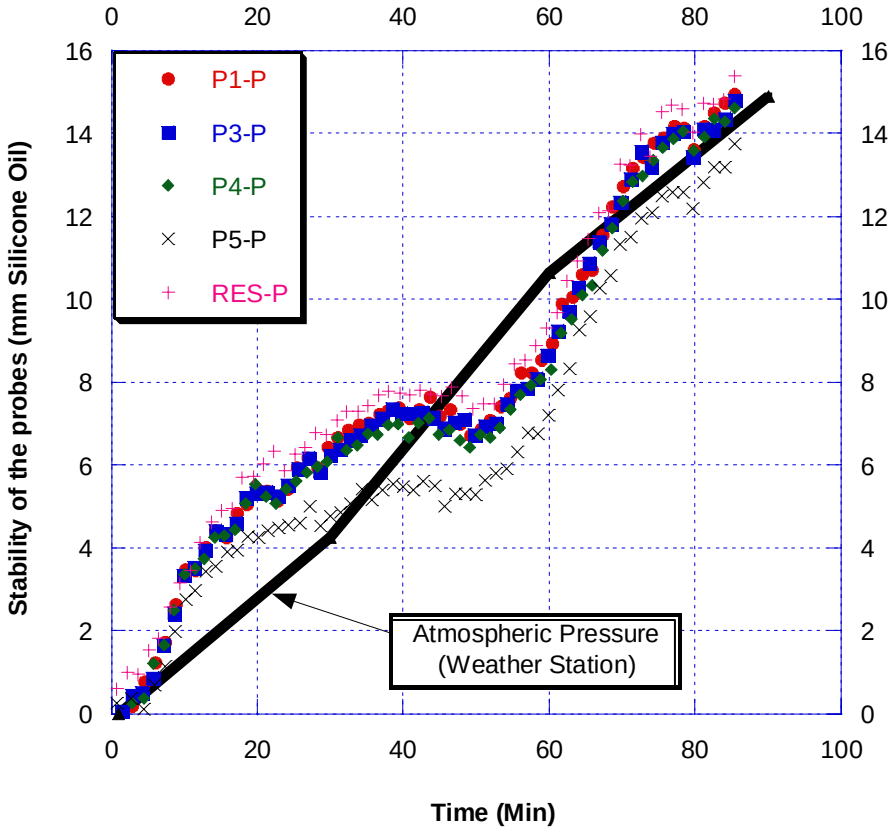

Figure 4.18: Stability of settlement cell transducers at constant temperature 24^{o}C.

Figure 4.19 shows the stability of the settlement probe after subtracting changes in the atmospheric pressure (i.e. subtracting the reservoir transducer readings) The probes, with the exception of P2, has standard deviations between 0.156mm to 0.477mm and mean of 0.05mm over a period of 90 minutes. Much of the stability fluctuations can be attributed to the stability of the central data acquisition.

.

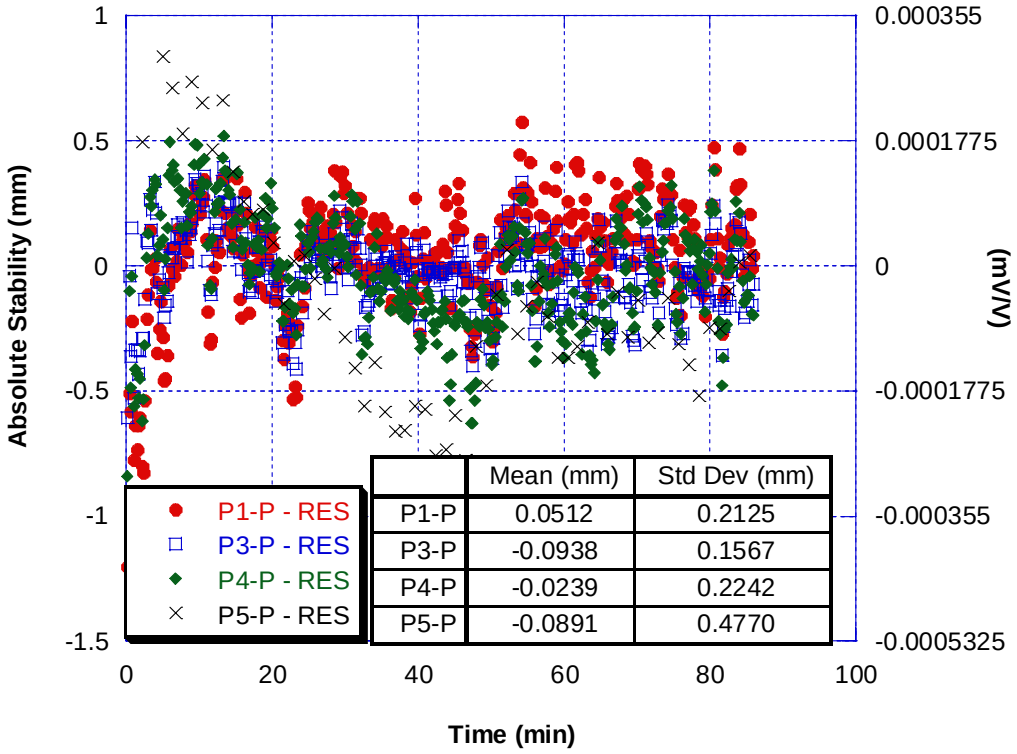

Figure 4.19: Absolute Stability of probe (no atmospheric pressure influence)

4.5 Piezometer

Unlike the settlement probes, the piezometer is not dependent on the pressure induced by the silicone oil and therefore is not subjected to atmospheric temperature fluctuations and changes in the density of the silicone oil. The manufacturer calibration of 50 kPa/(mV/V) is retained for pressure calibration. Similarly, the temperature calibration follows that of the MPX2200A performed earlier in Section *4.3.2*.

4.6 Conclusions

The MPX series absolute pressure transducers, 5 settlement probes and 1 piezometer have been calibrated and tested for stability, and the results are shown in are shown in *Table 4.2*:

Table 4.2: Resolution and stability of settlement probe and piezometers

	Lab Calibrated					
	Settlement Probe					**Piezometer**
	Probe 1	**Probe 2**	**Probe 3**	**Probe 4**	**Probe 5**	
Resolution* (mm)	0.085	NA	0.085	0.085	0.085	0.00015 kPa
Stability (mm)	1	NA	0.5	0.5	0.5	0.0094 kPa
Mid Term Drift (mm) for 1 day	1	NA	1	1	1	0.047 kPa
Calibration mm/(mV/V)	2712.23	NA	2683.84	2812.48	2701.97	50 kPa/(mV/V)

Note:
* Resolution based on DAQ 55

It has been shown that the pressure transducers are heavily influenced by the effects of atmospheric pressure and temperature (*Section 4.3.1*), and correction methods (*Section 4.3.2*) have been introduced to minimise these effects. The 5 settlement probes have been calibrated using a calibration procedure described in *Section 4.4.1*. In addition to influence of atmospheric pressure and temperature effects, the settlement probes are susceptible to changes in differential temperature (between the ground and the atmosphere) which will result in silicone oil density changes. As such, a density correction factor has been proposed to address this issue (*Section 4.4.2.2*).


Field
Installation

Chapter 5: Field Installation

5.1 FAST site at TTCI

The Transportation Technology Centre Inc, better known as TTCI, is located in Pueblo, Colorado (*Figure 5.1*). The Facility for Accelerated Service Testing (FAST) is a 4.8 mile loop dedicated for Heavy Axle Load (HAL) testing. Within FAST, a special 2.7 mile High Tonnage Loop (HTL) (*Figure 5.2*) was created to accommodate HAL trains. Test train operations are designed to accumulate 1.0 million gross tons (MGT) a day, with HAL trains operating at a maximum of 40 mph.

Figure 5.1: Map of TTCI in Pueblo, Colorado

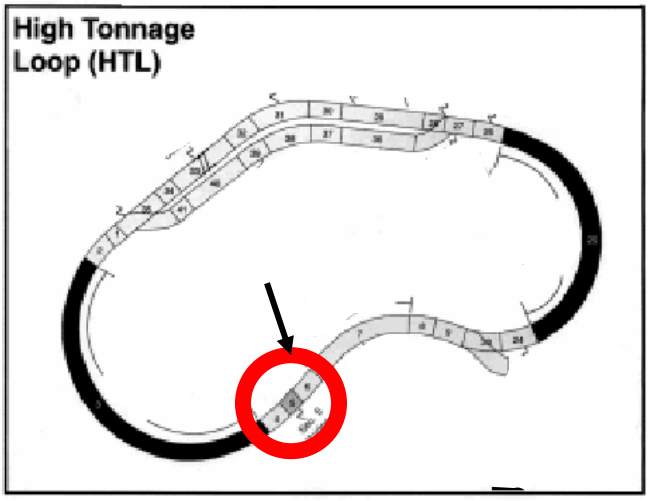

Figure 5.2: FAST section and the bridge approach

5.1.1 HAL Trains at HTL

The HAL train has 76 carriages, each weighing 329 tonnes, and a total combined weight of 12340 tonnes. The train is driven by two main engines and travels at an average velocity of 43 mph, thus going around the HTL (of 2.7 miles) every 4 minutes. Given that each carriage has 4 axles, the train has a total of 304 axles, with average axles weighing 40.6 tonnes. An average carriage has length of 15.75 metres, and the total length of the train is 1197 metres (0.75 miles).

Figure 5.3: HAL main engine.

Figure 5.4: 320 tonnes cargo carriage.

5.1.2 Weather at TTCI

The weather condition at TTCI is dry all year around. Temperatures can reach 35^0C during summer and can dip below -5^0C during winter (*See Figure 5.5*). Being a desert, the atmosphere does not retain heat at night resulting in high daily fluctuations (up to 20^0C). This large daily temperature variation has a significant effect on the sensors performance, in particular the pressure transducer in the reservoir and exposed liquid settlement tubing. Nevertheless, the ground temperature remains fairly constant at a given day due to the high ground latent heat. The atmospheric pressure may vary up to 3kPa yearly, with as much as 1kPa (100mm silicone oil head) per day (*Figure 5.6*). *Figure 5.7* and *Figure 5.8* show the expected weather conditions in Colorado.

The topsoil, which consists mainly of silty clay and sand, is completely dry due to the exposure to the sun. However, the soil is relatively moist under the ballast and at about 0.6 metres into the ground. The water table is not encountered at depths 1.2 metres below the ground.

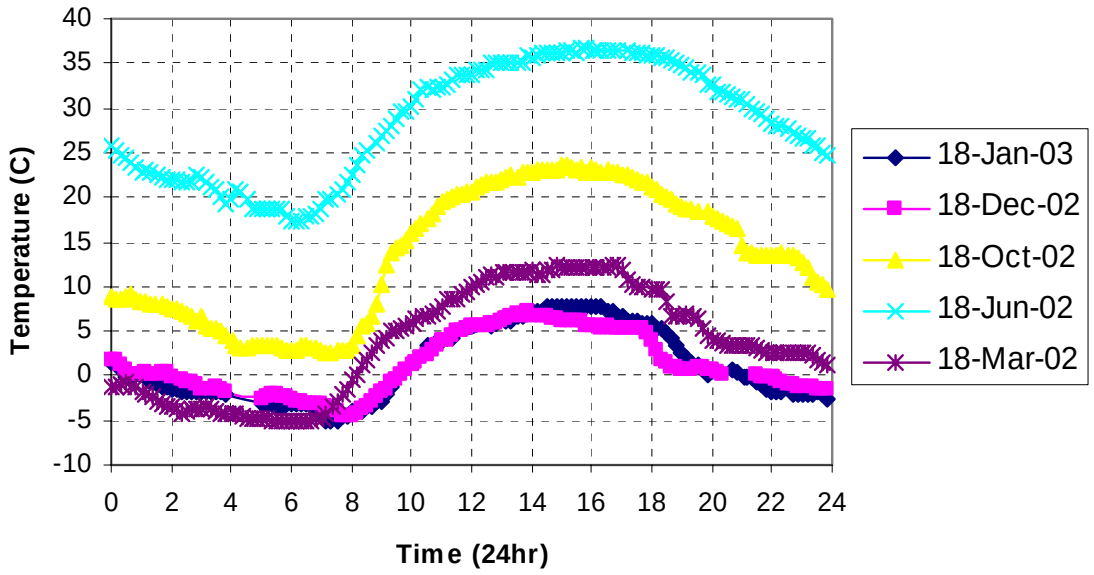

Figure 5.5: Typical daily atmospheric temperature in Pueblo, Colorado at various times of the year (Weather Underground)

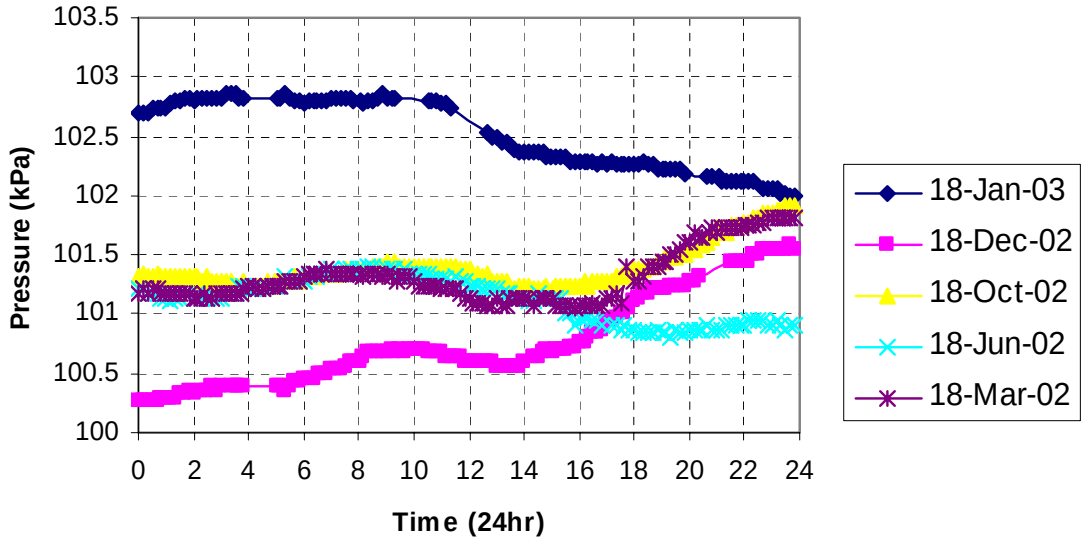

Figure 5.6: Typical daily atmospheric pressure in Pueblo, Colorado at various times of the year (Weather Underground)

Figure 5.7: Typical hot and dry climate at TTCI and Colorado where temperatures could soar up to 50°C and rain is few and far between.

Figure 5.8: Colorado is not all hot and dry. With temperatures dipping subzero during winter, it is vital that the monitoring system is able to perform in all weather conditions.

5.2 Monitoring system at TTCI

5.2.1 Introduction

The monitoring system was installed at the FAST bridge approach site in two phases, 16 Dec to 19 Dec 2002 and 16 April to 18 April 2003. The sensors and installation tools were properly packaged and air-delivered to TTCI from MIT. During the first installation phase, the physical layout of the monitoring system was put in place; the settlement probes and piezometers were installed in the subgrade, connected to the junction box and data acquisition. The first valuable experience learned from the site installation is the importance of good communication between different parties; the site specified physical layout and amenities discussed were different in the actual field. As a result, some overhaul in the monitoring system had to be performed, including extension of the wiring between the junction box and the data acquisition. The computer and communication system were found to be incompatible with TTCI's network, and the Internet connection could not be established. All these unexpected challenges, coupled with the time constraints, contributed to poor data collection and a second installation phase was immediately planned. During the second installation phase, the computer was replaced by a laptop and DAQ 55 data acquisition.

5.2.2 Aim of the installation

The installation process, in addition to the analyses of the long-term field results, serves as a learning process to better understand the practical issues involved in field conditions. Some of the aims are summarised below:

1. To investigate the best, most effective and easiest method of installing the sensors in the subgrade. Two methods of installation were performed: hand augering, and excavating the ballast from the top by hand.
2. To evaluate practicality of the field saturation and setting up the probes.
3. To communicate and work with the TTCI personnel.

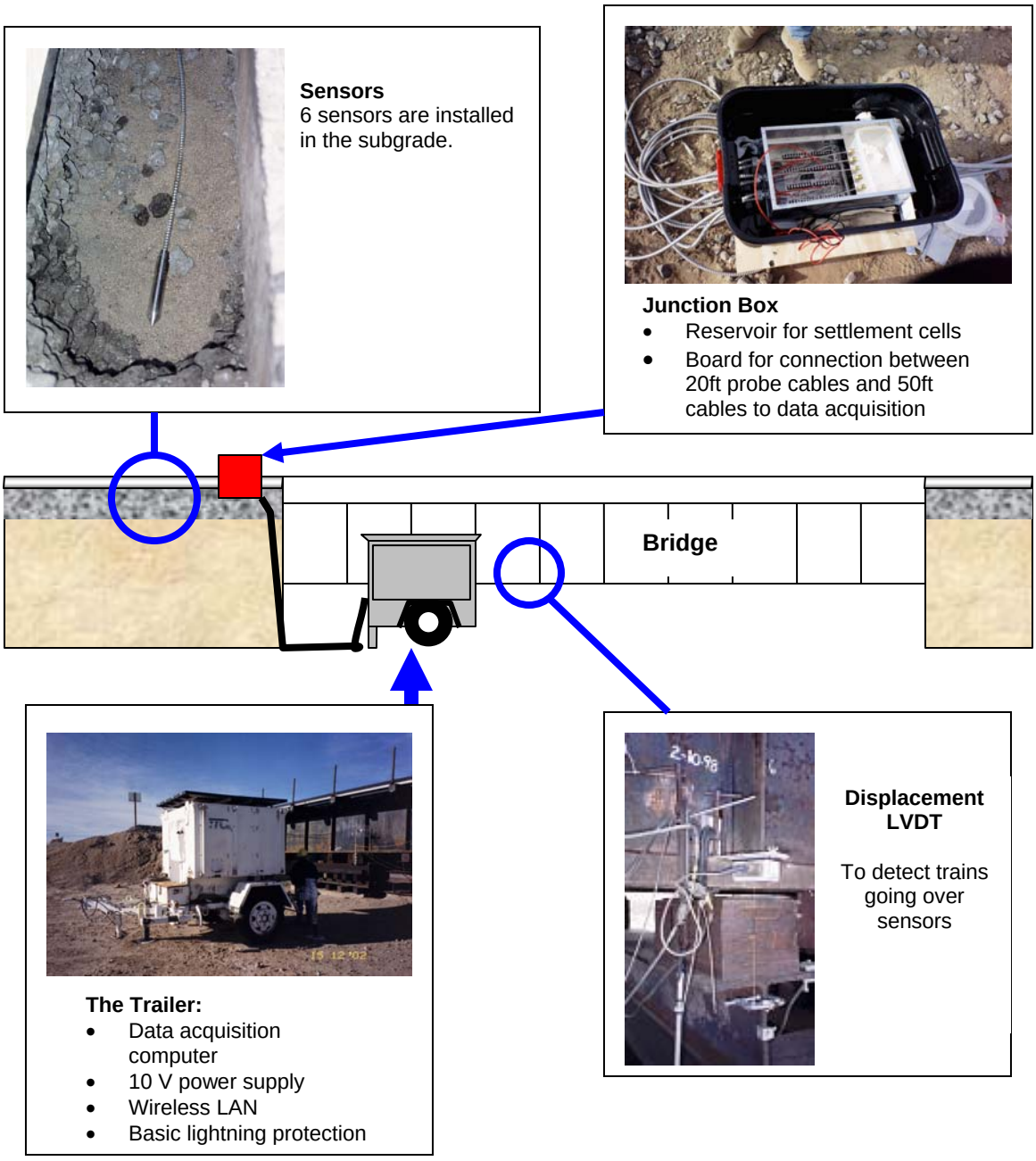

Figure 5.9: Location and layout of the monitoring system at TTCI.

5.3 Monitoring System Layout

The layout of the monitoring system at TTCI, consisting of the embedded probe (piezometer and settlement probes), junction box, and data acquisition is shown in *Figure 5.9*. The data acquisition, laptop and the power supply are housed in a trailer located 18 metres away from the probes.

5.4 Installation of the monitoring system

5.4.1 Setting up the Data acquisition

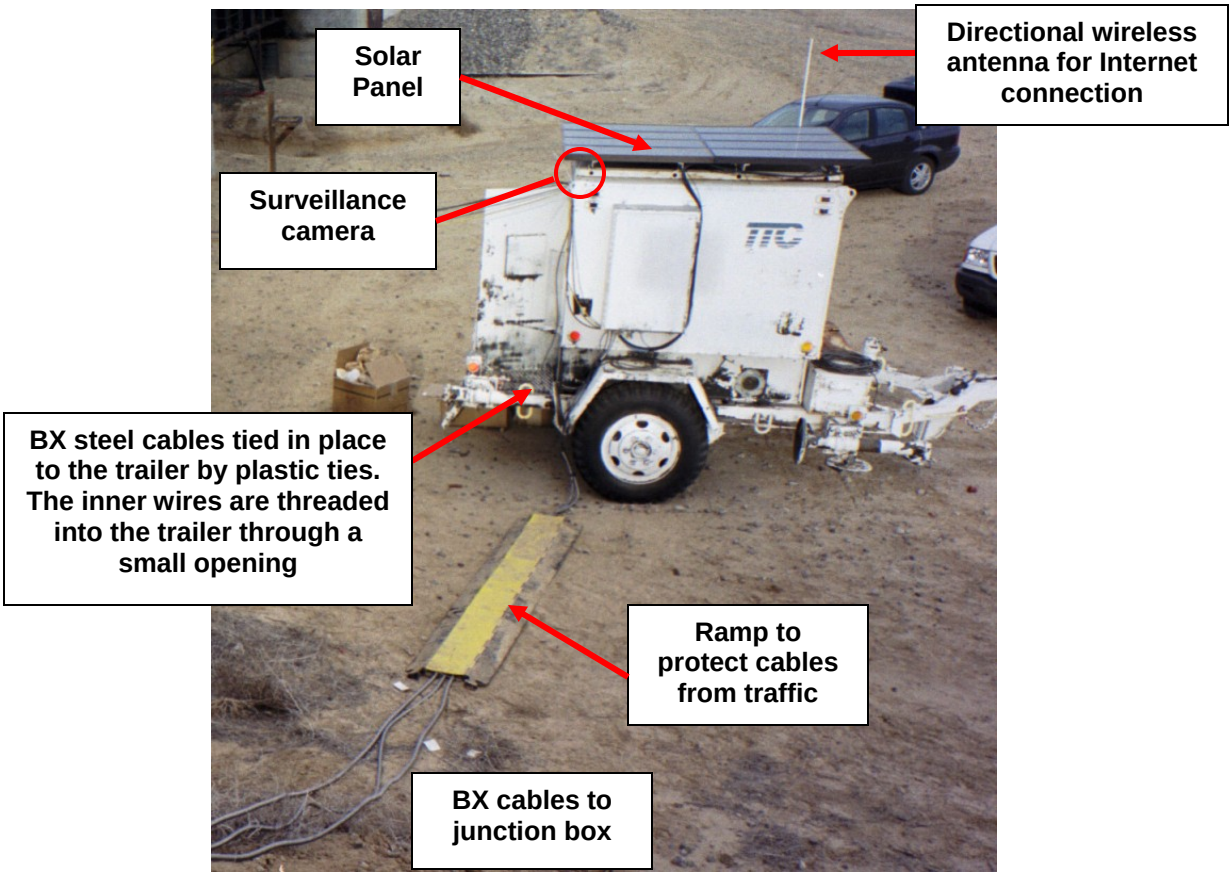

Figure 5.10: Layout of the data acquisition trailer on the site.

The data acquisition DAQ 55, laptop, power supply and the ac-dc converter were set up in a trailer (*Figure 5.11*). The trailer, which is also used for other instrumented projects, contains a directional antenna, providing wireless Internet connection with the

main LAN in the TTCI headquarters. The primary 120V alternating current power source is obtained from the TTCI electricity grid. In the event of power failure, the trailer can rely on four 45W Solarex Solar panels and batteries to provide power backup. The trailer is also equipped with basic lightning protection system consisting of eight-feet copper rod inserted into the ground.

The DAQ 55 and the laptop are housed within the trailer. The temperature in the trailer could soar up to 45°C, thus providing an opportunity to evaluate the robustness of the laptop and DAQ 55 (before being used in the problematic site). A unique IP address was assigned to the laptop to enable access to the TTCI LAN. The Internet connection in the trailer is rather good, with minimal connection interruptions.

An ac-dc converter (10Vdc) is plugged into the AC power supply. The low side (negative) of the power output is grounded to create a zero voltage reference point.

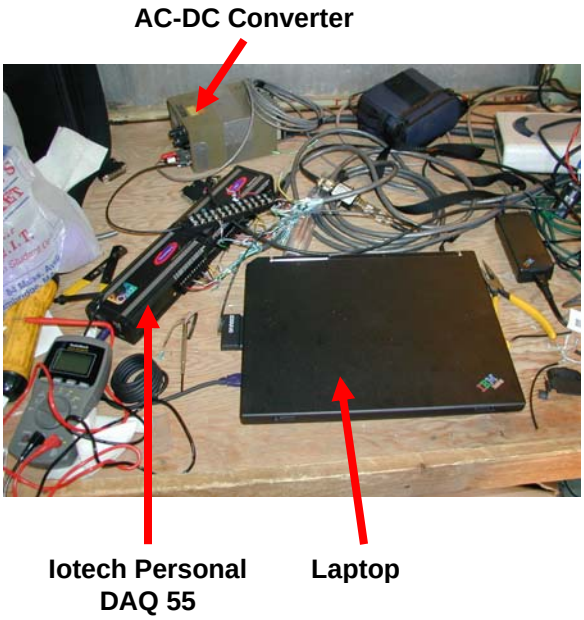

Figure 5.11: Layout of the system in the trailer

A digital surveillance camera is installed on the roof of the trailer to enable remote visualisation of the train passing the bridge. The camera is also capable of capturing video and the pictures and video images can be transferred back to MIT via the same communication network.

Figure 5.12: Digital surveillance camera

The 15-metre long BX steel cables are attached to the side of the trailer by plastic ties. The inner cables are threaded into the trailer through an opening on the wall. Installation of the cable proved to be a challenging task. The trailer was situated much further away from the monitored site, contrary to prior specification, and could not be moved. The 16 m data cables had to be hastily extended in situ to accommodate the increase in length.

5.4.2 Field installation of the sensors

The sensors were installed in the subgrade next to the bridge approach (around tie number 10 from the bridge). Five of the six sensors (including 1 piezometer) were installed in the subgrade while the sixth settlement probe was clipped onto the rail tie itself. The complete installation took about four hours to complete, with assistance from the TTCI staff using a variety of tools ranging from a lightweight backhoe to small hand-operated augers and shovels. The location of the sensors are summarised in *Table 5.1* and shown in *Figure 5.13*.

Table 5.1: Location of the sensors installed at TTCI

Probe	Location and installation Method	Comments
P1	Deepest location (1.43 m under the rail). Installed by augering.	The probe is installed at an angle of 45° to the horizontal.
P2	Between the ballast and the subgrade (under rail). Installed by shovelling the ballast from the top.	To test the robustness of the probe in withstanding the high stresses due by crushing action of the ballast from train loading.
P3	0.864m under the rail. Installed by augering	The probe is installed horizontally.
P4	Installed at 5 cm below the ballast-subgrade interface (0.74m). Installed by top excavation.	To test the robustness of the probe due to train loading. P4 lies close to the ballast interface and is protected only by 5cm of subgrade.
P5	Clipped on to the side of the tie (at the centre of the track).	To test the robustness and degradation from atmospheric exposure. Care is taken to ensure that the probe is not in the way of maintenance machines.
Piezometer	1.132 m under the rail. Installed by augering.	The probe is installed at 30° to the horizontal.

*Measurements are performed below the top of the tie.

P2, P3, P1 and piezometer were installed directly under the rail where the highest stresses and movement occurs, while. P4 was installed by excavating beneath the centre of the track where smaller movements (and stresses) are expected to occur.

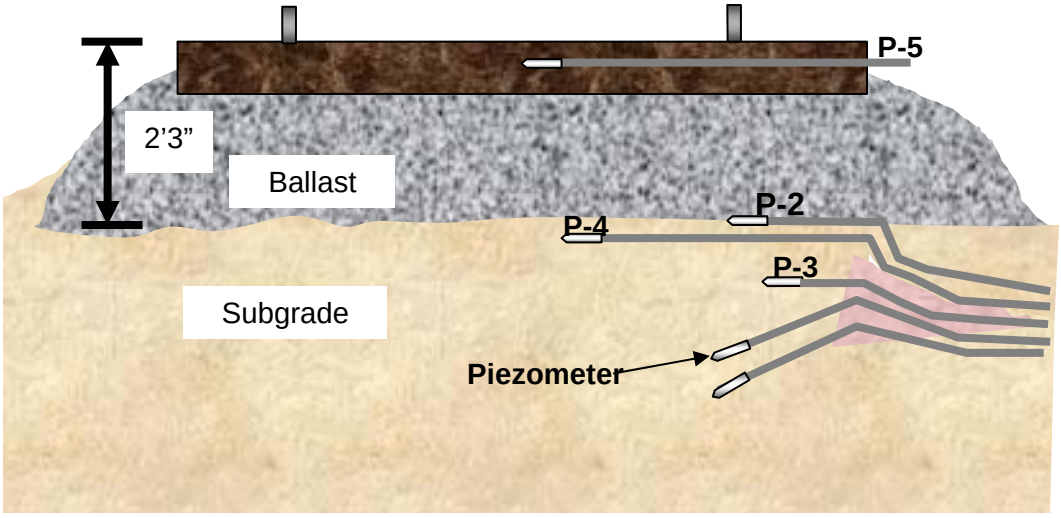

Figure 5.13: Location of the sensors installed in the subgrade

Saturation of probes

The settlement probes and piezometer were saturated on-site prior to installation. The porous stone for the piezometer was saturated at MIT by placing it in an ultrasonic bath (UV) bath for 24 hours and was transported to TTCI in a silicone oil bath container. The pressure transducers in the piezometer were saturated with de-aired silicone oil with a hypodermic syringe. A special sleeve, made by attaching an upturned plastic bottle to the body of the piezometer (*Figure 5.14*), supports a local reservoir of de-aired silicone oil around the head of the piezometer. The chamber and the pressure transducer are now completely submerged under the silicone oil. The internal conduits in the conical head were saturated with de-aired silicone oil by means of a hypodermic syringe and gently lowered into the bath, ensuring no air became trapped in the underside of the chamber. The conical head was then tightened and the piezometer was ready for field installation.

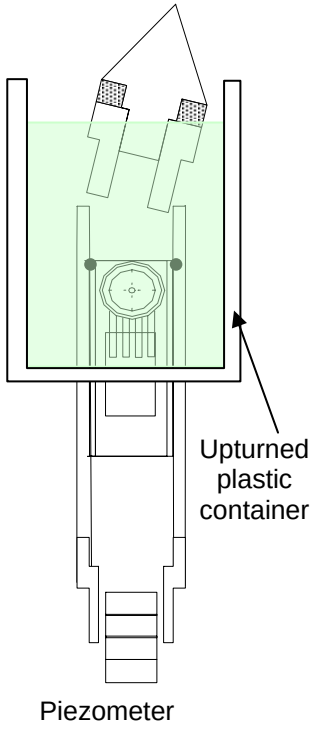

Figure 5.14: Saturating the piezometer

The settlement probes are connected to the reservoir and the conical head is removed to enable de-aired silicone fluid from the reservoir to flow through the probes. The silicone is allowed to flow freely out of the probe for a few minutes and the conical head is recapped. The strong winds and low temperature (about –10°C) made on-site saturation more challenging, and there were times when sand was blown into the reservoir. Unlike air bubbles, sand grains do not expand or contract with small changes in pressure and will not influence the pressure transfer mechanism between the reservoir and the pressure transducer in the embedded probe.

Figure 5.15: Field Saturation of the settlement probes.

5.4.2.1 Installation methods

The sensors were installed by two methods: a) hand excavation of the top ballast, and b) hand augering from the side, after ballast was removed from the side of rail.

5.4.2.1.1 Excavation from top of ballast

In theory, the top ballast (between the ties) could be hand-excavated by shovel up to 0.348 metres (1 foot) and settlement probe 2 will be laid at the interface between the subgrade and the ballast. However, years of train operation and track maintenance increase the depth of ballast to 0.65 metres (2 feet), making hand excavation more labour intensive (*Figure 5.16*). It is therefore possible for ballast in the problematic sites to extend more than 0.65 metres in depth. Excavations are generally easier at the centre of the track and became progressively tougher below the rails themselves. Settlement probe 2 is placed in the excavated area (*Figure 5.17*) and is backfilled with the original ballast materials. This operation required several hours of strenuous labour.

Figure 5.16: Excavating the top of the ballast by shovel.

Figure 5.17: Installing settlement probe 2 from the top of ballast

5.4.2.1.2 Hand-augering

Hand augering, if successful, offers an easy and effective method of installing the sensors at any possible inclination within the reach (or depth) of the auger (typically around 1 to 1.5 metres). Up to 1 metre of the ballast at the edge of the tie is removed with the help of a front-end-loader in *Figure 5.18*. The depth of the ballast was found to be 0.67 metres, leaving 0.33 metres of subgrade to work with. The excavation process took about 5 minutes to complete.

Figure 5.18: Excavation of the rail ballast using a front-end-loader

A hand auger of 1 m diameter is used to create three holes at three different inclinations. Initially, there were some doubts to whether hand augering would work since there is a possibility that the desert-dry sand subgrade would cave in once the auger is removed. All doubts were essentially quenched as the hole stayed open due to the arching action of the highly compacted moist sand.

The probe was marked at 1ft intervals, starting from the tip of the probe (so that the depth of installation can be back calculated later). A 2 m long steel rod is used to push the settlement probes and piezometer into the hole. The hole is backfilled with sand and the exposed BX cables are covered with gravel (*Figure 5.19*). The excavation is filled and the side ballast is replaced using the front-end loader.

Figure 5.19: The augered hole is back-filled with sand.

Figure 5.20: Hand installation of the probe in the augered hole using a rod.

5.4.2.2 Compaction

The ballast is compacted by a rail compaction machine to prevent settlement of the rail (*Figure 5.21*). The mechanical arms are inserted between the rails and vibrate to compact the gravels in that region. This process took about 15 minutes to complete.

Figure 5.21: Compaction process of the ballast after installation of the probe.

The tie and rail are marked with colours to indicate that sensitive instrumentations are installed in the section. The BX cables run out of the side of the ballast and are connected to the junction box at 4 metres away.

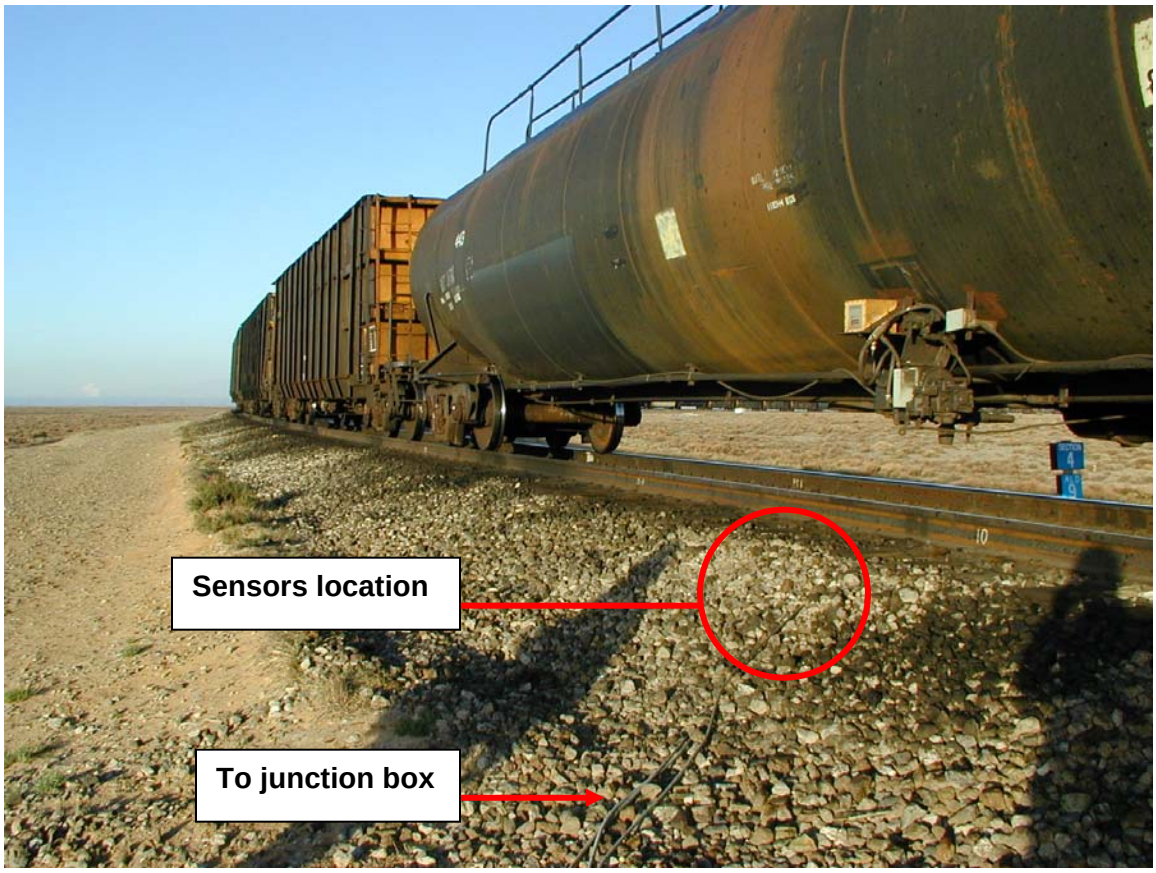

Figure 5.22: Picture of the sensors after the installation is completed. The BX cables runs out from the side of the ballast.

5.4.3 Junction Box

Field requirements dictated that the trailer (housing the data acquisition) and the instrument site were at least 16 m apart. Therefore, a junction box is used to provide intermediate connection between the sensors and the data acquisition.

The junction box rests on an elevated wooden platform supported by steel driven piles. The elevated platform discourages animals and water from entering the container. It also serves as the common grounding point for the system, achieved through installation of a 10 feet copper rod. The drain wires from the signal cable and Faraday-cage-acting BX cables are electrically connected to the earthed metal junction box.

The junction box is protected from the weather by a hard-waterproof plastic container. Holes are made in the side of the plastic container for the BX cables and are then sealed with silicone gel to prevent bugs and insects from entering.

The reservoir for the settlement probe, consisting of a Rubbermaid plastic container and Swagelok connections, are housed in the upper level of the junction box (*Figure 5.25*). The liquid settlement Probe 2 (because it is not working) is not connected to the reservoir and a close-ended tubing is used to block the connection (second tubing from the right). The reservoir is closed (to prevent bugs from entering) but not sealed (to retain atmospheric pressure in the reservoir).

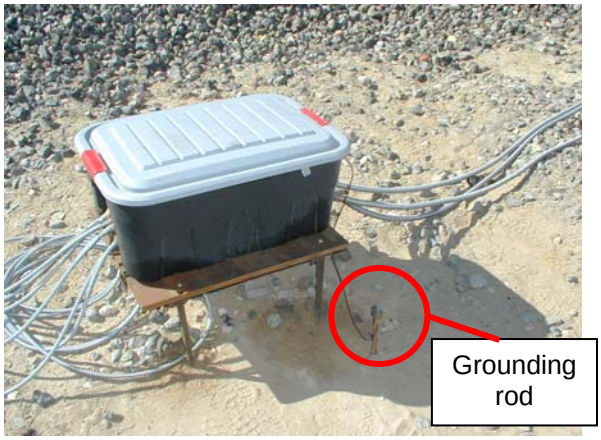

Figure 5.23: Junction box and lightning protection rod.

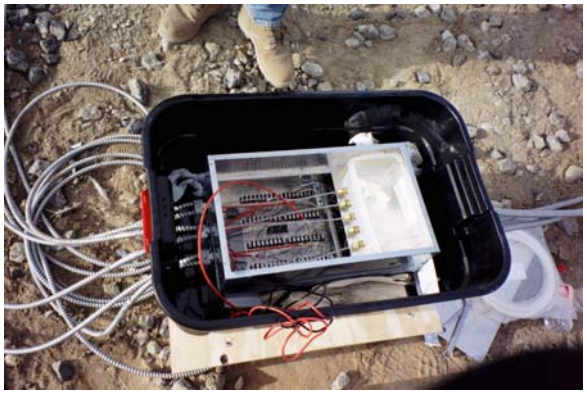

Figure 5.24 Junction box installed at the bridge.

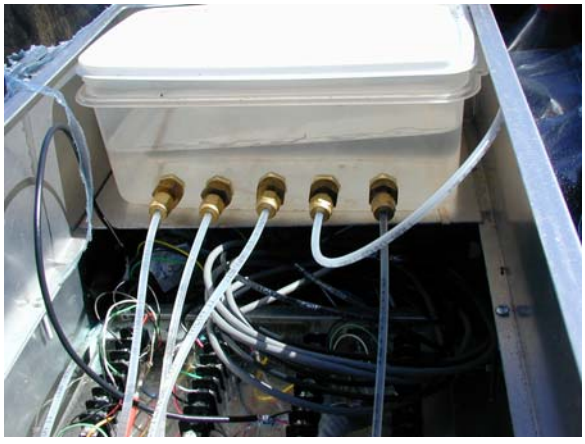

Figure 5.25: Reservoir for the settlement probe

5.5 System testing

Ideally, the initial zero reading (when the settlement probe is placed at the reservoir level) of each probe should be noted prior to field installation. This will enable precise location of the depth of installation. However, this was not possible during the field installation (December 2002) because the computer had compatibility problems with the TTCI network and was serviced by the computer technicians. Instead, the output readings from the probes were manually checked by using a handheld voltmeter to ensure that the readings fall within the desired range. During the second installation phase (April 2003), preliminary data were obtained from the sensors using the DAQ 55 and were instantly analysed. Sensors which were not working properly were immediately adjusted and corrected.

First Field Test Results

Chapter 6: First Field Test Results

6.1 Data collection

The data collection from the monitoring system began immediately after the second phase field installation is completed. Data were collected over a period of four weeks (18 April 2003 to 12 May 2003). The data acquisition was remotely controlled from MIT and the data were electronically transmitted via the Internet. Since the long-term stability of the subgrade (and sensors) is of importance, the data were collected at the maximum allowable (by DAQ 55) period of 20 minutes. The data collection is summarised in *Table 6.1*, and the system performance (at the end of the second phase) is summarised in.

Table 6.1: Data collection at TTCI

Channel	Range	Integration Rate	Bit	Sampling Period
P1-P	± 62.5 mV	610 ms	22	20 minutes
P1-T	± 156 mV	610 ms	22	20 minutes
P2-P	± 62.5 mV	610 ms	22	20 minutes
P2-T	± 156 mV	610 ms	22	20 minutes
P3-P	± 62.5 mV	610 ms	22	20 minutes
P3-T	± 156 mV	610 ms	22	20 minutes
P4-P	± 62.5 mV	610 ms	22	20 minutes
P4-T	± 156 mV	610 ms	22	20 minutes
P5-P	± 62.5 mV	610 ms	22	20 minutes
P5-T	± 156 mV	610 ms	22	20 minutes
RES-P	± 62.5 mV	610 ms	22	20 minutes
RES-T	± 156 mV	610 ms	22	20 minutes
PZT-P	± 62.5 mV	610 ms	22	20 minutes
PZT-T	± 156 mV	610 ms	22	20 minutes
Input Voltage	± 20V	610 ms	22	20 minutes
Shunt 1	± 62.5 mV	610 ms	22	20 minutes
Shunt 2	± 62.5 mV	610 ms	22	20 minutes

Note: P1-P = Settlement Probe 1: Pressure transducer
P1-T = Settlement Probe 1: Thermistor
RES-P = Reservoir: Transducer
PZT-P = Piezometer: Pressure transducer

Table 6.2: Prototype I System Performance

Probe	Location	Transducer		Thermistor	
		Lab	Field	Lab	Field
P1-P	Deepest (1.43m) from top of tie	Working	Working	Working	Working
P2-P	Interface between ballast & subgrade	Not working	Not working	Working	Failed
P3-P	0.86m deep	Working	Working	Working	Working
P4-P	5 cm below ballast interface	Working	Failed	Working	Working
P5-P	On rail tie	Working	Failed	Working	Failed
Piezometer	1.13 deep	Working	Working	Working	Working

6.2 Methods of data interpretation

It has been shown in Chapter 4 that the sensors are sensitive to the changes in temperature and atmospheric fluctuations. It is necessary to apply calibration and correction factors to the data as summarised in *Table 6.3*:

Table 6.3: Calibration and corrections for the sensors

Probe	Type	Equation
All Therm	Temperature Curve	T (C) = 0.5 exp(0.335 x mV/V) + 1.5 x (mV/V) – 0.5
P1	Calibration[1]	2712 (mm/mV/V)
	Temp Correction	ΔH (mm) = 2.6913 (T_{Probe}) -64.983
	Fluid Temp Correction[2]	ΔH (mm) = (-0.0477*T_{atm} + 0.7154)*1.1*1000/100
P2	Calibration	---
	Temp Correction	---
	Fluid Temp Correction	---
P3	Calibration	2683.84 (mm/mV/V)
	Temp Correction	ΔH (mm) = 2.9211(T_{Probe}) - 62.210
	Fluid Temp Correction	ΔH (mm) = (-0.0477*T_{atm} + 0.7154)*1.1*1000/100
P4	Calibration	2812.48 (mm/mV/V)
	Temp Correction	ΔH (mm) = 1.1830(T_{Probe}) - 21.532
	Fluid Temp Correction	ΔH (mm) = (-0.0477*T_{atm} + 0.7154)*1.1*1000/100
P5	Calibration	2701.97 (mm/mV/V)
	Temp Correction	ΔH (mm) = 3.8087(T_{Probe}) - 83.405
	Fluid Temp Correction	ΔH (mm) = (-0.0477*T_{atm} + 0.7154)*1.1*1000/100
Res	Calibration	2659.57 (mm/mV/V)
	Temp Correction	ΔH (mm) = 2.6913 (T_{Probe}) -64.983
	Fluid Temp Correction	NA
PZT	Calibration	50 kPa /(mV/V)
	Temp Correction	ΔH (mm) = 2.6913 (T_{Probe}) -64.983
	Fluid Temp Correction	NA

Note:

1. All the calibration factors and correction factors are applied for the probes. The offset will be set to zero at the start of the monitoring reading. Any deviation from the zero will constitute either settlement is occurring or drift is occurring.
2. The temperature in the ground is assumed as a constant 15°C, thus simplifying calculations.

6.3 Data interpretation

At least a hundred thousand data points have been collected during the monitoring period, and evaluated for short and long-term stability, and drift. The subgrade in TTCI is very stiff and not expected to settle due to train loading, providing a relatively easy reference state for evaluating the stability of the monitoring system. The temperature correction and silicone oil density correction are applied to each of the settlement probes and the absolute stability (removed of the atmospheric pressure influence) can be obtained by subtracting off the witness reservoir transducer. The readings are referenced to the starting point of the test on 18 April 2003.

6.3.1 HAL train operation

The HAL trains are scheduled to operate between 8pm until 7am, four days a week from Sunday night until Thursday morning. The train circles the HTL loop once every 4 minutes and takes about 1 minute to completely cross the sensors. The data acquisition is set to sample readings at every 20 minutes, but there will be instances when the reading coincides with the passing of the train.

The presence of the train is detected by a LVDT (Linear Variable Differential Transformer) installed under the steel bridge. The HAL train causes deflections up to 25mm in the bridge and is easily picked up by the LVDT. The rail loading is plotted in the settlement graphs, appearing as series of long spikes that represent deflection of the bridge. As it turns out, lots of the collected data happened to occur over the weekend when there is no train operation, and there are times when the train operation is cancelled due to track maintenance or rail problems. Train loadings appear in the first week (18-23 April 03, Friday to Tuesday), as shown in *Figure 6.6*.

6.3.2 Performance of the prototype probes

The performance of the sensors is investigated by analysing the stability and settlement graphs with respect to time. The stability graphs (or transducer output graphs) represent the temperature-corrected readings from the pressure transducer, and most of the large fluctuations (up to 100mm) with time are direct results of atmospheric pressure changes. The stability graphs are useful for observing trends of each individual sensor and identify non-performing devices. The settlement graphs (with settlement as

positive and heave as negative), can be derived from the stability graphs by subtracting the readings of the probe from the reservoir pressure transducer (and thus eliminating the effects of atmospheric pressure). The averaging technique (5 point moving window) is applied to smooth out small reading fluctuations.

The performance of the sensors will be characterised in three ways; the first being short-term stability (defined as events occurring less than an hour); and the second, the mid-term stability (events occurring up to a day), and finally, the long-term stability (1month period). Drift refers to the changes in the offset of the transducer with time, and are often long-term events.

As previously mentioned, 3 probes (P1, P3 and piezometer; *Figure 5.13*) have been installed in the “safe” subgrade section. Another 3 settlement probes (P2, P4, P5; *Figure 5.13*) have been installed in more hazardous environments with the intent of evaluating the robustness of the probes.

6.3.2.1 Reservoir Transducer

The reservoir transducer, acting as the witness transducer and a barometer, has rather good stability over the period of two months. Analysing the stability of the reservoir transducer is not quite straightforward, since the “real” value is not known. One way of determining the stability of the reservoir transducer is by comparing it with an independent barometric pressure obtained from the local Pueblo weather station forecast (www.weatherunderground.com). The reading follows the barometric pressure rather closely, with small deviations resulting from localised pressure difference between the sensor location and the weather station (*Figure 6.1*). In addition, the reservoir transducer trends coincide rather closely with other absolute pressure transducers. As such, the reservoir transducer is suitably stable to be used as a reference transducer for all other analyses.

The atmospheric temperature, as measured by the reservoir thermistor (stored in a junction box which is covered by a heat absorbingly black out shell), fluctuates between 8°C and 38°C, which is slightly different than the temperature obtained from the weather station (8°C and 28°C) (*Figure 6.1b*). The temperature different is most notable during the day when heat from the sun is absorbed and trapped in junction box (accounting up to additional of 10°C).

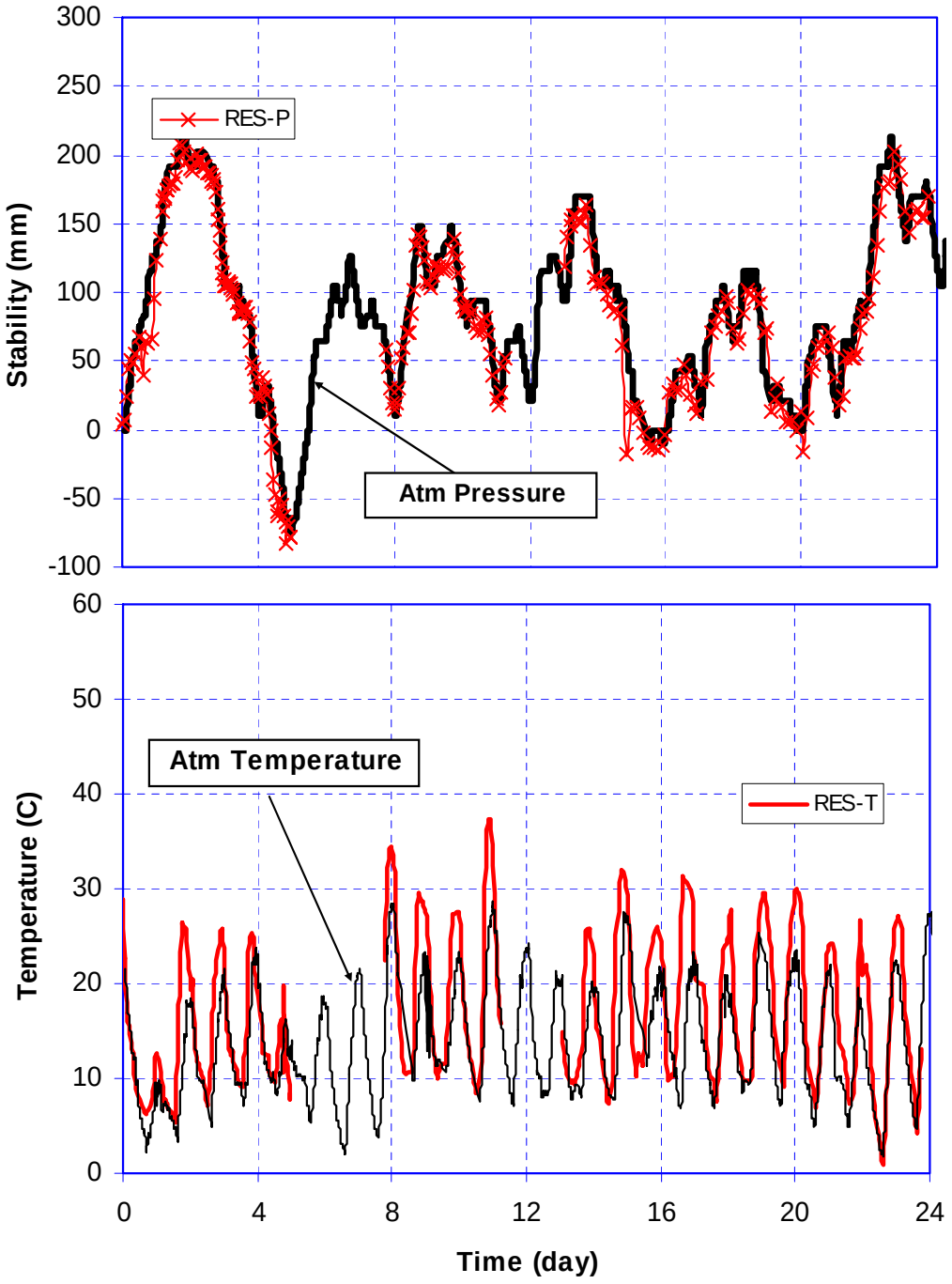

Figure 6.1 : a) Comparison between the reservoir pressure transducer (RES-P) and the atmospheric pressure (from weather station), and b) comparison between the reservoir thermistor and the atmospheric temperature for the period 18 April – 12 May 2003.

6.3.2.2 Piezometer (PZT-P)

The measurement of the piezometer is normally in kPa but for simplicity and ease of comparison, the absolute stability of the piezometer is plotted with the settlement probes in mm. For analysing purposes, a change in 1mm of silicone oil is equivalent to 0.0094 kPa. Since no pore water pressure is expected to develop in the sandy subgrade (and any fast impulse of pore pressure due to train loading will not be detected by the piezometer), the ideal absolute stability of the piezometer is expected to be zero.

In general, there is a good agreement between the piezometer and the reservoir transducer over the period of two months, with the average absolute stability of zero kPa. There are times when the absolute stability reaches 40mm, before returning to the zero regions. The temperature in the ground is relatively constant, pegging at 10°C (April) and 12°C (May) and temperature correction is not critical for piezometers. The thermistor is working very well, as illustrated in *Figure 6.5*.

6.3.2.3 Settlement Probe 1 and 3

The temperature-corrected output readings (termed stability graphs in the figures) and the absolute stability of probe 1 and 3 are shown in *Figure 6.4* and *Figure 6.5, Figure 6.3.* The absolute stability profile is obtained by subtracting the readings from the settlement probe and the reservoir transducer in order to remove the effect of the atmospheric pressure.

During the first week (18 – 24 April 2003), P1-P showed short-term (1 hour) and mid-term (1 day) absolute stability of 0.4mm and 20 - 80 mm respectively. P3-P, on the other hand, showed short-term and mid-term absolute stability of 0.4mm and 40 cm respectively (*Figure 6.6*). In the second week, P1-P was temporary disconnected from the data acquisition and no data were available. P3-P showed short-term and mid-term absolute stability of ± 20mm (*Figure 6.7*). In the third week, P1-P registered short and mid term absolute stability of 0.4mm and 80mm (although the mid term stability improved to 20mm from days 15 to 18). P3-P had short and mid term stability of 0.4mm and ±20mm (*Figure 6.8*). This result is similar in the final week of data gathering (*Figure 6.9*).

In conclusion, the settlement probes P1-P has short, mid, and long term absolute stability of 0.4mm, 20 – 80mm, and 80 mm respectively. P3-P has short, mid, and long term absolute stability of 0.4mm, ±20mm and ±20mm respectively. The overall results are summarised in *Figure 6.3*.

So what causes these big stability issues in the prototype probes? The short term absolute stability of both settlement probes seems to be affected by the atmospheric temperature, despite being buried the ground with almost constant temperature. The data acquisition is not susceptible to temperature fluctuations, discussed in Section 4.2.1. The absolute stability is obtained by subtracting the readings of the reservoir transducer from the settlement probe. The temperature correction equation of the reservoir transducer is by no means perfect and may have contributed up to ±5mm of error (see *Figure 4.9*). Coupled with the errors from the silicone oil density-temperature corrections in the 10m tubing, this may well add up to the localised temperature related absolute stability. Using the field data, the difference between having a density correction factor and one without could account up to 5mm for a 15°C differential temperature (between the atmospheric and ground temperature), or 10mm for 30°C differential temperature (*Figure 6.2*).

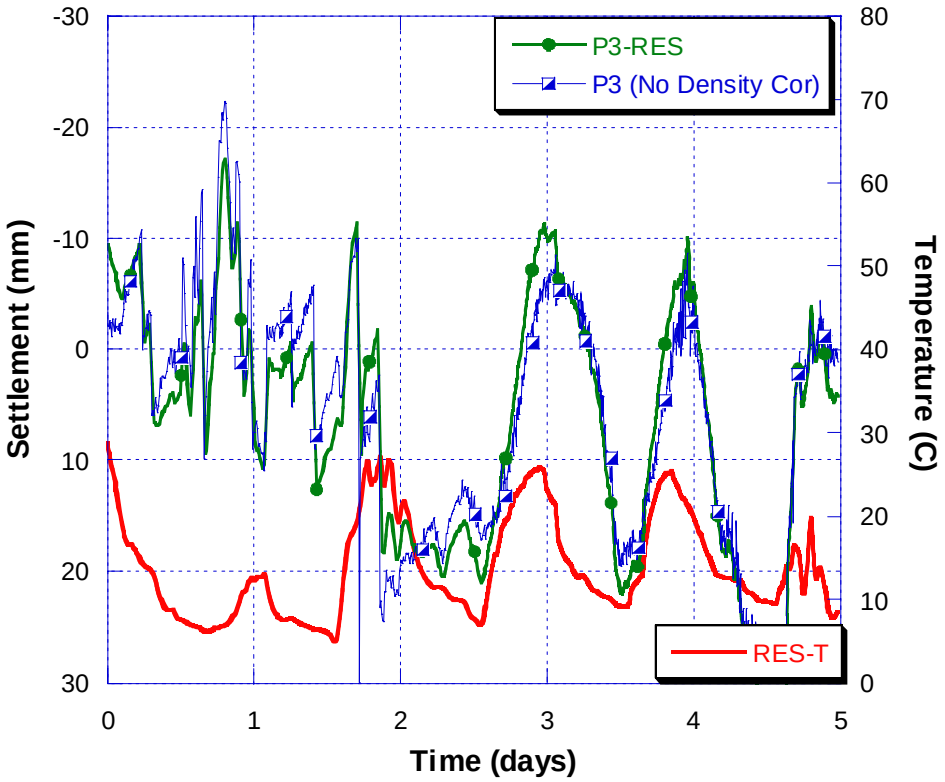

Figure 6.2: Comparison between density-corrected P3-P (for silicone oil in the tubing) and no density correction.

Arguably, the short term temperature influence may not be a critical issue for this application where the overall settlement picture is obtained over period of three to twelve

months. These fluctuations can be ironed out and the long term stability is more important.

The underlying reasons for the unsatisfactorily long term drift of the settlement probes are unclear. The reservoir transducer and the piezometer, have simpler construction and operation, and show rather good long term correlation with each other. This suggests two possible explanations for the settlement probes: a) The dependence of silicone oil head over 10m of tubing might have added complexity to the problem, or b) better soldering and wiring techniques are needed during the construction of the settlement probe. The former should not contribute more than 10 or 15 mm of error. The latter is likely to be the cause for the poor field performance. The allowable soldering temperature of the MPX2100A and MPX2200A pressure transducers are limited to 260°C. These specifications were not appreciated in advance of fabrication, and it is highly likely that the temperature limits were exceeded in preparing for the first field deployment. More stringent controls on the fabrication are expected to solve the problem in a second field at TTCI, currently in preparation.

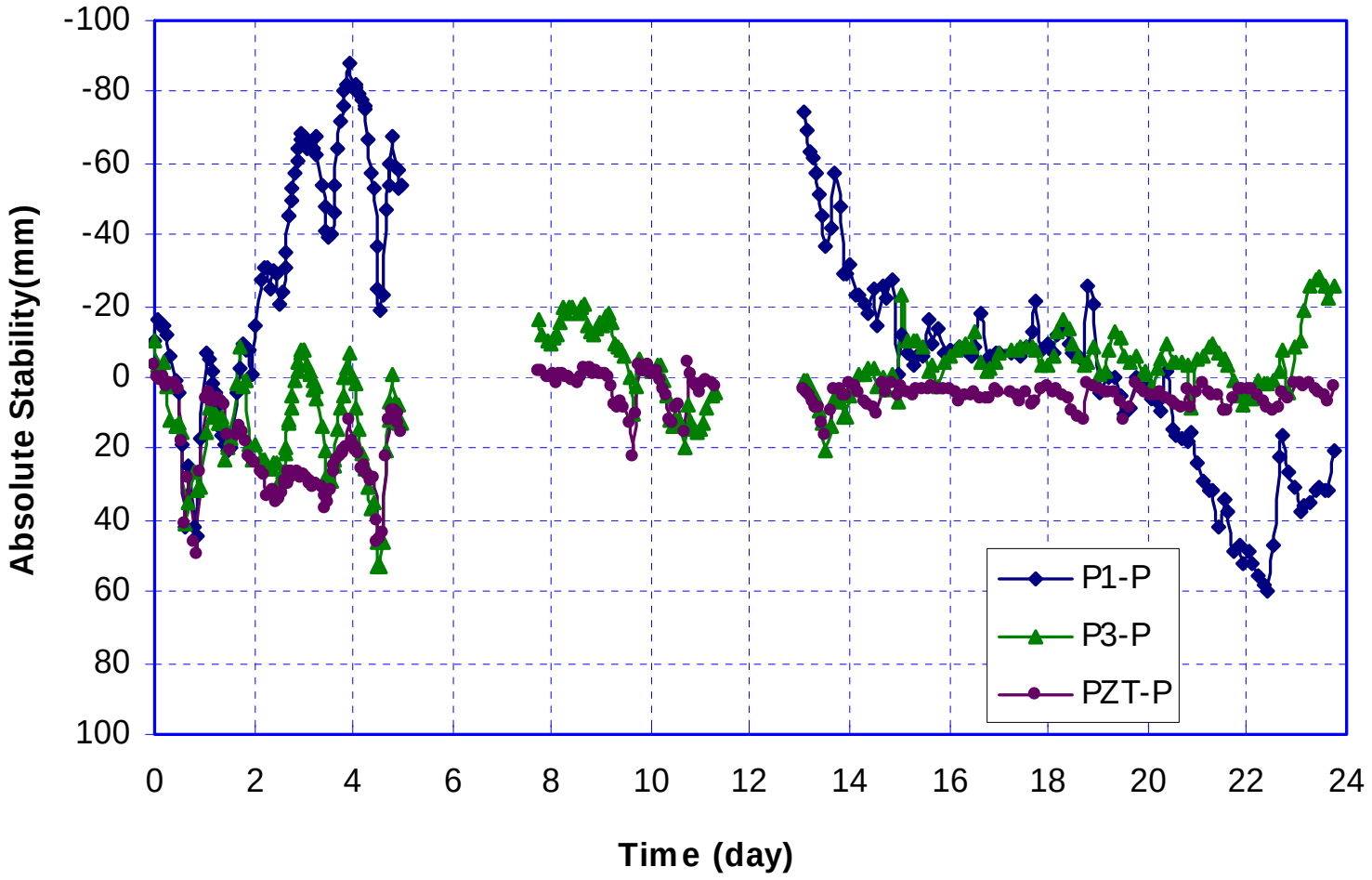

Figure 6.3: Absolute stability of settlement probe 1, 3, and piezometer (18 April – 12 May 2003)

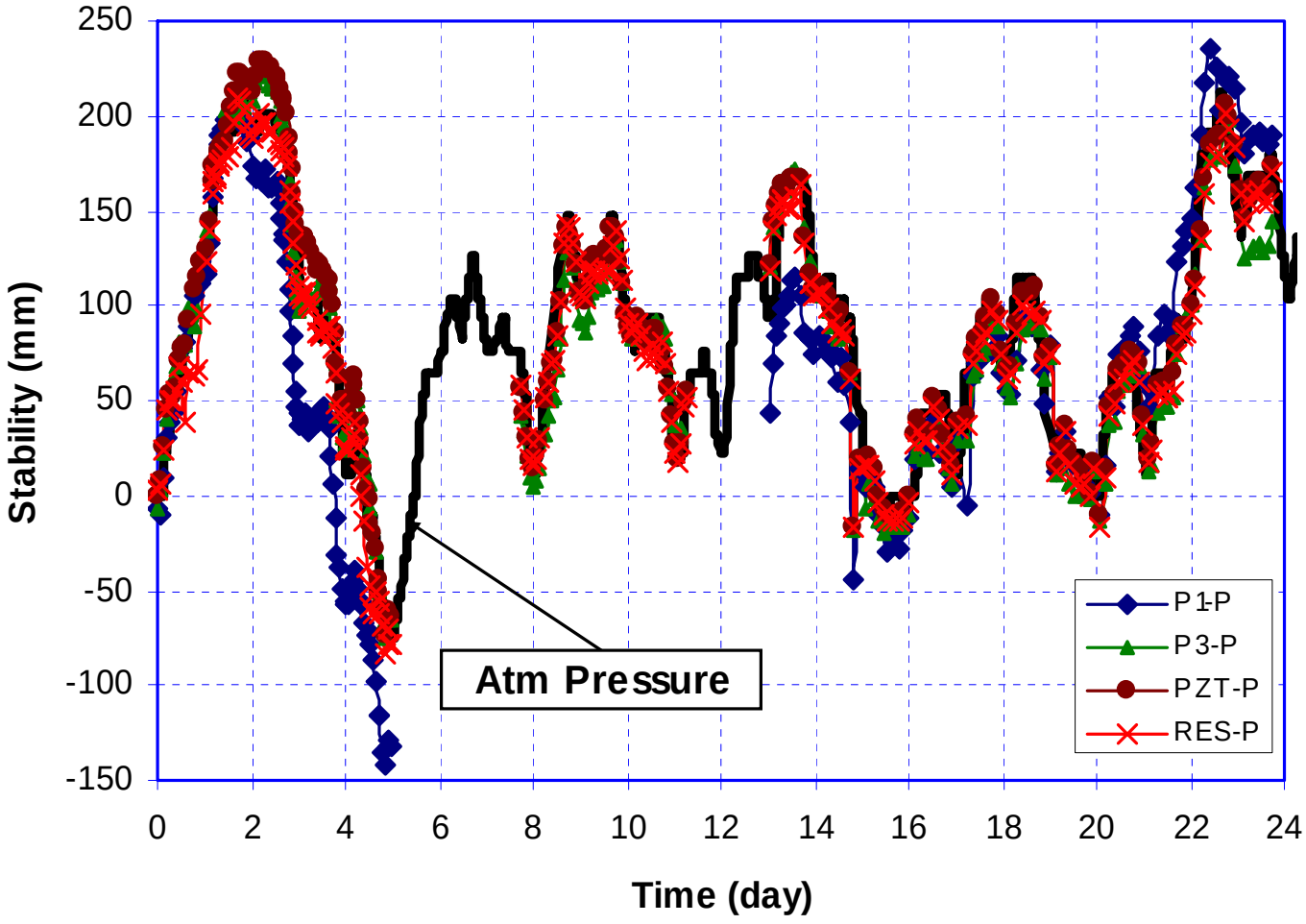

Figure 6.4: Stability of settlement probe 1, 3, and piezometer (18 April – 12 May 2003)

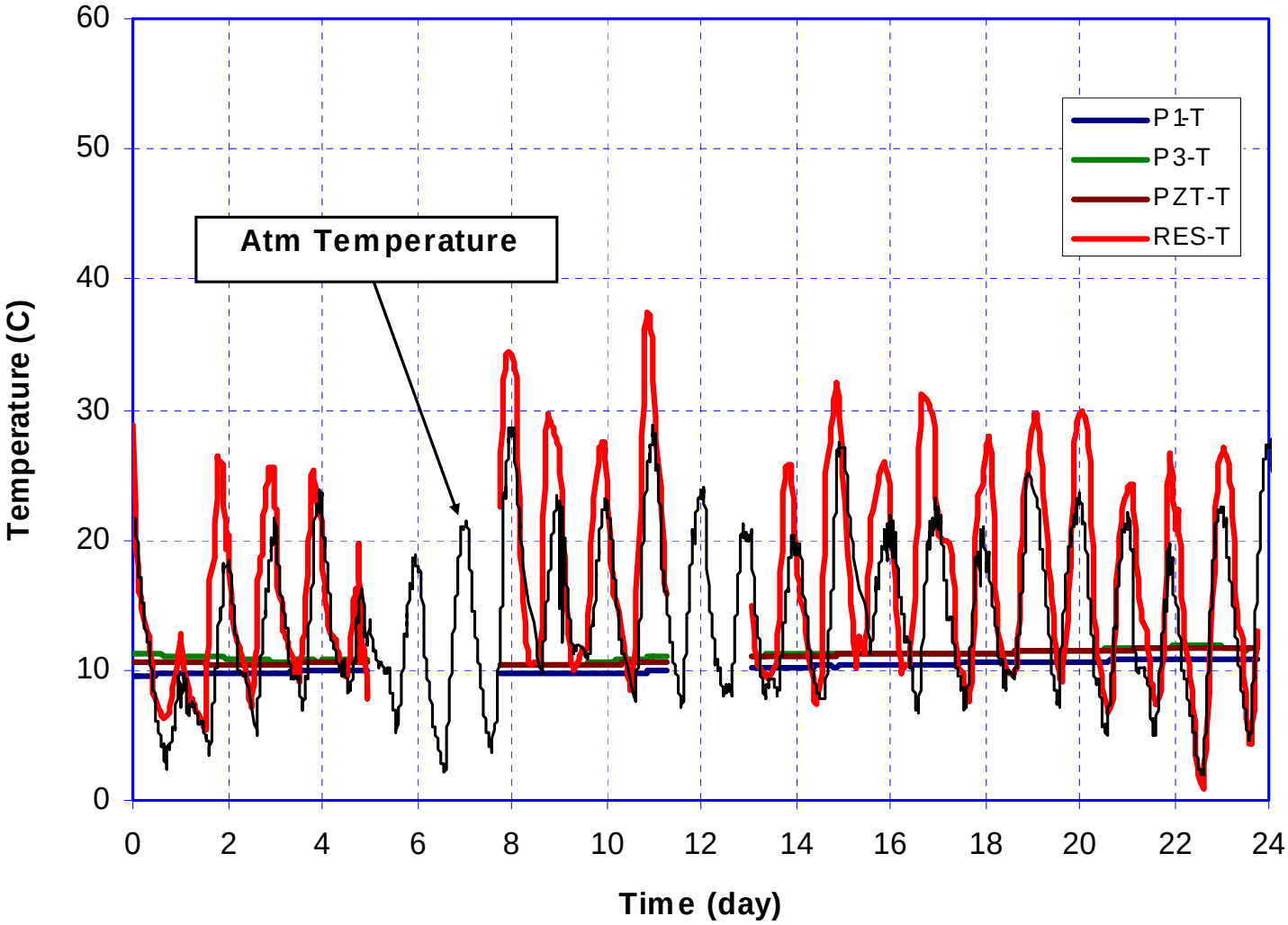

Figure 6.5: Temperature readings for settlement probe 1, 3, piezometer and reservoir thermistor (18 April – 12 May 2003)

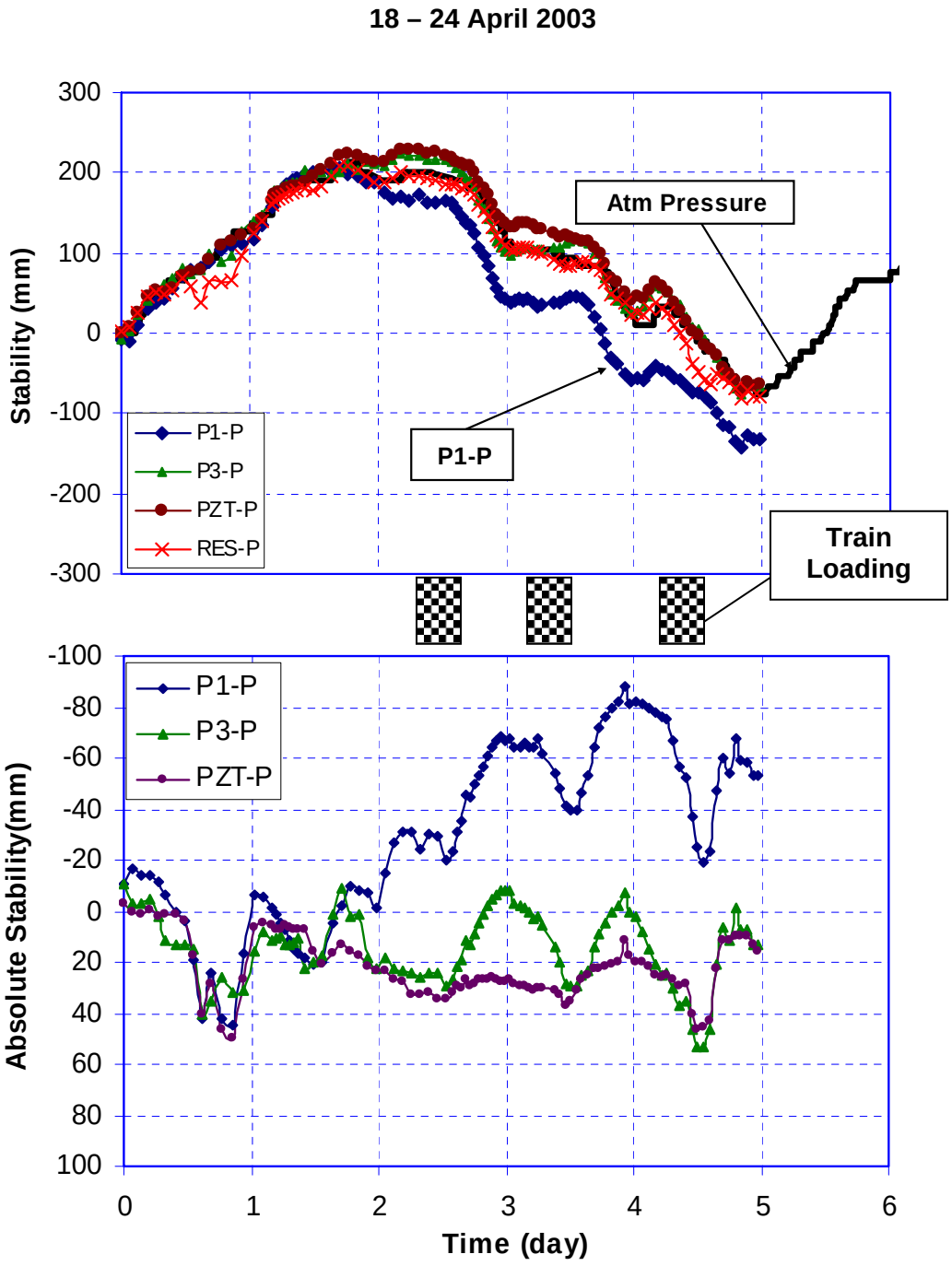

Figure 6.6: a) Stability and b) Absolute stability of sensors between 18 – 24 April 2003

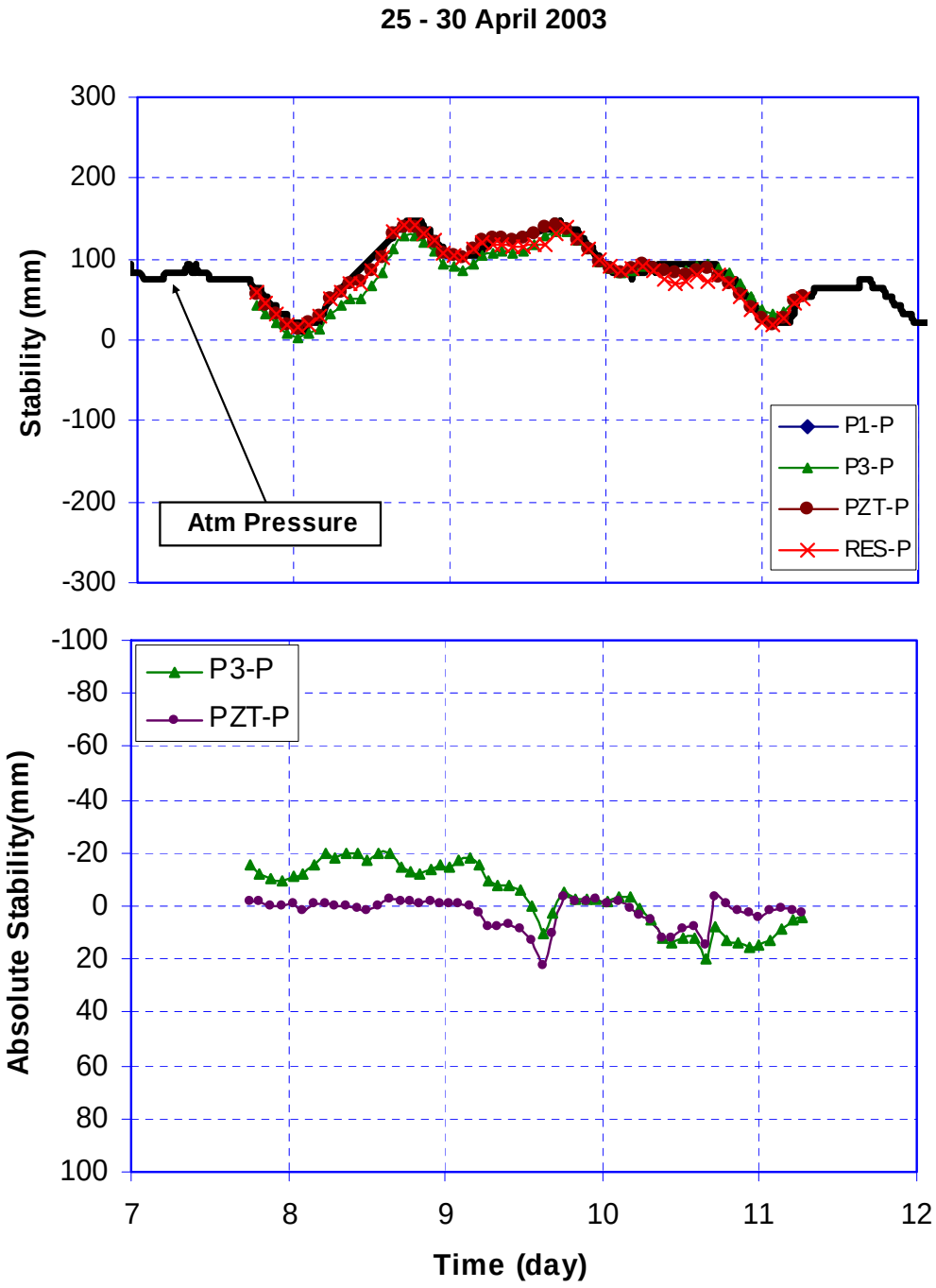

Figure 6.7: a) Stability and b) Absolute stability of sensors between 25 - 30 April 2003

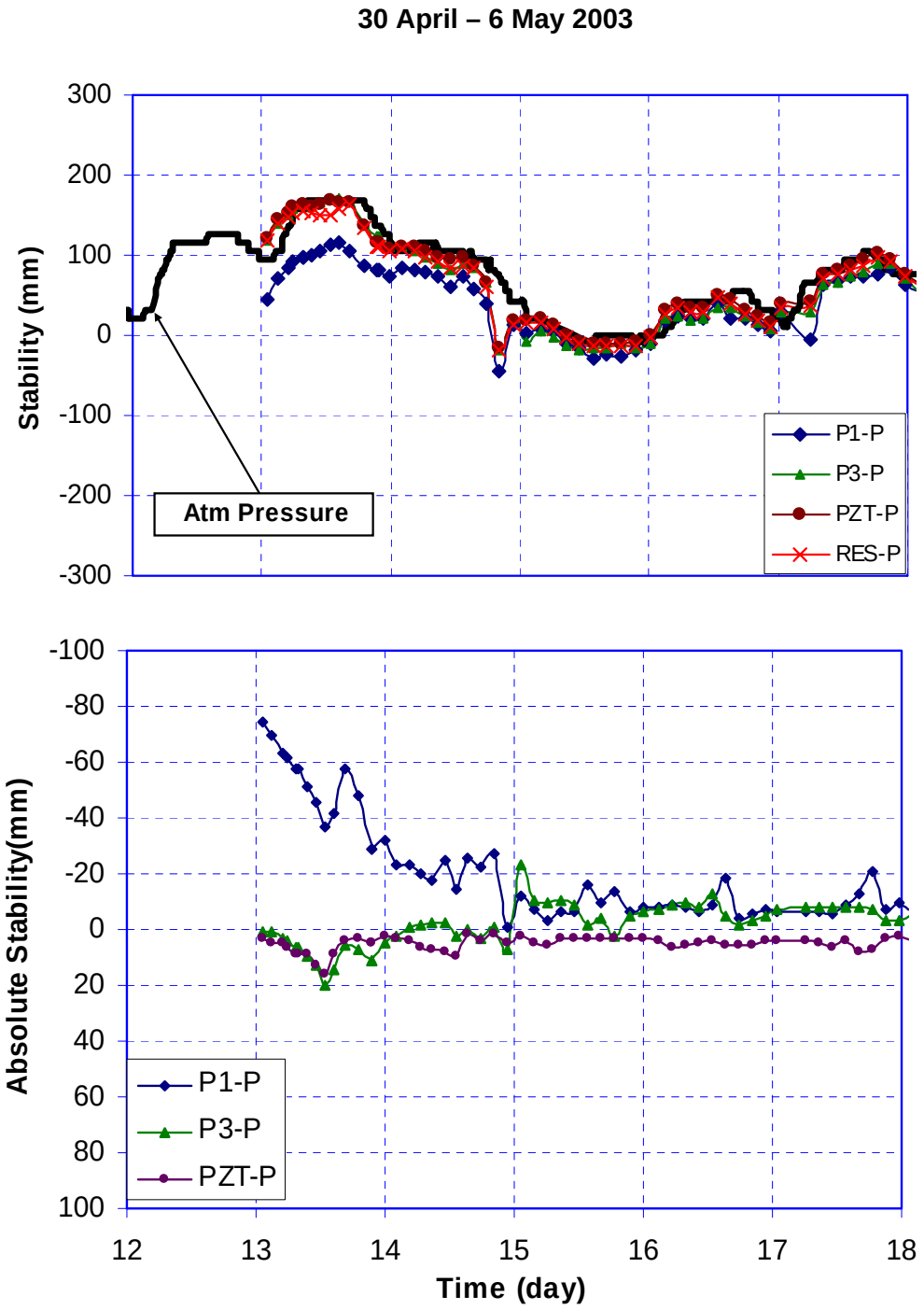

Figure 6.8: a) Stability and b) Absolute stability of sensors between 30 April – 6 May 2003

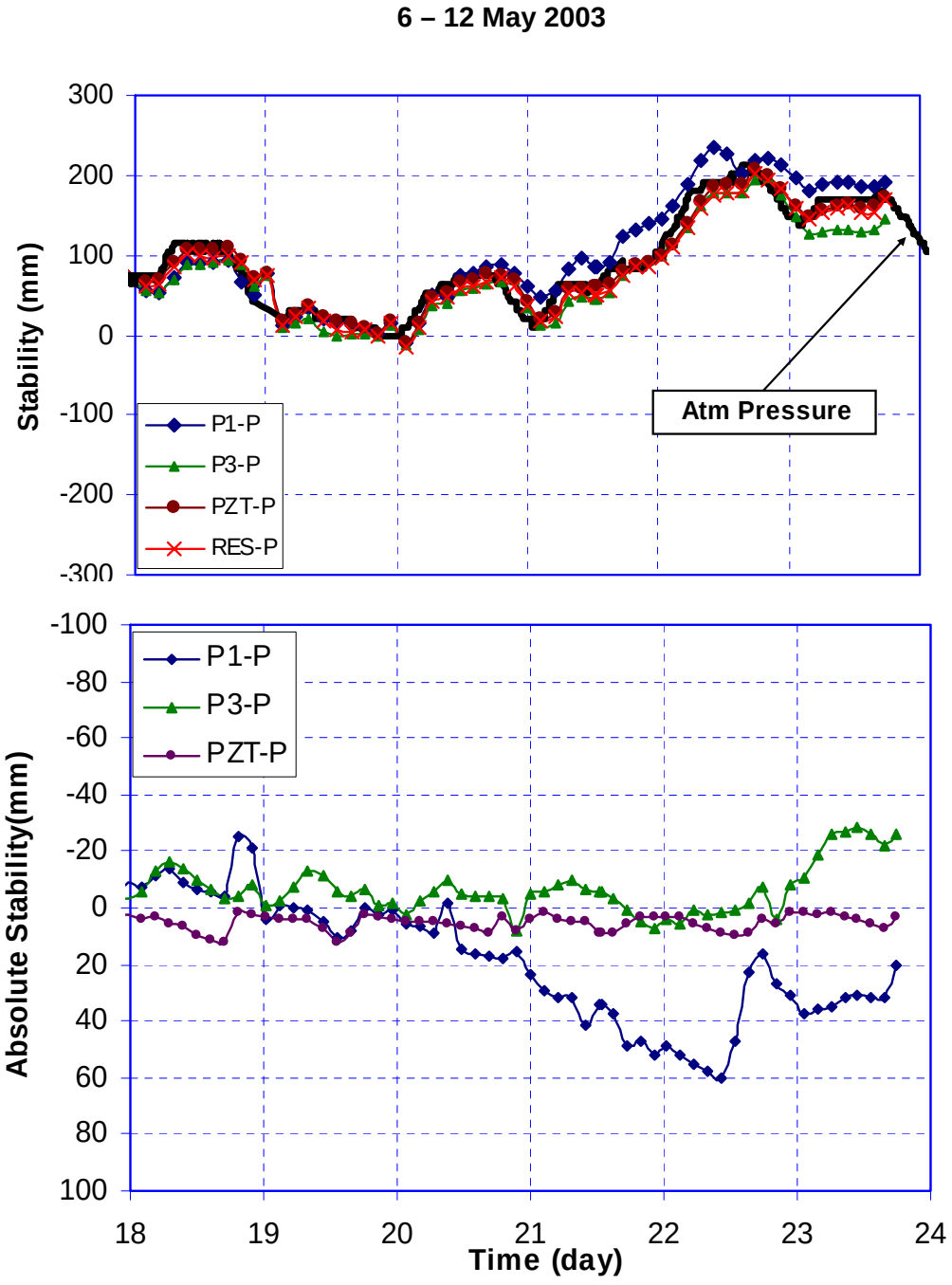

Figure 6.9: a) Stability and b) Absolute stability of sensors between 6 – 12 May 2003

6.3.2.4 Settlement Probe 2

The settlement probes and piezometer installed deep in the subgrade have been, so far, resilient to the train loadings. The robustness of the sensors will be further tested by installing a settlement probe (P2) at the very high stress interface between the ballast and the subballast. Since the pressure transducer for P2 settlement probe was not functioning (during fabrication and was not replaced due to time constraint), it now relies on its working thermistor (*Figure 6.10*) to act as a ground thermometer. As postulated, the crushing action of the ballast proved to be too great and P2 ceased to function (*Figure 6.11*). The temperature readings are now in the region of 2000°C as opposed to the ground temperature of 11°C. The probe failure occurred sometime between the first instalment and the second instalment in April.

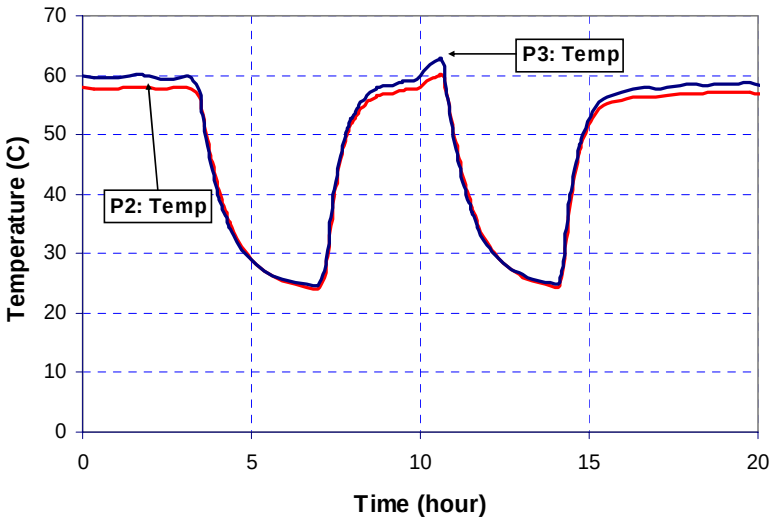

Figure 6.10: Stability of P2 during the laboratory temperature calibration testing (compare with P3)

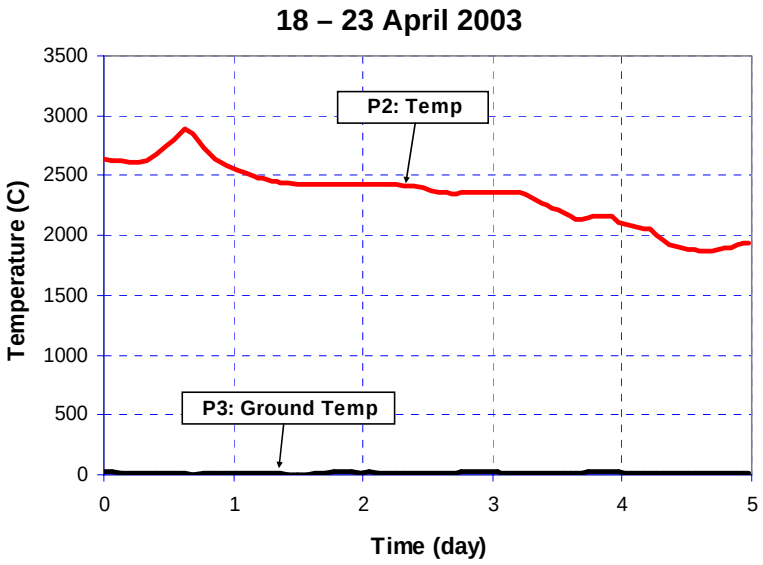

Figure 6.11: Stability of P2 after field installation.

6.3.2.5 Settlement Probe 4

P4 is installed at a depth of 5 centimetres below the highly stressed ballast–subballast interface. P4 is one of the few probes which had been monitored after the first installation phase in December 2002. The readings from the pressure transducer (during the first installation phase) seem to fluctuate with the atmospheric temperature, despite being buried in the ground where the temperature is expected to be nearly constant. The thermistor was not monitored in the first installation phase due to wiring problems.

During the second installation phase, the thermistor and the pressure transducer is now connected to the Iotech data acquisition and the wiring at the junction box is checked. However, by now, the offset of P4 has shifted to 6.4 (mV/V), well above the 4 (mV/V) maximum transducer output and exceeded the 64mV data acquisition voltage sampling range. However, the thermistor shows good readings and is measuring the correct ground temperature four months after then installation (*Figure 6.13*). It is possible that the train loading may have crushed the probe, and thus destroying the pressure transducer (which has questionable performance in the first phase) while keeping the thermistor intact. The probe is robust enough to withstand most of the high stresses just below the ballast/subgrade interface.

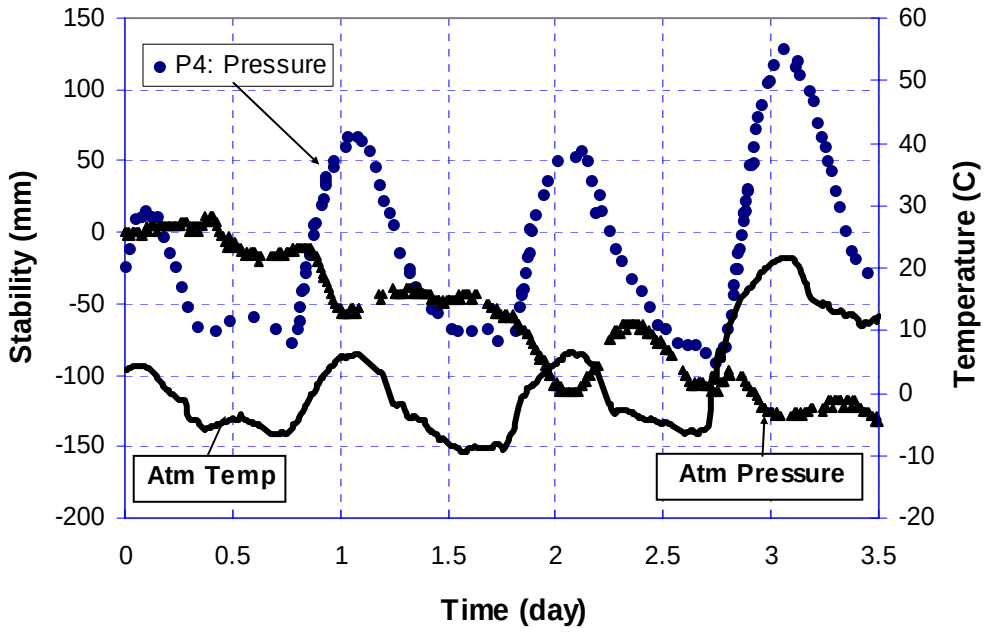

Figure 6.12: Performance of P4: First phase (16 to 20 Jan 2003)

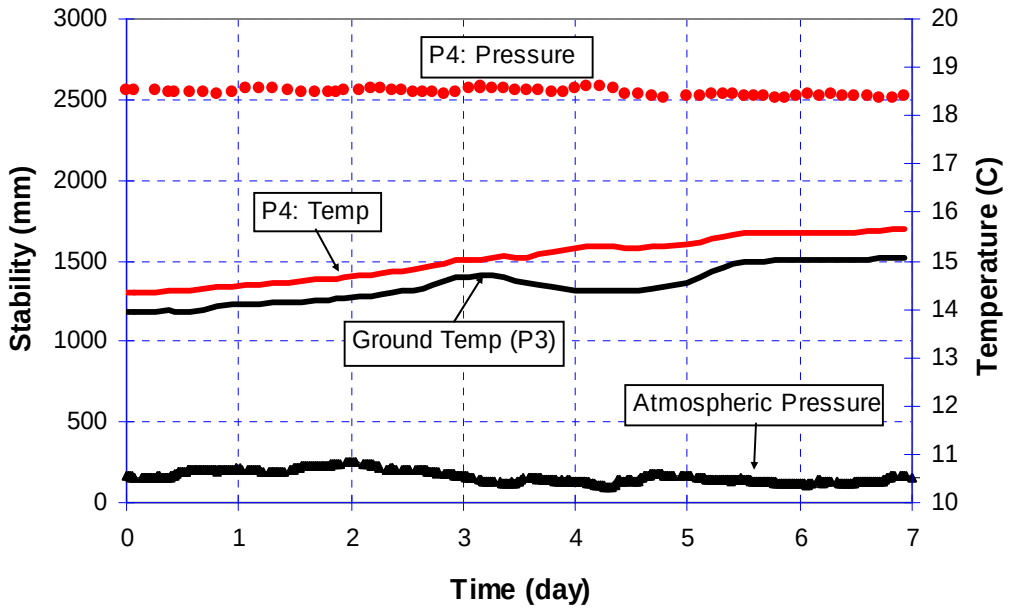

Figure 6.13: Performance of P4: Second phase (26 – 30 May 2003)

6.3.2.6 Settlement Probe 5

The performance of the settlement probe when exposed to the full brunt of atmospheric weathering, high electrostatic charges in the rail track, and track maintenance machines is evaluated by installing a settlement probe (P5) onto the rail tie (*Figure 6.14*). It is also installed at an elevation higher than the reservoir and is subjected to negative silicone head.

Figure 6.14: P5 clipped on the rail tie.

The performance of P5 after the first phase installation is shown in *Figure 6.15*. The temperature readings follow the atmospheric temperature (www.wunderground.com) rather closely. However, the transducer output appears to fluctuate (between 1000 and -800mm) with the atmospheric temperature rather than the atmospheric pressure, despite application of temperature correction factors detailed in *Table 6.3*. The (apparently) temperature related fluctuations far exceeds the 40mm / 10°C temperature calibration curve for the pressure transducers. This means the pressure transducer is electronically dead.

During the second installation phase in mid April, the connections at the junction box and to the Iotech data acquisition were checked for bad wiring conditions. However, the condition persisted (*Figure 6.16*) and the transducer has mostly likely failed. The thermistor is now showing big temperature fluctuations, occasionally returning to the correct atmospheric temperature (*Figure 6.17*). However, after 23 April 03, the thermistor failed. The extended exposure to the harsh wintry condition (-15°C) proves to be detrimental to the probe.

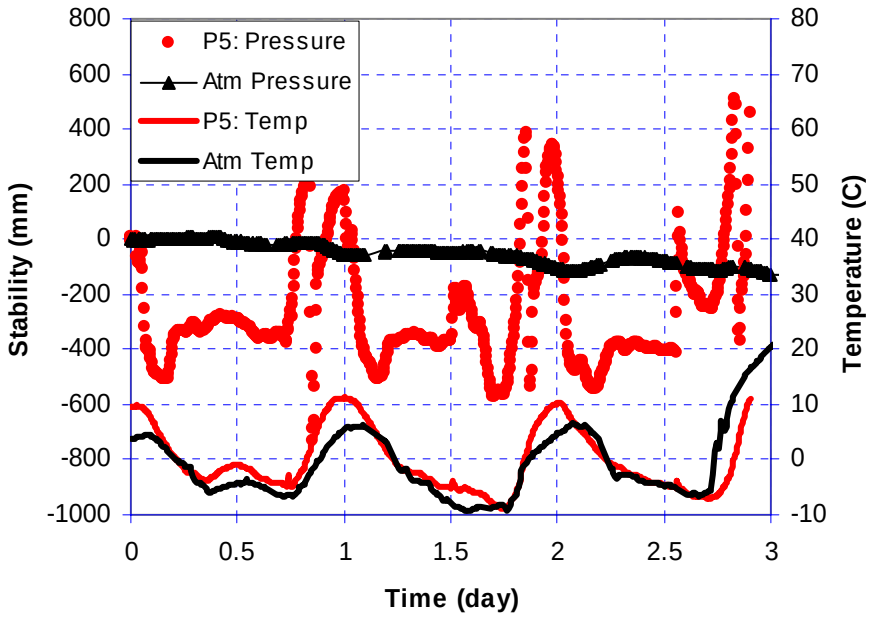

Figure 6.15: Performance of P5 (at rail tie) after first installation phase (16 – 20 Jan 03)

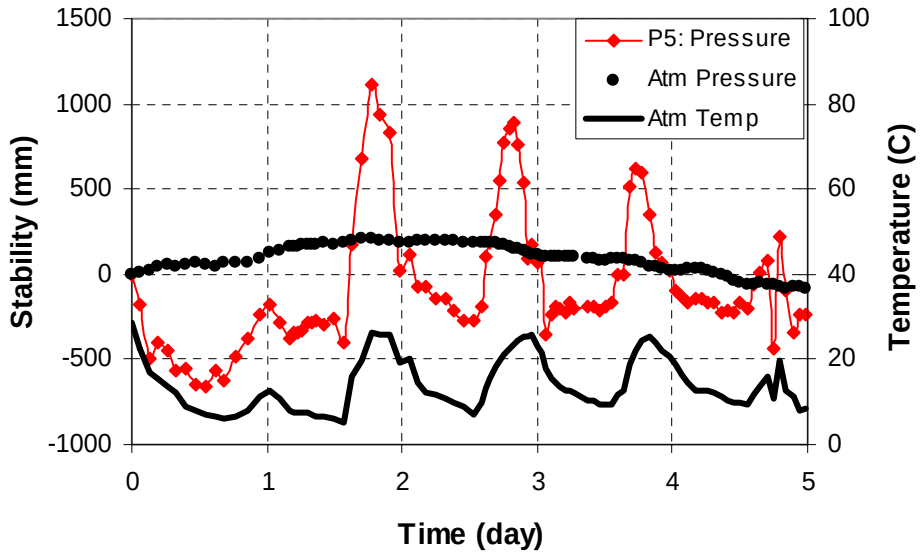

Figure 6.16: Performance of P5 three months after installation (18-23 April 03.)

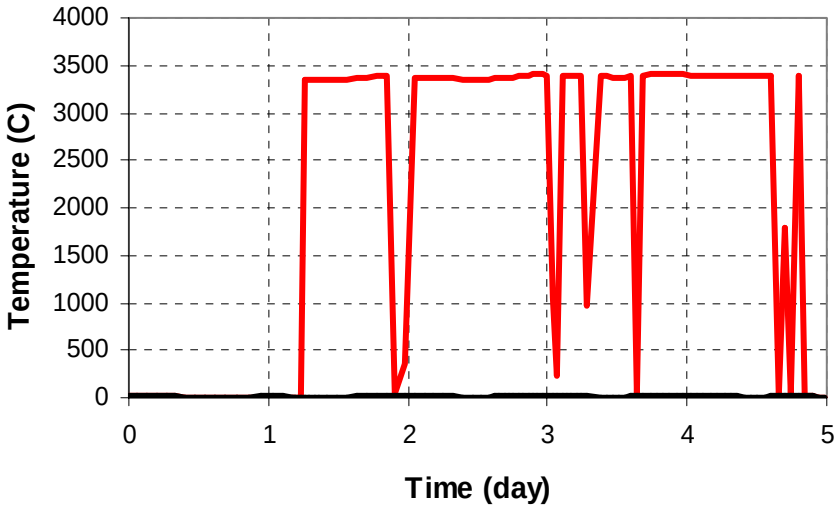

Figure 6.17: Performance of thermistor in P5 (18-23 April 03).

6.3.2.7 Remarks about P2, P4 and P5

All three settlement probes have been installed in areas of high risk zones: P2 and P4 were installed close to the highly stressed ballast and subgrade interface, and P5 was clipped onto the rail tie and is susceptible to environmental degradation and track maintenance vehicles. These probes (except P4) failed at a period between 2 weeks to 2 months, suggesting that these zones should perhaps be avoided. *Table 6.4* summarises the observations.

Table 6.4: Performance of settlement probe P2, P4, and P5, before and after installation.

Probe	Location	Transducer		Thermistor	
		Laboratory	Field	Laboratory	Field
P2	Interface between ballast & subgrade	Not Working	Not Working	Working	Failed
P4	2 cm below P2	Working	Failed(?)	Working	Working
P5	On the rail tie	Working	Failed	Working	Failed

The failures are experienced by both the pressure transducer and the thermistor, and in the case of P4, only one of them failed. There are several reasons that could contribute to these failures. P2 is exposed to the harsh wintry weather which may have

damaged the sensor. Another plausible reason would be failure at the electronic circuit board in the embedded probe caused by train loading. The combined diameter of the data cable and the nylon 11 tubing is almost equal to the inner diameter of the BX cable, thus causing them to “lock-tight” with the BX cable. There is virtually no leeway for the BX cable to slide over the data cable and the fluid tubing. It is possible that the high stresses and vibrations exerted by the ballast due to train loadings may have displace the BX cable from the embedded probe, and in the process, pulled the data cable out from the electronic circuit board. This hypothesis can be confirmed by excavating the probes and performed physical examination. Alternatively, a resistance check on the output of the transducer can be performed and values of 2kΩ are expected.


VII
Conclusions

Chapter 7: Conclusions

The advent of electronic sensors in the 80s has spawn new ways of field data collection and has certainly changed the way traditional methods of measurements are being made. While being vigorously embraced in other high technology fields such as aerospace, automotive industry, etc, electronic instrumentation is slowly creeping its way into the geotechnical community, in this particular case, the railroad industry. Rail alignment problems are characterised by high maintenance costs, and many of these sections are in remote areas where it is often uneconomical to employ traditional (manual) instrumentations, and this is where the strength of remote monitoring systems can be fully realised.

This thesis presents the first development phase of a remote and low cost monitoring system aimed at characterising site-specific subgrade problems. This project offers exciting opportunities to be involved in a variety of disciplines, starting from problem definition and identification, designing the complete monitoring system and fabrication of sensors, laboratory testing, field installation, data collection, and results interpretation.

7.1 Instrumentation

7.1.1 The monitoring system

The prototype monitoring system currently consists of 5 settlement probes, a piezometer and an on-site data acquisition system installed at TTCI for field evaluation. The sensors are tailor-made to meet the needs of railway subgrade monitoring, in particular the cost, resolution of measurement and flexibility of installation of the sensors. The piezometer is a 27 x 187 mm probe capable of measuring pore pressure up to 200 kPa at resolution of 0.01 kPa (Section 3.3). The liquid settlement probe is used to measure the settlements and is capable of measuring up to 10m with resolution of 0.09 mm (Section 3.4). The analogue signal produced by the sensors is converted into digital signal by an on-site data acquisition module (Iotech DAQ55) before being transmitted back to MIT via the Internet for further processing. The USB-based DAQ 55 is small, low cost, good long-term stability (Section 4.2.1), and portable, thus making it an ideal unit

for on-site data acquisition. At the moment, the monitoring system is dependant on the power supply (115 V_{ac}) and Internet connection provided by TTCI.

7.1.2 Design and fabrication of sensors

Design, fabrication and laboratory testing of the sensors constitute a major portion of this research. The design methodology and blueprints for the piezometer and settlement probes are described in Section 3.3.3 and 3.4.2 respectively. Care has to be taken when handling and soldering the pressure transducers (Section 3.3.3.9). The sensors have to be properly saturated before installation to ensure good performance (Section 3.3.3.9) & (Section 3.4.2.6). Proven procedures have been developed for this application.

Each of the probes typically takes ten hours of fabrication time using a conventional manual lathe, although the time can be considerably reduced with automatic lathe machine and production manufacturing. The settlement probe and the piezometer share many similar components but this advantage will be fully utilised by an production manufacturing.

7.1.3 Laboratory Testing

The laboratory test programs serve two aims: a) to identify all factors which may affect the readings of the sensors, and b) to experimentally characterise these influencing factors. The absolute pressure transducers are affected by the fluctuations in atmospheric pressure, temperature, and environmental noise (Section 4.3.1 & 4.3.2). The settlement probes, being dependent on the silicone fluid for pressure measurement, have additional fluid density-temperature corrections (Section 4.4.2.2). Without these temperature and density correction factors, it is usual to expect up to 100 mm errors in measurements. Unfortunately, the correction factors are specific to each transducer and cannot be used interchangeably between them. All transducers have to be calibrated separately due to inherent differences between them, possibly from imperfect manufacturing.

Laboratory testing suggests that the low-cost MPX transducers have good stability and resolution (Section 4.3.1), which is often limited by the inherent stability of the data acquisition.

7.1.4 Installation process

The field installation process took place in two phases; first in December 2002, and the second in April 2003. The physical installation of the sensors and data acquisition was completed in the first phase and the data acquisition system was upgraded during the second phase. The monitoring system is designed for easy installation with minimal machinery, manpower and time. The installation of the probes in the subgrade is achieved by means of a shovel (top ballast excavation), front end loader machine and a hand auger for side installation (Section 5.4.2.2). The data acquisition system and the remote control link were easily set up in the trailer (Section 5.4.1).

The field installation of the sensors (including excavation of the ballast, augering, refilling and compaction) took only four hours to complete. There were no problems with installing the probe in the required orientations and locations. The successful field installation exercise offered the author an opportunity to evaluate the design of the sensors and the installation procedures. The augering and shovelling method will be incorporated in future installation programmes whereas the installation procedures can be further improved (Section 5.6)

7.1.5 Field Data Interpretation and Discussions

The field data were collected over a period of four weeks, starting from 18 April 2003 to 12 May 2003. The Heavy Axle Load (HAL) train operates four days a week and simulates the actual (problematic) field conditions. In addition, the monitoring system is subjected to the harsh Colorado environment, spanning from the winter of 2002 (since the first field installation) to the hot summer of May 2003. Since there is virtually no movement and pore pressure developing in the hard sandy subgrade, this provide an excellent platform to evaluate the stability of the sensors.

Over a hundred thousand data points have been collected and evaluated for short and long term stability, and drift. The correction factors are applied to the respective sensors and the results are presented in Section 6.3. The reservoir transducer and the piezometer show good short and long-term stability (Section 6.3.1.1 & 6.3.1.2 respectively). The settlement probes P1 and P3 have reasonable short-term stability, although they are more susceptible to long-term drift (Section 6.3.1.3). The higher short-term fluctuations could be due to the combination of inadequacies in the model of fluid density correction and various unknown environmental interference.

DUNNICLIFF (1988) has observed that the accuracy of a liquid settlement probe (with the vibrating wire transducer) is typically between 6 to 25 mm.

Important lessons can be drawn from the performance of P2, P4 and P5 (Section 6.3.1.4, 6.3.1.5 & 6.3.1.6). The three settlement probes are installed in high-stressed zones and two of the three probes failed from repeated train loadings (6.3.1.7). The laboratory and field performance of the sensors are summarised in *Table 7.1*.

Table 7.1: Performance of the sensors.

Probe	Laboratory Testing		Field Testing	
	Short Term Stability*	Mid Term Stability**	Short Term Stability	Long term Stability***
P1	0.4mm	3 mm	0.4 mm	80 mm
P2	NA	NA	NA	NA
P3	0.4 mm	5 mm	0.4 mm	±20 mm
P4	0.4 mm	6 mm	Failed	Failed
P5	0.4 mm	2 mm	Failed	Failed
PZT	0.0094 kPa	0.047 kPa	0.02 kPa	0.05 kPa

Note:

* Short term stability defined as events occurring under 1 hour
** Mid term stability defined as events occurring over 1 day
***Long term stability defined as events occurring over 1 month

Overall, the prototype field instrumentation program and data analyses have been successful. However, there are serious stability issues in the settlement probes which are believed to be caused by overheating during the soldering process. This problem will be addressed at next phase of settlement probe designs.

7.2 Recommendations for future research

A second phase monitoring system to be installed at a site with problematic subgrade is being designed and built. Key emphasis will be placed on evaluating the reliability and the stability of the second wave of settlement probes.

The current monitoring system will be expanded to include power supply and remote data transfer. This may include the solar panels and batteries for renewable power backup, satellite Internet or mobile phone connection to relay data back to MIT. The satellite Internet allows the flexibility of installing the system almost anywhere in the

United States. The methodology for the complete package is illustrated in *Figure 7.1*. The monitoring system will be installed at a problematic site.

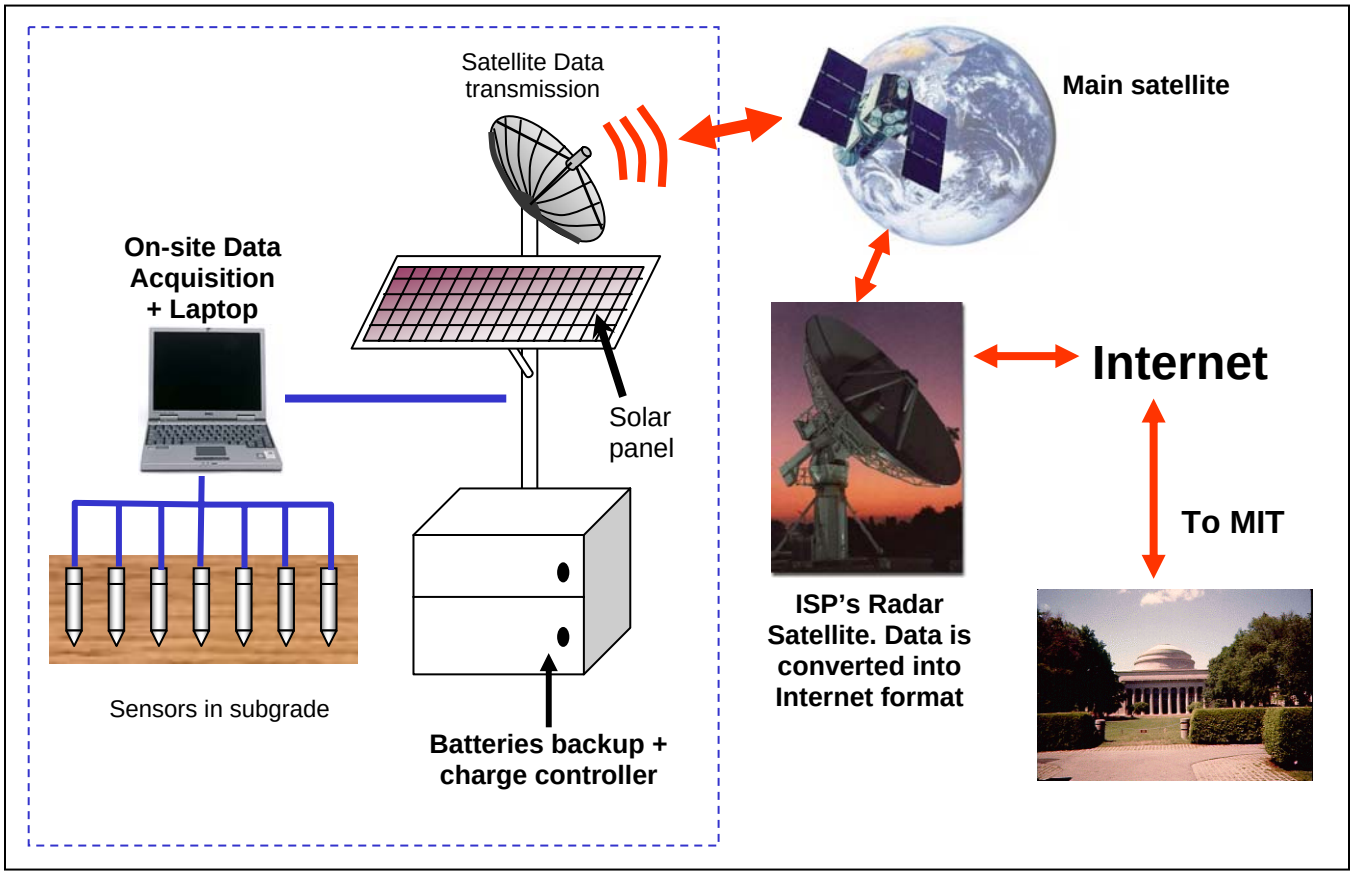

Figure 7.1: Remote monitoring system package of the future.


References

Chapter 8: References

Andersen, K.H, Brown S.F, Foss I, Pool J.H, Rosenbrand W.F (1976), '*Proc., Conf. on Des. and Constr. of Offshore Structures*', Institute of Civil Engineers, London, p1–5

Ayres D.J (1986), '*Geotextiles or Geomembranes in Track? British Railways' Experience*,' Geotextiles and Geomembranes **3,** p129 – 142

Bishop A.W, Kennard M., Penman A.D.M (1960), '*Pore pressure Observations at Selset Dams'*, in *Proceedings of the Conference on Pore Pressure and suction in Soils'*, Butterworths, London, p91-102

Bishop A.W, Alpan I, Blight G.E and Donald I.W (1960), '*Factors Controlling the Strength of Partly Saturated Cohesive Soils*', Proceedings, Conference on the Shear Strength of Cohesive Soils, American Society of Civil Engineers, p503 – 532

Drumm, Reeves, Madgett, Trolinger, (1997), '*Subgrade Resilient Modulus Correction for Saturation Effects'*, ASCE, Journal of Geotechnical and Geoenvironmental Engineering, July

Da Re, (2000), '*Physical Mechanisms Controlling the Pre-failure Stress-strain Behaviour of Frozen Sand'*, MIT, PhD Thesis,

Dunnicliff J (1988), *Geotechnical Instrumentation for Monitoring Field Performance*', Wiley, p199 - 295

Fluet, J.E Jr (1986), '*Geosynthetics and North American Railroads*', Geotextiles and Geomembranes **3**, p201 – 218

Hanna T.H (1985), '*Field Instrumentation in Geotechnical Engineering'*, Trans Tech Publications, Vol. 10

Hayward A.T.J, (1959), "*The Choice of Flexible Tubing for Use in a Vacuum System*", National Engineering Laboratory, Fluids Note No. 83, October 1959.

Iotech Personal DAQ User's Manual (June 2001), *USB Data Acquisition Module,* p/n 491-0901 Rev 3.0

Larew H. G & Leonards G. A (1962), '*A strength criterion for repeated loads.*', Proceedings HRB, No 41, p529 – 556

Li D, Selig E.T (1996),' *Cumulative Plastic Deformations for Fine-grained Subgrade Soils'*, ASCE, Journal of Geotechnical Engineering, p1006 – 1013

Li D, Selig E.T (Apr 1998a), '*Method for railroad Track Foundation Design I: Development'* ASCE, Journal of Geotechnical and Geoenvironmental Engineering, v124 p316 – 322

Li D), Selig E.T (Apr 1998b), '*Method for railroad Track Foundation Design II: Application'* ASCE, Journal of Geotechnical and Geoenvironmental Engineering, v124 p323 - 329

Li D (2000), '*Deformations and Remedies for Soft Railroad Subgrades Subjected to Heavy Axle Loads'*, Geotechnical-Special-Publication, n103, ASCE, Reston, VA, USA p307 – 321

Martinek K (1986), '*Geotextiles used by the German Federal Railway – Experiences and Specifications'*, Geotextiles and Geomembranes **3,** p175 – 200

Matsui T, Ohara H, and Ito T (1980), '*Cyclical Stress-Strain History and Shear Characteristics of Clay*', Journal Geotechnical Engineering Division, ASCE, 106(10), p1101–1119

Miller (Feb 2000), Li D, '*Cyclic Shear Strength of Soft Railroad Subgrade'*, ASCE, Journal of Geotechnical and Geoenvironmental Engineering, p139 - 147

Mitchell R.J & King R.D (1977), '*Cyclical Loading of an Ottawa area Champlain Sea Clay*', Canadian Geotechnical Journal, Ottawa, Canada, 14, p52–62

Möller B. & Löfroth B. (1999), '*Remote Monitoring System for Geotechnical Applications, Descriptions and Case Records*', Field Measurements in Geomechanics, Leung, Tan & Phoon (eds), Balkema, Rotterdam, p139 – 144

Motorola MPX2100/D Semiconductor Technical Data
Motorola MPX2200/D Semiconductor Technical Data
Motorola (2003) DL200/D, Rev 5

Nielsen J C O & Stensson A (1999), *'Enhancing Freight Railways for 30 tonne Axle Loads*' Proceedings of the I MECH E Part F Journal of Rail and Rapid Transit, Vol 217, p225 - 263

Penman A.D.M (1956), "*A Field Piezometer Apparatus*", *Geotechnique,* 6, No.2, 57

Penman A.D.M (1960), '*A Study of the Response Time of Various Types of Piezometers*', in *Proceedings on the Conference on Pore Pressure and Suction in Soils,* Butterworths, London, p53 – 58

Penman A.D.M, Charles J.A, Nash J.K.T.L, and Humphreys J.D (1975), *"Performance of Culvert Under Winscar Dam"*, *Geotechnique*, Vol 25, No4. p713 - 730

Penman A.D.M (1978), "*Pore Pressure and Movement in Embankment Dams*," *Int. Water Power & Dam Construction,* London, Vol 30, No. 4, p32 - 39

Potchana P, Vavassori M, Zattoni A (1999), '*Automatic Data Acquisition System (ADAS): Monitoring System of Khao Laem Dam, Thailand*', Field Measurements in Geomechanics, Leung, Tan & Phoon (eds), Balkema, Rotterdam, p145 - 150

Rad N.S & Tumay M.T, (September 1985), "*Pore-Pressure Response of the Piezocone Penetrometer"*, Geotechnical Testing Journal, GTJODJ, Vol 8, No 3, p125 – 131

Raymond G.P (1999), '*Railway Rehabilitation Geotextiles*', Geotextiles and Geomembranes **17,** p213 – 230

Read D. and Li D (1995), '*Subballast Considerations for Heavy Axle Load Trackage*', TD 95-028, Technology Digest, Association of American Railroads, Research and Teset Department, Pueblo, Colorado

Selig E.T & Water JM (1994), '*Track Geotechnology and Substructure Management'*, Thomas Telford, p10.9 – 10.19

Shackel, B. (1973), '*Repeated Loading of Soils – a review*', *Australian. Road Res.,* Melbourne, 5(3), p22–49

Weather Underground, www.wunderground.com

Whittle A.J, Ling H.I (2002), '*Geosynthetics in Construction*', Encyclopaedia of Materials: Science & Technology, Elsevier